

**On the enzymatic mechanism of 4-hydroxybutyryl-CoA  
dehydratase and 4-hydroxybutyrate CoA-transferase  
from *Clostridium aminobutyricum***



Dissertation  
zur  
Erlangung des Doktorgrades  
der Naturwissenschaften  
(Dr. rer. nat.)

dem  
Fachbereich Biologie  
der Philipps-Universität Marburg  
vorgelegt von

**Jin Zhang**  
aus Xi'an, V.R. China  
Marburg/Lahn, Germany 2010

Die Untersuchungen zur vorliegenden Arbeit wurden von April 2006 bis März 2010 im Laboratorium für Mikrobiologie, Fachbereich Biologie, der Philipps Universität Marburg unter der Leitung von Prof. Dr. W. Buckel durchgeführt.

Vom Fachbereich Biologie  
der Philipps-Universität Marburg  
als Dissertation am 04. 2010 angenommen.

Erstgutachter: Prof. Dr. Wolfgang Buckel  
Zweitgutachter: Prof. Dr. Lars-Oliver Essen

Tag der mündlichen Prüfung am .

Die im zeitlichen Rahmen dieser Dissertation erzielten Ergebnisse sind in folgenden Publikation veröffentlicht:

**Martins, B., Messerschmidt, A., Friedrich, P., Zhang, J. & Buckel, W. (2007)**

4-Hydroxybutyryl-CoA Dehydratase.

In: *Handbook of Metalloproteins Online Edition* (A. Messerschmidt, ed.) John Wiley & Sons Ltd., Sussex, UK. (Review)

**Li, F., Hinderberger, J., Seedorf, H., Zhang, J., Buckel, W. & Thauer, R. K. (2008)**

Coupled ferredoxin- and crotonyl-CoA reduction with NADH catalyzed by the butyryl-CoA dehydrogenase/ETF complex from *Clostridium kluyveri*.

*The Journal of Bacteriology*. 190, 843-850.

**Macieira, S.\*, Zhang, J.\*, Velarde, M., Buckel, W., Messerschmidt, A. (2009)**

Crystal Structure of 4-hydroxybutyrate CoA-Transferase from *Clostridium aminobutyricum*.

*Biological Chemistry*. 390 (12): 1251-1263

(\* contributed equally to this work)

**Macieira, S.\*, Zhang, J.\*, Velarde, M., Buckel, W., Messerschmidt, A. (2010)**

Crystal Structure of the complex between 4-hydroxybutyrate CoA-Transferase from *Clostridium aminobutyricum* and butyryl-CoA.

*The FEBS Journal*. (in submitting)

(\* contributed equally to this work)

**Zhang, J., Friedrich, P., Martins, B., Kim, J., Buckel, W. (2010)**

Mutations in the active centre of 4-hydroxybutyryl-CoA dehydratase from *Clostridium aminobutyricum*. (in preparation)

# Contents

<b>Abbreviations .....</b>	<b>8</b>
<b>Zusammenfassung .....</b>	<b>9</b>
<b>Summary .....</b>	<b>11</b>
<b>1. Introduction .....</b>	<b>13</b>
1.1 Overview of anaerobic energy metabolism.....	13
1.2 Glutamate fermentation pathway in anaerobic bacteria .....	14
1.3 <i>Clostridium aminobutyricum</i> .....	18
1.4 Fermentation of 4-aminobutyrate in <i>C. aminobutyricum</i> .....	19
1.5 4-Hydroxybutyrate CoA-transferase from <i>C. aminobutyricum</i> .....	21
1.6 4-Hydroxybutyryl-CoA dehydratase from <i>C. aminobutyricum</i> .....	23
1.7 Proposed mechanism of dehydration via a ketyl radical .....	26
1.8 Cofactors in 4-hydroxybutyryl-CoA dehydratase .....	29
1.9 4-Hydroxybutyryl-CoA dehydratase in the 5 <sup>th</sup> CO <sub>2</sub> -fixation pathway.....	33
1.10 Goals of this work .....	35
<b>2. Materials and Methods .....</b>	<b>36</b>
2.1 Materials .....	36
2.1.1 Chemicals and reagents.....	36
2.1.2 Instruments, gases and columns.....	36
2.1.3 Bacterial strains and cultures .....	37
2.1.4 Plasmids.....	38
2.1.5 Oligonucleotides .....	38
2.1.6 Media .....	41
2.1.7 Antibiotics.....	41

2.1.8	Molecular biology kits .....	42
2.2	Molecular Biological Methods .....	43
2.2.1	Isolation of genomic DNA from <i>C. aminobutyricum</i> .....	43
2.2.2	Isolation of plasmid DNA .....	44
2.2.3	Determination of DNA concentration and purity .....	44
2.2.4	Agarose gel electrophoresis .....	44
2.2.5	DNA extraction from agarose gel .....	45
2.2.6	DNA restriction and ligation .....	45
2.2.7	Preparation of competent <i>Escherichia coli</i> cells for electrotransformation .....	46
2.2.8	Electrotransformation .....	46
2.2.9	PCR reaction .....	46
2.2.10	Cloning of the genes .....	48
2.2.11	Sequencing of the cloned genes .....	48
2.2.12	Site directed mutagenesis .....	48
2.3	Biochemical methods .....	50
2.3.1	Gene expression in <i>E. coli</i> and protein purification .....	50
2.3.2	Purification of other proteins .....	52
2.3.3	Determination of protein concentration .....	54
2.3.4	Sodium dodecylsulfate-polyacrylamide gel electrophoresis (SDS-PAGE) .....	54
2.3.5	Gel-filtration .....	56
2.3.6	Enzyme activity assays .....	57
2.3.7	Iron protein reconstitution .....	59
2.3.8	Non-heme iron determination with Ferene .....	59
2.3.9	Acid-labile sulfur determination .....	60
2.3.10	Flavin determination by UV-Vis .....	62

2.3.11	MALDI-TOF Mass Spectrometry.....	62
2.3.12	EPR Spectroscopy.....	63
2.4	Chemical synthesis.....	63
2.4.1	Acetyl-CoA, butyryl-CoA and crotonyl-CoA synthesis by anhydride.....	63
2.4.2	CoA-esters synthesis by 4-hydroxybutyryl-CoA transferase .....	64
2.4.3	4-Hydroxyvaleryl-CoA synthesis .....	64
<b>3.</b>	<b>Results.....</b>	<b>65</b>
3.1	The recombinant 4-hydroxybutyryl-CoA dehydratase (AbfD) in <i>E. coli</i> .....	65
3.1.1	Sequence analysis of <i>abfD</i> .....	65
3.1.2	Cloning and expression of <i>abfD</i> in <i>E.coli</i> .....	68
3.1.3	Purification of the recombinant AbfD .....	68
3.1.4	Physical and chemical characterization of the recombinant protein.....	69
3.1.5	Vinylacetyl-CoA $\Delta$ -isomerase .....	77
3.1.6	Mutagenesis of recombinant AbfD .....	80
3.2	The recombinant 4-hydroxybutyrate CoA-transferase (AbfT) in <i>E. coli</i> .....	85
3.2.1	Sequence analysis of AbfT .....	85
3.2.2	Cloning and expression of <i>abfT</i> in <i>E.coli</i> .....	87
3.2.3	Protein purification and analysis.....	90
3.2.4	Mutagenesis in the active site of recombinant AbfT .....	91
3.2.5	Crystal structure analysis .....	93
3.3	AbfD in new CO <sub>2</sub> -fixation .....	104
3.3.1	Cloning and expression of two different AbfD from <i>Metallosphaera sedula</i> .....	104
3.3.2	Protein purification .....	106
<b>4.</b>	<b>Discussion .....</b>	<b>107</b>

4.1	4-Hydroxybutyryl-CoA dehydratase .....	107
4.1.1	Recombinant 4-hydroxybutyryl-CoA dehydratase .....	107
4.1.2	Mutagenesis of 4-hydroxybutyryl-CoA dehydratase.....	110
4.1.3	Vinylacetyl-CoA $\Delta$ -isomerase .....	112
4.1.4	Proposed mechanism via a ketyl radical .....	114
4.2	4-Hydroxybutyrate CoA-transferase .....	117
4.2.1	Recombinant 4-hydroxybutyrate CoA-transferase .....	117
4.2.2	Identification of the catalytic glutamate residue in the active site.....	119
4.2.3	Crystal structure and mutation studies .....	120
4.2.4	The crystal structure of enzyme & butyryl-CoA complex.....	122
4.3	AbfD in new CO <sub>2</sub> -fixation pathway in <i>M. sedula</i> .....	123
<b>References .....</b>		<b>124</b>

## Abbreviations

DTT	Dithiothreitol
TEMED	N,N,N',N'-Tetraethylethylenediamine
AHT	Anhydrotetracycline
DTNB	5,5'-Dithiobis(2-nitrobenzoate)
IPTG	Isopropyl thio- $\beta$ -D-galactoside
AbfD	4-Hydroxybutyryl-CoA dehydratase
AbfT	4-Hydroxybutyrate CoA-transferase
MS_1, MS_2	Two different copies of 4-hydroxybutyryl-CoA dehydratases in <i>Metallosphaera sedula</i>



## Zusammenfassung

**Die 4-Hydroxybutyryl-CoA-Dehydratase** aus *Clostridium aminobutyricum* katalysiert die ungewöhnliche reversible Dehydratisierung von 4-Hydroxybutyryl-CoA zu Crotonyl-CoA. Das Enzym ist im nativen Zustand ein Homotetramer mit einer Masse von 232 kDa, und besteht aus zwei katalytisch aktiven Dimeren mit je zwei aktiven Zentren. Darin befinden sich je ein  $[4\text{Fe-4S}]^{2+}$  Cluster, ein nicht kovalent gebundenes FAD und einige konservierte Aminosäurereste, deren Oberflächen an einen schmalen Substrat-Bindungskanal grenzen.

Die ungewöhnliche Dehydratisierung erfordert die Abstraktion des nicht aktivierten 3Si-Protons ( $\text{pK} \approx 40$ ) vom 4-Hydroxybutyryl-CoA, die das Enzym über eine transiente Deprotonierung und Oxidation zu radikalischen Zwischenstufen bewerkstelligt. Das Hauptziel dieser Arbeit war die Aufklärung der Funktionen hoch konservierter Aminosäuren im aktiven Zentrum. Dabei wurden die Liganden des  $[4\text{Fe-4S}]^{2+}$  Clusters, H292C/E, C99A, C103A und C299A, sowie E257Q, E455Q, Y296F, A460G, Q101E, T190V und K300Q durch ortsspezifische Mutagenese verändert. Die sieben erstgenannten Varianten waren enzymatisch völlig inaktiv. Die übrigen zeigten geringe Restaktivitäten (0.4 – 4%).

Zusätzlich katalysiert die 4-Hydroxybutyryl-CoA Dehydratase die Isomerisierung von Vinylacetyl-CoA zu Crotonyl-CoA. Alle Varianten katalysierten diese Reaktion, wobei E455Q (7%), H292E (1%) und C99A (1%) die geringsten Aktivitäten aufwiesen. Überraschenderweise wurden die aktivsten E257Q (92%) und C299A (76%) Varianten durch Luft nicht inaktiviert, während der Wildtyp unter gleichen Bedingungen 90% seiner Aktivität verlor. Die Ergebnisse zeigen, dass wahrscheinlich H292 und E455 sowohl in der Dehydratisierung als auch in der Isomerisierung als katalytische Säure/Basen wirken. Möglicherweise ist E257 an der Stabilisierung des FAD beteiligt und somit für die Isomerisierung ohne Bedeutung.

Vor kurzem wurde ein neuer  $\text{CO}_2$ -Fixierungsweg in Archaeen gefunden, der sogenannte 3-Hydroxypropionat/4-Hydroxybutyrat Zyklus. In diesem wurde die 4-Hydroxybutyryl-CoA Dehydratase ebenfalls als ein Schlüsselenzym nachgewiesen. Interessanterweise sind zwei

unterschiedene Kopien der 4-Hydroxybutyryl-CoA Dehydratase in *Metallosphaera sedula* vorhanden. Ein weiteres Ziel dieser Arbeit war die Aufklärung der Funktionen dieser beiden Dehydratasen. Die Gene wurden bereits erfolgreich in Plasmide kloniert, aber eine Produktion in *Escherichia coli* führte nur zu inaktivem Protein. Deshalb ist in Zukunft die Genexpression in *Sulfolobus solfataricus* geplant, weil sowohl *Metallosphaera* als auch *Sulfolobus* zu den thermophilen *Crenarchaeota* gehören.

**Die 4-Hydroxybutyrat CoA-Transferase** katalysiert die Aktivierung von 4-Hydroxybutyrat zu 4-Hydroxybutyryl-CoA. Im Rahmen dieser Arbeit wurde mit ortsspezifischer Mutagenese herausgefunden, dass E238 während der Katalyse mit CoA ein Thioesterintermediat bildet. Dieses Intermediat wurde auch über den Ping-Pong-Mechanismus, die Reduktion mit  $\text{NaBH}_4$  und durch thermische Fragmentierung der Peptidkette identifiziert. Die Kristallstruktur mit Butyryl-CoA als Substrat zeigt, dass das aktive Zentrum des homodimeren Enzyms zwischen den beiden Untereinheiten einen schmalen Kanal bildet, an dessen Ende sich E238 befindet. Diese Struktur eines Michaelis Komplexes ist bisher unter den CoA-Transferasen einmalig.

## Summary

**4-Hydroxybutyryl-CoA dehydratase** from *Clostridium aminobutyricum* catalyzes the unusual reversible dehydration of 4-hydroxybutyryl-CoA to crotonyl-CoA. The enzyme is a homotetramer with the molecular mass of 232 kDa in native form, which consists of two catalytically functional dimers with two active sites in each dimer. Each active site contains one  $[4\text{Fe-4S}]^{2+}$  cluster and one not covalently bound FAD moiety. The surface of these two cofactors and several in the active site located amino acids forms a narrow substrate binding channel.

This unusual dehydration reaction involves the removal of the non-activated 3 $^{\text{rd}}$ -hydrogen ( $\text{p}K \approx 40$ ) of 4-hydroxybutyryl-CoA, which is carried out via transient deprotonation and oxidation generating radical intermediates. This work aimed to explain the catalytic functions of highly conserved amino acids in the active centre. Thereby, the ligands of  $[4\text{Fe-4S}]^{2+}$  cluster, H292C/E, C99A, C103A, and C299A, as well as E257Q, E455Q, Y296F, A460G, Q101E, T190V, and K300Q were generated by site-directed mutagenesis. The first variants from H292C to E455Q abolished the dehydratase activities. The others showed low residual activity (0.4 – 4%).

Moreover, 4-hydroxybutyryl-CoA dehydratase also catalyzes the isomerization of vinylacetyl-CoA to crotonyl-CoA. All mutants were able to catalyze this reaction, in which E455Q (7%), H292E (1%) and C99A (1%) exhibited the smallest activities. Surprisingly, the mutants E257Q (92%) and C299A (76%) were not inactivated by exposure to air, whereas the wild type lost 90 % of the initial value under the same conditions. The results showed that H292 and E455 probably act as catalytic acid/base in the dehydration as well as in the isomerization. E257 most likely participates in the stabilization of FAD and therefore is insignificant for the isomerization.

Recently a new  $\text{CO}_2$ -fixation pathway has been reported in archaea, namely the 3-hydroxypropionate/4-hydroxybutyrate pathway, which contains 4-hydroxybutyryl-CoA

dehydratase as the key enzyme. However, the genome of the autotrophic thermophile *Metallosphaera sedula* revealed two different copies of 4-hydroxybutyryl-CoA dehydratase. This work also aimed to uncover the functions of these two copies through cloning of their genes in plasmid and analysis of the purified recombinant proteins. Unfortunately, the purified recombinant protein produced in *Escherichia coli* expression system showed no dehydratase activity. Therefore, in the future the recombinant protein will be produced in *Sulfolobus solfataricus*, because both *Metallosphaera* and *Sulfolobus* belong to the thermophilic *Crenarchaeota*.

**The 4-hydroxybutyrate CoA-transferase** catalyzes the activation of 4-hydroxybutyrate to 4-hydroxybutyryl-CoA. In this work it has been detected by site-directed mutagenesis that E238 is responsible to form the CoA-enzyme thioester intermediate. This intermediate was identified by the ping-pong mechanism, the reduction with NaBH<sub>4</sub> and also by thermal fragmentation of the peptide chain. The crystal structure with butyryl-CoA as substrate exhibited that the active centre is forming a narrow substrate binding channel between both subunits, and E238 is located at the end of this channel. This structure of the Michaelis complex is unique in the CoA-transferases.

## 1. Introduction

### 1.1 Overview of anaerobic energy metabolism

Under anoxic conditions many organisms are able to use organic or inorganic compounds other than molecular oxygen as electron acceptors. During energy conservation reactions the organic substrates or hydrogen are oxidized and the electron acceptors, such as nitrate, nitrite, sulfate, carbon dioxide, fumarate, the substrate itself or a derivative thereof are reduced. In *Clostridium aminobutyricum* crotonyl-CoA, a derivative of the substrate 4-aminobutyrate, acts as electron acceptor.

In the reductive branch, an electron is transferred from the donor with a negative redox potential to an acceptor with a more positive redox potential. The electron transfer is coupled to the synthesis of ATP (adenosine-5'-triphosphate). This process is known as electron-transport phosphorylation (ETP) or anaerobic respiration. It is different to aerobic respiration, in that oxygen is replaced by other electron acceptors. However most of them have a less positive redox potential than oxygen, which leads to the less energy available for ATP-synthesis [1-4].

In the oxidative branch, during the degradation of organic substrates, a high-energy phosphoanhydride bond containing compound is formed, from which ATP is generated by substrate level phosphorylation (SLP).

Fermentation is the process of deriving energy from the oxidation of organic compounds using an endogenous electron acceptor. It occurs mainly in soil, marine, and anoxic sewage sludge environments, as well as in the intestinal tract and other anoxic niches of the animal and human body. Three types of fermentation have been observed [5]:

- Fermentation in which two substrates participate, one acting as electron donor and the other as electron acceptor (e.g., amino acid fermentation called Stickland).
- Fermentation in which a single substrate is fermented, such that the oxidative step is

followed by the reductive step (e.g., homolactate fermentation).

- Fermentation in which a single substrate serves both as electron donor and as electron acceptor (e.g. glutamate fermentation). This occurs in the majority of cases.

### 1.2 Glutamate fermentation pathway in anaerobic bacteria

In the anoxic environments, the polypeptide and proteins are hydrolyzed by exogenous proteases to small peptides and single amino acids, which are taken up by fermentative bacteria and degraded to ammonia, CO<sub>2</sub>, H<sub>2</sub>, acetate and short chain fatty acids. Acetogenic organisms can then use the byproducts CO<sub>2</sub> and H<sub>2</sub> for acetate synthesis, while syntrophic bacteria can oxidize the short chain fatty acid to acetate, CO<sub>2</sub> and H<sub>2</sub>. The latter reaction happens only if the H<sub>2</sub> pressure is kept at a very low level by reacting with CO<sub>2</sub> to produce methane, which occurs in methanogenic archaea. The biochemically most versatile organisms in this process are the fermentative bacteria. A special case is glutamate fermentation by anaerobic bacteria of the orders Clostridiales and Fusobacteriales [6-10].

These bacteria are able to degrade glutamate to fatty acids, ammonia, CO<sub>2</sub> and H<sub>2</sub> by at least five different pathways, most of which contain reactions with radical intermediates.

#### The two coenzyme B<sub>12</sub>-dependent 3-methylaspartate pathways

In the first half of the two pathways glutamate is degraded to ammonia, acetate and pyruvate via a catalytically interesting coenzyme B<sub>12</sub>-dependent glutamate mutase. Pyruvate then disproportionates either to CO<sub>2</sub> and butyrate or to acetate, CO<sub>2</sub> and propionate.

The classic glutamate fermentation pathway was first discovered in *Clostridium tetanomorphum* [10, 11]. In this pathway, glutamate is converted via (2*S*, 3*S*)-3-methylaspartate to mesaconate, which is hydrated to (*S*)-citramalate. Citramalate is then cleaved to acetate and pyruvate. The most interesting enzyme, glutamate mutase, catalyzes the reversible re-arrangement of (*S*)-glutamate to (2*S*,3*S*)-3-methylaspartate. It contains two

subunits, which in the presence of coenzyme B<sub>12</sub> forms the active complex. When the substrate is added to the active complex, the carbon-cobalt bond of the coenzyme is cleaved into cob(II)alamin and the 5'-deoxyadenosine radical. The radical can then abstract the 4*S*i hydrogen to form 5'-deoxyadenosine and the 4-glutamate radical. The glutamate radical fragments to acrylate and the glycine radical, which recombines to the 3-methylaspartate radical. The 3-methylaspartate is formed during the regeneration of the 5'-deoxyadenosine radical.

These two coenzyme B<sub>12</sub>-dependent pathways have been detected in some clostridia, such as *C. cochlearium*, *C. lentoputrescens*, *C. lismosum*, *C. malenominatum* and *C. tetani* [12-14]. The pathway leading to propionate has been found in several bacteria of the family Acidaminococcaceae.

### The 2-hydroxyglutarate pathway

In this pathway, glutamate is initially oxidized to 2-oxoglutarate by NAD<sup>+</sup>, then reduced to 2-hydroxyglutarate by NADH. After activation to 2-hydroxyglutaryl-CoA, it is dehydrated to glutaconyl-CoA and then decarboxylated to crotonyl-CoA, which disproportionates to acetate, butyrate and H<sub>2</sub> [15-21].

This pathway yields the same products as the butyrate forming coenzyme B<sub>12</sub> dependent pathway, but in the absence of coenzyme B<sub>12</sub>. The mechanism involves the reversible *syn*-elimination of water by 2-hydroxyglutaryl-CoA dehydratase. This oxygen sensitive enzyme contains two components, a homodimeric activator with a [4Fe-4S]<sup>2+</sup> cluster and a heterodimeric dehydratase with either one or two [4Fe-4S]<sup>2+</sup> clusters. Upon addition of ATP the helix-cluster-helix angle in the activator is probably enlarged from 105° to 180°. This conformational change moves the cluster towards the dehydratase component in order to facilitate the electron transfer, which reduces the electrophilic carbon to a negative charged ketyl radical. After elimination of the hydroxyl group the formation of the enoxyradical lowers the p*K* of the β-hydrogen from 40 to 14. Now the β-hydrogen can be removed easily by a base of the enzyme leading to a second ketyl radical. Finally, it is oxidized to glutaconyl-

CoA.

This pathway has been detected in *Acidominococcus fermentans*, *C. sporosphaeroides*, *C. symbiosum*, *Fusobacterium nucleatum* and *Peptostreptococcus asaccharolyticus* [16, 19-21].

### The 4-aminobutyrate fermentation pathway

This pathway is different from the three pathways described above, because a second organism decarboxylates glutamate to 4-aminobutyrate, such as *E. coli*. 4-Aminobutyrate is used by several anaerobic bacteria for energy conservation. In this pathway 4-aminobutyrate is fermented via 4-hydroxybutyrate to acetate and butyrate [22]. The oxygen sensitive 4-hydroxybutyryl-CoA dehydratase catalyzes the mechanistic most interesting reversible dehydration of 4-hydroxybutyryl-CoA to crotonyl-CoA using a ketyl radical. More details will be described in chapter 1.5.

### The fermentation pathway via 5-aminovalerate

Under osmotic stress, glutamate is reduced to the osmoprotective amino acid proline by *Bacillus subtilis*, which is further reduced to 5-aminovalerate by *Clostridium sporogenes*. *Clostridium viride* then ferments 5-aminovalerate via 5-hydroxyvaleryl-CoA and 2-pentenoyl-CoA to ammonia, acetate, propionate and valerate. During the dehydration of 5-hydroxyvaleryl-CoA to 4-pentenoyl-CoA a non-activated  $\gamma$ -hydrogen has to be removed. The activation of this hydrogen is achieved by participation of FAD as a prosthetic group. Firstly, a double bond is generated using 5-hydroxyvaleryl-CoA dehydratase/dehydrogenase with help of FAD resulting 5-hydroxy-2-pentenoyl-CoA and FADH<sub>2</sub>, which can be dehydrated by acid base catalysis. The resulting 2,4-pentadienoyl-CoA is reduced to 3-pentenoyl-CoA, whereby oxidized FAD is regenerated [23].



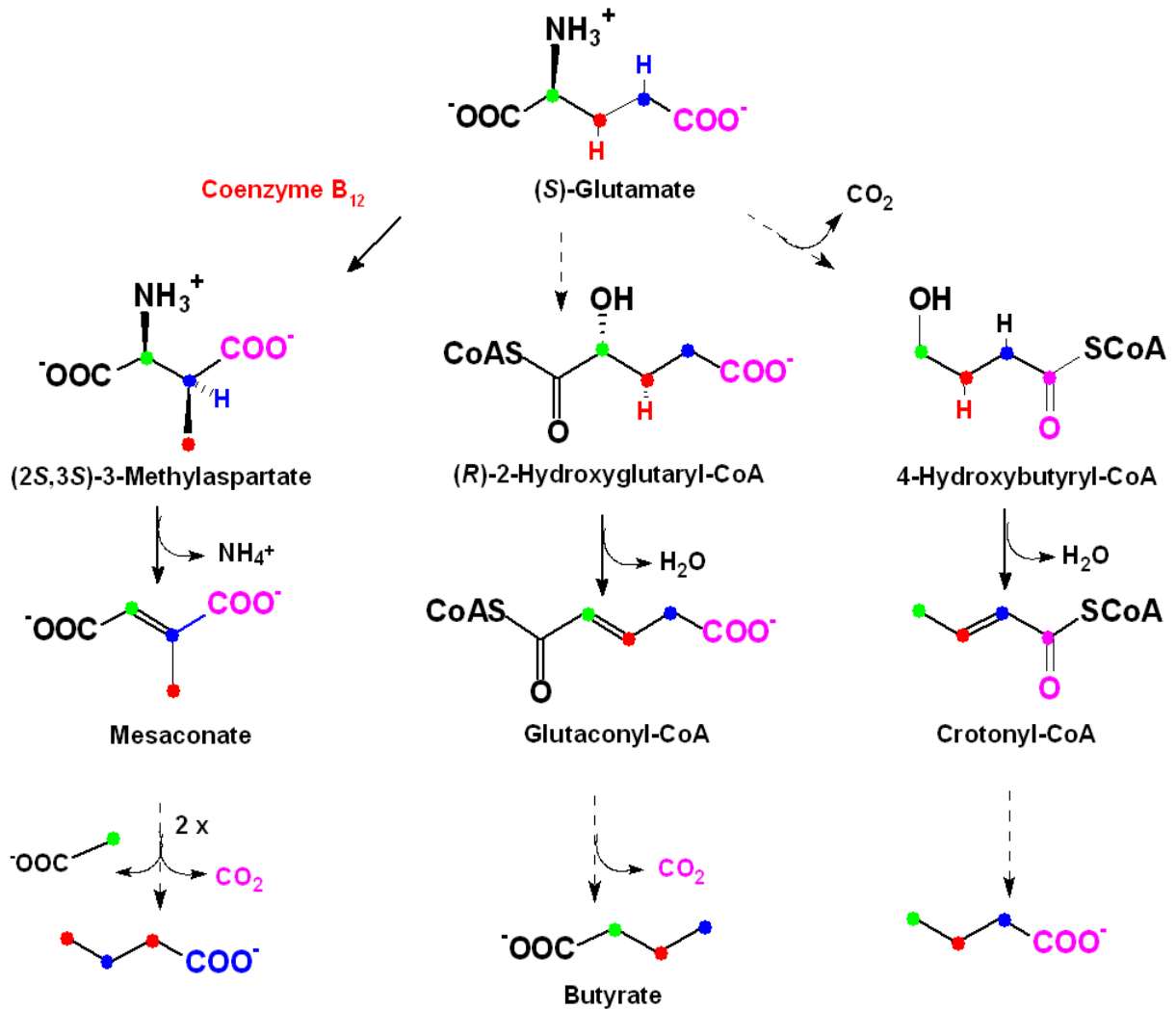


Figure 1-1. Glutamate fermentation pathway via (2S,3S)-3-methylaspartate, 2-hydroxyglutaryl-CoA and 4-hydroxybutyryl-CoA.

### 1.3 *Clostridium aminobutyricum*

Clostridia are bacteria, which probably evolved in the anoxic atmosphere before oxygen became available. They can produce spores during the resting stage, which are resistant to physical and chemical stress. Some species, such as *C. difficile* and *C. tetani*, cause diseases. On the other hand, most of them are harmless, and use sugars or amino acids as energy sources [24].

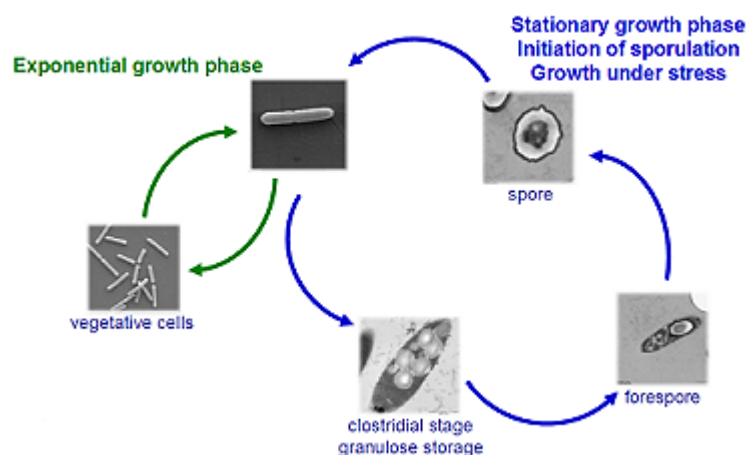


Figure 1-2. Growth phases of *Clostridium*

Most clostridial species form spores, are Gram positive, motile, and able to degrade organic materials to acids, CO<sub>2</sub> and H<sub>2</sub>. Their 16S ribosomal RNAs show very low sequence similarity, which indicates early divergence of the species during evolution [24, 25].

The strict anaerobic *Clostridium aminobutyricum* was first isolated from North Carolina swamp mud [26-29] and grows on 4-aminobutyrate, but not on closely related compounds. It forms acetate, butyrate and ammonia.

## 1.4 Fermentation of 4-aminobutyrate in *C. aminobutyricum*

*Escherichia coli* is able to decarboxylate glutamate to 4-aminobutyrate, which is then fermented by *C. aminobutyricum* via 4-hydroxybutyryl-CoA and crotonyl-CoA to acetate and butyrate [22].



$$\Delta G^{o'} \approx -50 \text{ kJ/mol 4-aminobutyrate}$$

Initially, the amino group of 4-aminobutyrate is exchanged with the keto-group of 2-oxoglutarate by 4-aminobutyrate aminotransferase [30] producing succinate semialdehyde. This is then reduced to 4-hydroxybutyrate with the help of NADH using 4-hydroxybutyrate dehydrogenase. The activation of 4-hydroxybutyrate to 4-hydroxybutyryl-CoA is catalyzed by 4-hydroxybutyrate CoA-transferase, followed by dehydration of 4-hydroxybutyryl-CoA to crotonyl-CoA using 4-hydroxybutyryl-CoA dehydratase/vinylacetyl-CoA  $\Delta$ -isomerase, a bifunctional oxygen sensitive cofactor containing enzyme. The resulting crotonyl-CoA then disproportionates to acetate and butyrate. The reductive branch leads to butyrate, whereas the oxidative branch via 3-hydroxybutyryl-CoA and acetoacetyl-CoA yields two acetyl-CoA, one of which is used for substrate level phosphorylation. On the other hand, *C. aminobutyricum* is also able to use vinylacetate, which is activated by 4-hydroxybutyrate CoA-transferase to vinylacetyl-CoA, afterwards it is converted to crotonyl-CoA by the same enzyme, namely 4-hydroxybutyryl-CoA dehydratase/vinylacetyl-CoA  $\Delta$ -isomerase [22, 31-34].

Additional, energy may be conserved via electron bifurcation in the reduction of crotonyl-CoA to butyryl-CoA by NADH. The highly exergonic reaction is used to drive the endergonic reduction of ferredoxin by a second NADH. Ferredoxin is then reoxidized by  $\text{NAD}^+$  catalyzed by a membrane-bound ferredoxin NAD-reductase (Rnf) that generates  $\Delta\mu\text{H}^+$  equivalent to about  $\frac{1}{4}$  ATP. Hence the total yield of ATP will be increased from 1.0 to 1.25 per two 4-hydroxybutyrate giving 80 kJ/ATP, which approaches the theoretical value of 70 kJ/ATP.

*C. kluyveri* can grow on succinate [35]. The dicarboxylic acid is activated by succinate CoA-transferase to succinyl-CoA followed by reduction to succinate semialdehyde by succinate semialdehyde dehydrogenase using NADH. The resulting succinate semialdehyde is able to participate in the above described 4-aminobutyrate pathway [32, 36].

This pathway has been detected also in *Fusobacterium varium* and *F. mortiferum*, both of which are normally isolated from the gastrointestinal tract.

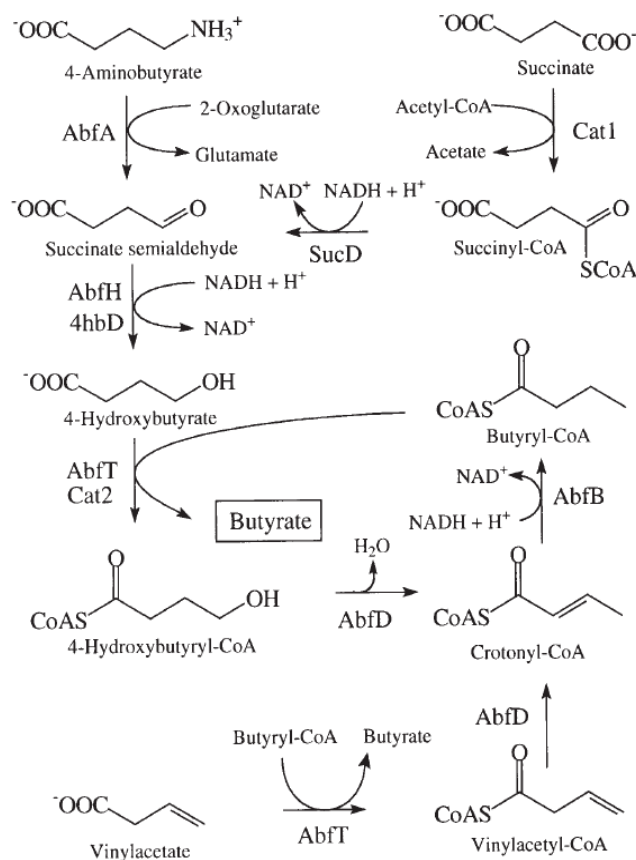


Figure 1-3. Proposed pathways of the reduction of 4-aminobutyrate and vinylacetate in *C. aminobutyricum* as well as succinate in *C. kluyveri*.

AbfA, 4-aminobutyrate aminotransferase; AbfH and 4hbD, 4-hydroxybutyrate dehydrogenase; AbfT and Cat2, 4-hydroxybutyrate CoA-transferase; AbfD, 4-hydroxybutyryl-CoA dehydratase/vinylacetate  $\Delta$ -isomerase; AbfB, butyryl-CoA dehydrogenase; SucD, succinate semialdehyde dehydrogenase.

## 1.5 4-Hydroxybutyrate CoA-transferase from *C. aminobutyricum*

CoA-transferases exist mainly in energy-limited anaerobic bacteria. It catalyzes the reversible transfer of the CoA-group from the donor, a CoA-thioester, to the CoA-acceptor, a free acid. CoA-transferases are grouped into three enzyme families [37].

In family I the reaction proceeds via a ping-pong mechanism, involving an active site glutamate residue that participates in the reaction mechanism [38, 39]. The reaction (Fig. 1-4, I) is started by a nucleophilic attack of the catalytic glutamate residue at the CoA-thioester substrate to form an enzyme-bound acyl-glutamyl anhydride. Then the released CoAS<sup>-</sup> anion participates in another nucleophilic attack at the mixed anhydride, which leads to an enzyme-bound glutamyl-CoA thioester and liberation of the acid of the donor thioester. The CoA-accepting carboxylate then attacks the glutamyl-CoA to generate the second mixed anhydride with the enzyme, and the liberated CoAS<sup>-</sup> anion reacts with this anhydride to produce the end product thioester. This enzyme family contains CoA-transferases for 3-oxoacids (EC 2.8.3.5; EC 2.8.3.6), short chain fatty acids (EC 2.8.3.8) [40] and glutaconate (EC. 2.8.2.12). Most of them use succinyl- and acetyl-CoA as CoA donors and are composed of two distinct subunits.

Family II consists of only the homodimeric  $\alpha$ -subunits of the octadecameric citrate or citramalate lyases (EC 2.8.3.10, EC 2.8.3.11) and catalyzes a partial reaction (Fig.1-4, II). These lyases consist of three subunits with different functions, a CoA-transferase ( $\alpha$ ), a lyase ( $\beta$ ) and an acyl-carrier protein ( $\gamma$ , ACP). Firstly, the thiol of the prosthetic group is converted to an acetyl-thioester in order to activate the enzyme [41]. The enzyme then catalyzes the acetylation of citramalate to an active acetyl-citramalyl-anhydride intermediate. The generated CoAS<sup>-</sup> anion from ACP reacts with this anhydride leading to the release of acetate and the production of citryl-CoA followed by cleavage to oxaloacetate and recycling of the acetyl-thioester.

In family III (Fig.1-4, III) the mechanism of CoA-transferase is analogous to that of family I, but not via the ping-pong reaction. This family includes an aspartate residue in the active

centre, which leads to the formation of aspartyl mixed anhydride intermediate. Most of them catalyze CoA-transfer reactions in a highly substrate- and stereospecific manner. This family contains formyl-CoA: oxalate CoA-transferase (EC 2.8.3.2), succinyl-CoA: (*R*)-benzylsuccinate CoA-transferase (EC 2.8.3.15), cinnamoyl-CoA: phenyllactate CoA-transferase (EC 2.8.3.17) and isocarproyl-CoA: 2-hydroxyisocaproate CoA-transferase.

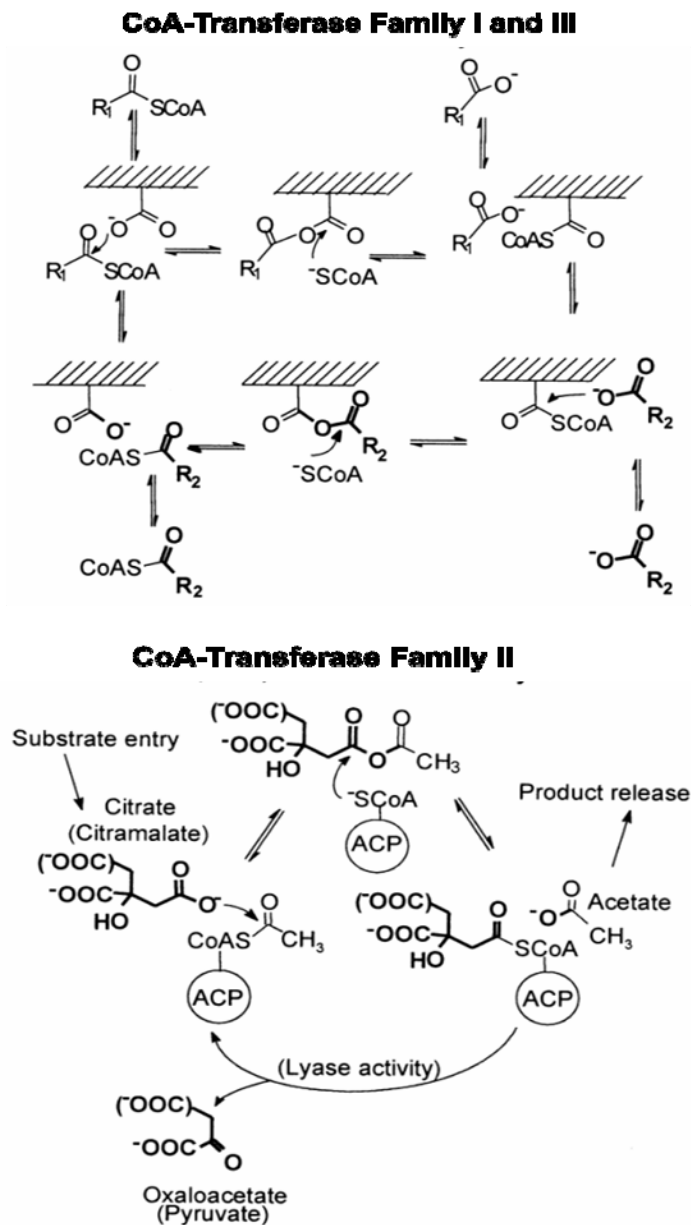


Figure 1-4. Mechanisms of CoA-transferases of families I, II and III

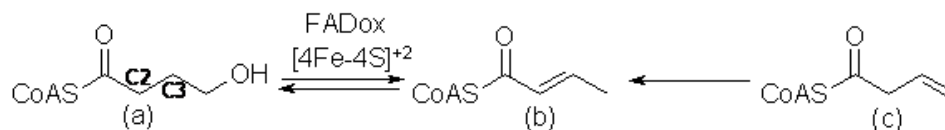
4-Hydroxybutyrate CoA-transferase takes part in the fermentation pathway of 4-aminobutyrate in anaerobic bacteria such as *C. aminobutyricum* or *Porphyromonas gingivalis* or in facultative bacteria as *Shewanella oneidensis*. It catalyzes the CoA transfer from acetyl-CoA to 4-hydroxybutyrate. The colorless 4-hydroxybutyrate CoA-transferase was isolated from *C. aminobutyricum*, purified and characterized several years ago [42]. The molecular mass was determined as 110 kDa and indicated a homodimeric structure with 54 kDa per subunit. The enzyme does not consist of prosthetic groups and is capable of taking butyrate, propionate and its CoA-thioester, in addition to 4-hydroxybutyrate, acetate and vinylacetate as well as their CoA-thioesters as substrates. In contrast, 3-hydroxybutyrate and *trans*-crotonate are not esterified.

However, the classification of 4-hydroxybutyrate CoA-transferase is not clear from its amino acid sequence alignment, although a relationship with the  $\alpha$ -unit of citrate lyase has been suggested [22]. Moreover, according to glutaconate CoA-transferase from *A. fermentas* [34, 38, 43], a thiol ester should be formed between the catalytic glutamate residue in the active site and the CoAS-moiety of the acyl-CoA substrate. This glutamate residue in 4-hydroxybutyrate CoA-transferase could not be identified previously [22].

## **1.6 4-Hydroxybutyryl-CoA dehydratase (AbfD) from *C. aminobutyricum***

Most of the dehydratases catalyze the  $\alpha,\beta$ -elimination of water. The  $\alpha$ -hydrogen is removed as a proton, which is activated by an adjacent electron withdrawing functional group, such as carboxylate, carbonyl or CoA-thioester, and the hydroxyl-group is eliminated from the  $\beta$ -position. However, 4-hydroxybutyryl-CoA dehydratase has to remove a non-activated hydrogen at the  $\beta$ -position of 4-hydroxybutyryl-CoA, which is the mechanistically most interesting reaction in the 4-aminobutyrate fermentation pathway in *C. aminobutyricum*. Furthermore, 4-hydroxybutyryl-CoA dehydratase can also catalyze the irreversible isomerization of vinylacetyl-CoA to crotonyl-CoA. Interestingly, in previous studies it has been shown that incubation of the native dehydratase under aerobic conditions resulted in the

complete loss of the dehydratase activity within 40 min, whereas the isomerase activity dropped to 40 % of the initial value.



4-Hydroxybutyryl-CoA dehydratase (Fig. 1-5, A) contains a  $[4\text{Fe-4S}]^{2+}$  cluster and a non covalently bound FAD moiety in each 54 kDa subunit [44, 45]. It is active only as a homotetramer composed of two catalytically functional dimers with two active sites in each dimer [46]. The monomer consists of three domains (Fig. 1-5, B). The N- and C-terminal domains (residues Met1 - Leu143 and Glu277 – Lys490) are mainly  $\alpha$ -helical, while the middle domain is predominantly  $\beta$ -structured. A similar structural fold is found in FAD-containing medium chain acyl-CoA dehydrogenase (MCAD) from pig liver [47, 48], which catalyzes the reversible oxidation of an acyl-CoA derivative to form the  $\alpha,\beta$ -double bond in the corresponding enoyl-CoA. However, both enzymes show only 16% amino acid sequence identity. Interestingly, both of them cleave the non-activated C-H bond at  $\beta$  position.

The active site (Fig. 1-6, a) is built by a narrow substrate binding channel leading from the surface of the molecule of the  $[4\text{Fe-4S}]^{2+}$  cluster and FAD. The Fe atoms of the  $[4\text{Fe-4S}]^{2+}$  cluster are covalently bound to the protein by three cysteine and one histidine residues, C99 and C103 from the N-terminal, and H292, C299 from C-terminal domain (Fig. 1-6, b). Interestingly, in all iron sulfur cluster containing metalloproteins the distances between  $\text{Fe}_1$  and  $\text{Ne}_2$  of a histidine ranges from 1.9 Å to 2.1 Å, but in AbfD the  $\text{Fe}_1-\text{Ne}_2$  bond of H292 length is 2.4 Å. Three residues located also in the active centre, Y296, K300, E455 and E257 are highly conserved among all known 4-hydroxybutyryl-CoA dehydratases [49].



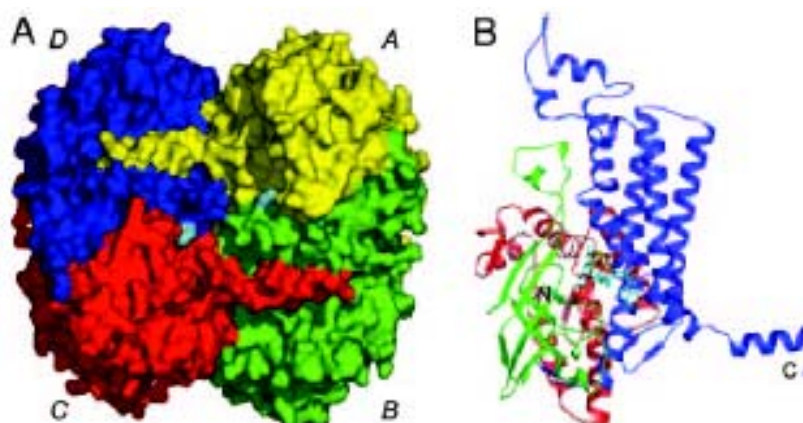


Figure 1-5. Crystal structure. A, surface representation of AbfD homotetramer, each monomer is individually colored; B, secondary structure topology of the monomer with the N-terminal domain in red, the middle domain in green and the C-terminal domain in blue, the iron sulfur cluster is shown as ball and sticks with Fe and S atoms in red and yellow, FAD shows in cyan.

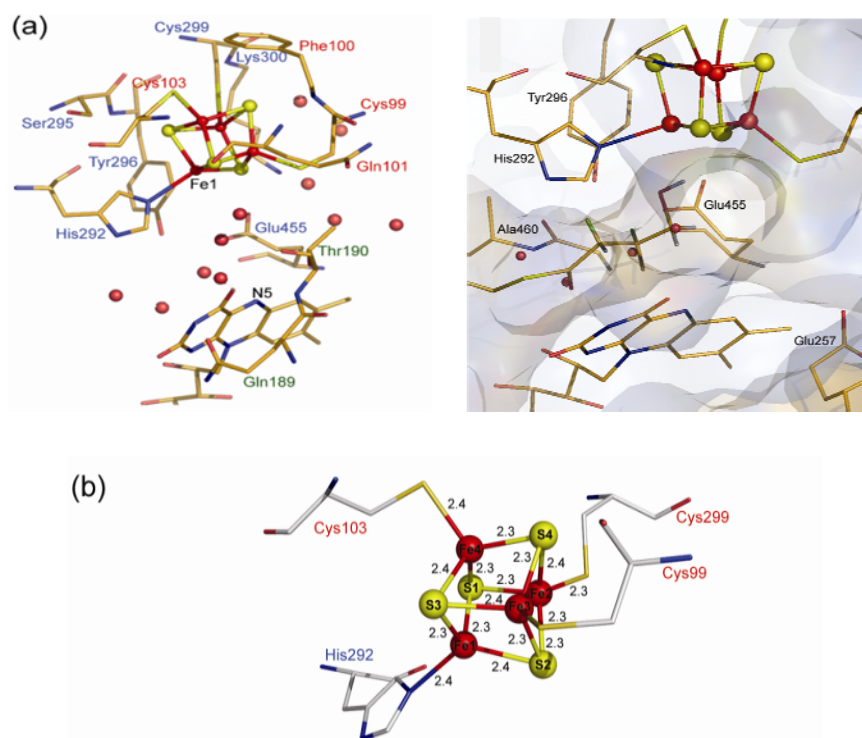


Figure 1-6. The active site. (a) Stereo view of AbfD active site environment, color code for residues and FAD is in cream for carbon, red for oxygen, blue for nitrogen and yellow for sulfur. (b) Amino acids coordinating the  $[4\text{Fe-4S}]^{2+}$  cluster.

## 1.7 Proposed mechanism of dehydration via a ketyl radical

Recently many enzymes have been found to act by a radical mechanism, which use the high reactivity of radicals to perform the catalytic reaction. The word ‘radical’ means a species with an unpaired electron, which is usually very reactive.

Nature has evolved low-energy pathways via simple acid-base mechanisms wherever possible, but for some ‘chemically difficult’ reactions, where there is no alternative, high-energy radical mechanisms are used. Because radicals react irreversibly with dioxygen, most of these enzymes occur in anaerobic bacteria and archaea [7, 50], apart from some B<sub>12</sub>- and S-adenosylmethionine (SAM)-dependent radical enzymes that occur also in aerobic bacteria and even in humans.

There are three different ways to generate radicals: homolysis of a weak covalent bond, one-electron oxidation and one-electron reduction. Well studied radical generators act via homolysis of adenosylcobalamin (coenzyme B<sub>12</sub>) as described for glutamate mutase (see above) or via reductive cleavage of S-adenosylmethionine that also leads to the 5'-deoxyadenosine radical. The latter type, called SAM radical enzymes, catalyzes a variety of unusual chemical transformations such as the migration of the  $\alpha$ -amino group of lysine to the  $\beta$ -position. This increasing number of enzymes is also involved in the activation of glycyl radical enzymes, hydrogenases and sulfatases, the biosynthesis of thiamin, biotin, porphyrin, molybdenum cofactor and lipoic acid, and the maturation of tRNA. An example of radical formation by one-electron reduction are the [4Fe-4S]<sup>2+</sup> cluster containing 2-hydroxyacyl-CoA dehydratases [15, 51], which consist of two components, a homodimeric activator and a heterodimeric dehydratase. Upon addition of ATP to the activator, the angle of helix-cluster-helix architecture opens from 105° to 180°, which facilitates the transfer of a highly energized electron to the dehydratase and leads to the formation of a ketyl radical at the thioester carbonyl. This nucleophilic radical expels the hydroxyl group to yield the enoxy radical. This elimination increases the acidity of the  $\beta$ -proton from  $pK \approx 40$  to  $pK \approx 14$ , which can be removed by a base of the protein.

The oxygen sensitive 4-hydroxybutyryl-CoA dehydratase is an example, in which a ketyl radical is formed by one-electron oxidation [52-55].

It has been proposed that during the catalytic reaction 4-hydroxybutyryl-CoA enters the active centre of enzyme as substrate with its hydroxyacyl part sandwiched between the two prosthetic groups. This results in the displacement of H292 from Fe<sub>1</sub> of the iron sulfur cluster. Then H292 as a base abstracts the 2*Re*-proton from the  $\alpha$ -position and the enolate is oxidized by FAD to an enoxy radical, which acidifies the  $\beta$ -proton from p*K* 40 to p*K* 14. The flavin semiquinone anion acts as a base removing the 3*Si*-proton from the  $\beta$ -position to yield neutral semiquinone FADH<sup>•</sup> and a ketyl radical anion. After elimination of the hydroxyl group to a dienoxyl radical, it is reduced to the dienolate by the semiquinone regenerating the flavin quinone. Lastly, dienolate is protonated to crotonyl-CoA. Overall, the dehydration of 4-hydroxybutyryl-CoA to (*E*)-crotonyl-CoA can be described as anti-elimination of the 2*Re*- and the 3*Si*-hydrogen as well as substitution of the hydroxyl group by hydrogen with retention of configuration [55-58].

The postulated mechanism of the dehydration of 4-hydroxybutyryl-CoA is based on the catalytic mechanism of medium-chain acyl-CoA dehydrogenase (MCAD) [48, 59, 60], since a similar fold is found in both proteins, although these two shows just 16% amino acid sequence identity. Similarity is that both of AbfD and MCAD require the rupture of non-activated  $\beta$ -C-H bond. MCAD is a FAD containing protein as AbfD, but devoid of an iron sulfur cluster. As in AbfD, the reaction initiates with deprotonation at the  $\alpha$ -carbon and a consecutive one electron transfer from the enolate of acyl-CoA to FAD resulting in the enoxy radical and the flavin semiquinone anion, which could remove the  $\beta$ -proton as a base. The generated ketyl radical transfers a second electron to the flavin, whereby the hydroquinone anion and the product enoyl-CoA are formed. The mechanistic similarity suggests that the introduction of a [4Fe-4S]<sup>2+</sup> cluster converted the acyl-CoA dehydrogenase into a 4-hydroxybutyryl-CoA dehydratase, a process called “evolution by selection of (small) modifications of existing catalytic systems” (Sir John W. Comforth).

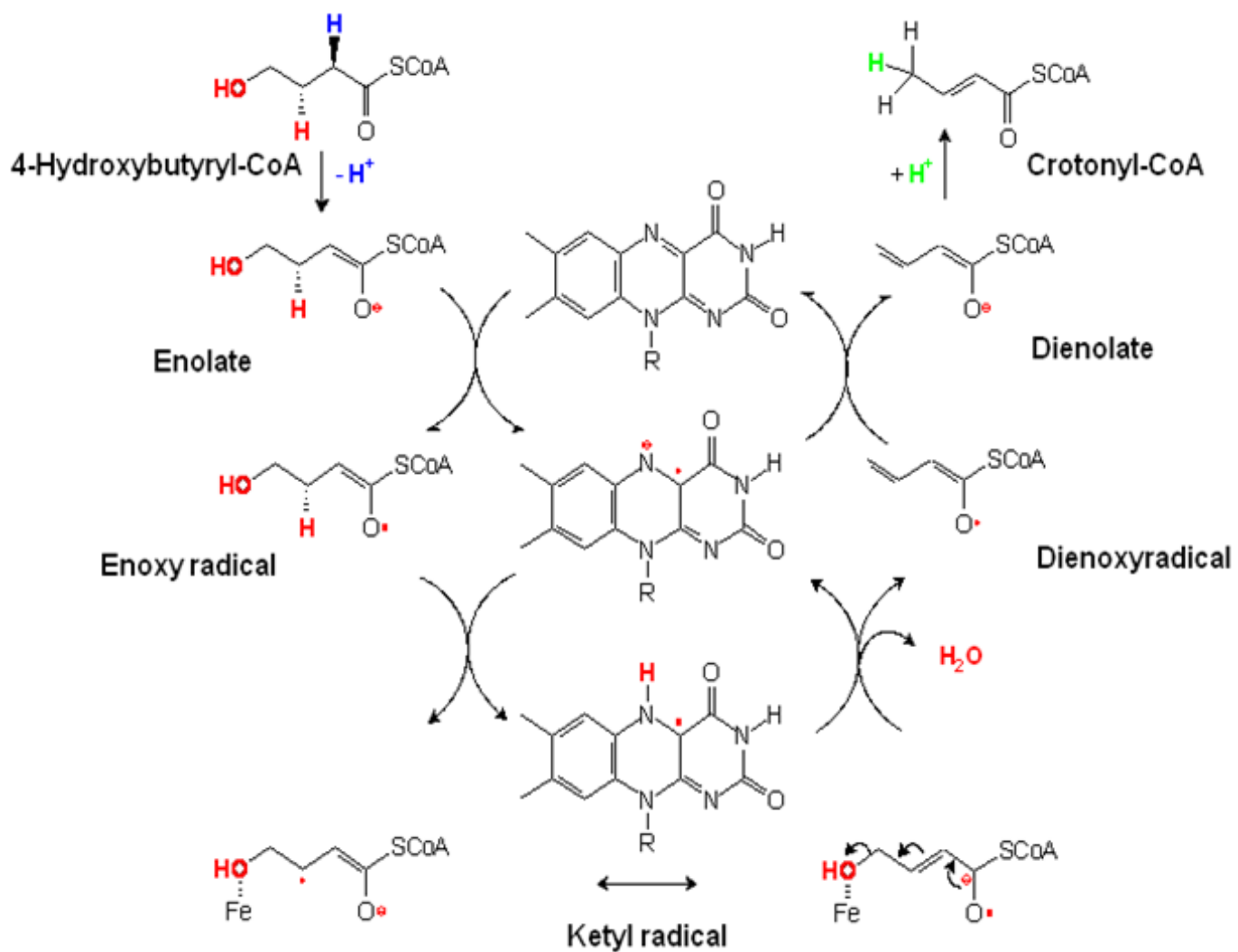


Figure 1-7. Proposed radical-intermediated mechanism of 4-hydroxybutyryl-CoA dehydratase.

## 1.8 Cofactors in 4-hydroxybutyryl-CoA dehydratase

### Iron sulfur cluster

Iron sulfur clusters have been found in a variety of metalloproteins, such as nitrogenase, hydrogenase, aconitase and so on, which contain sulfide-linked di-, tri- and tetrairon in variable oxidation states [61-63]. The simplest example of the iron sulfur protein is rubredoxin (Fig. 1-8). It has been detected in various sulfur anaerobic bacteria, where it serves as an electron transfer protein during oxygen detoxification by reduction. Ferredoxin is a classical iron sulfur protein, which has an electron transfer function and contains the iron sulfur cluster in the protein centre. The [2Fe-2S] cluster is built by two irons bridged by two sulfide ions and coordinated by either four cysteine, or two cysteine and two histidine residues of protein. The oxidized form contains two  $\text{Fe}^{3+}$  iron atoms, whereas the reduced form contains one  $\text{Fe}^{3+}$  atom and  $\text{Fe}^{2+}$  atom.

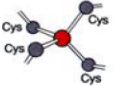
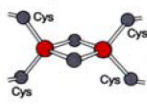
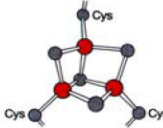
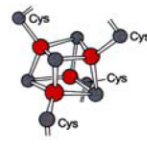
Protein	Cluster		Oxidations- zustand	formale Wertig- keit	EPR g-Werte (Temp.)	Mößbauer- Isomeriever- schiebung [mm s <sup>-1</sup> ]	$\lambda_{\text{max}}$ [nm], Extinktionskoeffizient ( $\times 10^{-3}$ , pro Fe)
Rubredoxin	1Fe-OS		oxidiert	$\text{Fe}^{3+}$	4.3, 9 ( $< 20$ K)	0.25	390(10.8), 490(8.8)
			reduziert	$\text{Fe}^{2+}$	keine	0.65	310(10.8), 335(6.3)
2Fe-Ferredoxin	2Fe-2S		oxidiert	$2\text{Fe}^{3+}$	keine	0.26	325(6.4), 420(4.8), 465(4.9)
			reduziert	$1\text{Fe}^{3+}$ , $1\text{Fe}^{2+}$	1.89, 1.95, 2.05 ( $< 100$ K)	0.25, 0.55	Absorption geht bei der Reduktion um 50 % zurück
3Fe-Ferredoxin	2Fe-4S		oxidiert	$3\text{Fe}^{3+}$	1.97, 2.00, 2.02 ( $< 20$ K)	0.27	305(7.7), 415(5.2), 455(4.4)
			reduziert	$2\text{Fe}^{3+}$ , $1\text{Fe}^{2+}$	keine	0.30, 0.46	425(3.2)
4Fe-Ferredoxin	4Fe-4S		oxidiert	$3\text{Fe}^{3+}$ , $1\text{Fe}^{2+}$	2.04, 2.04, 2.12 ( $< 100$ K)	0.31	325(8.1), 385(5.0), 450(4.6)
			Zwischen- form	$2\text{Fe}^{3+}$ , $2\text{Fe}^{2+}$	keine	0.42	305(4.9), 390(3.8)
			reduziert	$1\text{Fe}^{3+}$ , $3\text{Fe}^{2+}$	1.88, 1.92, 2.06 ( $< 20$ K)	0.57	uncharakteristisch; Absorp- tion bricht bei der Reduktion zusammen

Figure 1-8. Iron sulfur clusters and their spectroscopical characterizations.

[3Fe-4S] clusters have been also detected in proteins, in which each of three sulfide ions bridge two iron ions, while the fourth sulfide bridges three iron ions. It could act as an inactive intermediate stage of a [4Fe-4S] cluster, e.g., the inactive form of aconitase possesses a [4Fe-3S] cluster and activated by addition of an  $\text{Fe}^{2+}$  atom.

The most common iron sulfur cluster type in protein is the [4Fe-4S]-center, which is called “bacterial ferredoxin”. The iron centre is coordinated typically by cysteine ligands. The [4Fe-4S] containing protein can be subdivided into low potential (bacterial type) and high potential iron sulfur protein (HIPIPs), which are related by the following electron transfer process (Fig. 1-9). HIPIP has a redox potential of ca. to + 500 mV; this speciality allows electron transfer in photosynthesis and aerobic bacterial metabolism.

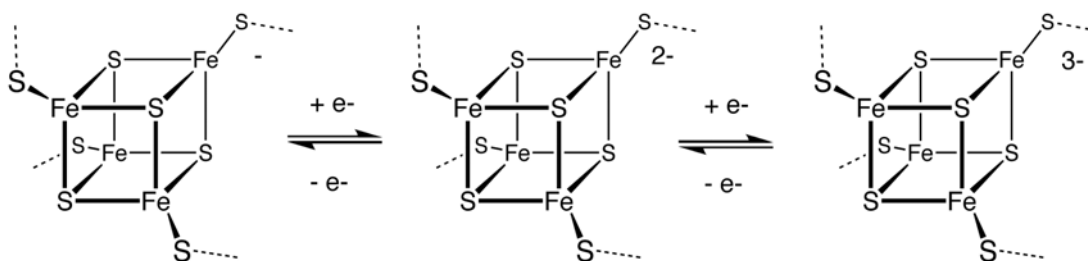


Figure 1-9. Redox states of [4Fe-4S] proteins

4-Hydroxybutyryl-CoA dehydratase contains a total of four  $[\text{4Fe-4S}]^{2+}$  clusters in the whole enzyme, with one in each subunit. This has been confirmed by UV-vis, EPR- and Mössbauer-spectroscopic experiments [45, 52, 64]. Three iron ions are coordinated by C99, C103 and C299, while the fourth iron is coordinated by H292 (Fig.1-6, b). The low redox potential of the  $[\text{4Fe-4S}]^{2+}$  cluster assures that the transient one electron oxidation of the substrate results only in the reduction of FAD. Interestingly, after addition of crotonyl-CoA as substrate the redox potential is increased by ca. 200 mV, which indicates a direct interaction of the substrate with the iron sulfur cluster. The best studied example of substrate interaction is aconitase, which catalyzes the isomerization of citrate to isocitrate without any redox change. Aconitase contains a cubane-type  $[\text{4Fe-4S}]^{2+}$  cluster in its active site with three iron atoms bound to three cysteines and four inorganic sulfur atoms and a fourth labile

iron atom, which is not bound to a protein cysteine, but to a hydroxyl group of the substrate or water [65-67].

Under air the native 4-hydroxybutyryl-CoA dehydratase is irreversibly inactivated, while vinylacetyl-CoA isomerase activity of the protein is decreased slowly and 40% of activity remains [32, 44]. We assumed that the inactivation of dehydratase by oxygen is based on destroying or degradation of the  $[4\text{Fe-4S}]^{2+}$  cluster to  $[3\text{Fe-4S}]$  or  $[2\text{Fe-2S}]$  clusters. But the mechanism is unknown yet.

### Flavin in proteins

Flavoproteins include a group of enzymes containing protein bound flavin, such as flavin adenine dinucleotide (FAD) or flavin mononucleotide (FMN, riboflavin-5'-phosphat) [68, 69]. From the isolation of the “old yellow enzyme”, as the first flavoprotein, up to now more than hundred flavoproteins have been detected, which are widely involved in biological processes, including bioluminescence, respiration and many dehydrogenases. Flavoproteins are able to accept either one by one electron in a two-step process or two electrons simultaneously.

The redox active centre of flavin coenzyme is the isoalloxazine ring system that is found in three redox states [53]. The fully oxidized quinone form of FAD and FMN can be reduced with one electron to the blue semiquinone anion and protonated to the neutral semiquinone. Further addition of one electron leads to the colorless hydroquinone anion. During the catalytic reaction of the 4-hydroxybutyryl-CoA dehydratase, the enolate reduces the quinone to the semiquinone radical, which deprotonates the resulting enoxy radical at the  $\beta$ -position and the neutral semiquinone is formed [70, 71]. Upon addition of substrate, 4-hydroxybutyryl-CoA dehydratase exhibits an absorbance decrease of the peak at 438 nm and an increase around 550 nm, which is due to formation of the neutral flavin semiquinone.

Furthermore, the formation of the neutral flavin semiquinone radical can be identified by its EPR spectrum at 77 K. At a temperature lower than 40 K more radical signals can be

observed, probably due to the reduction of the cluster to  $[4\text{Fe-4S}]^+$  and a substrate based radical [44, 53, 72].

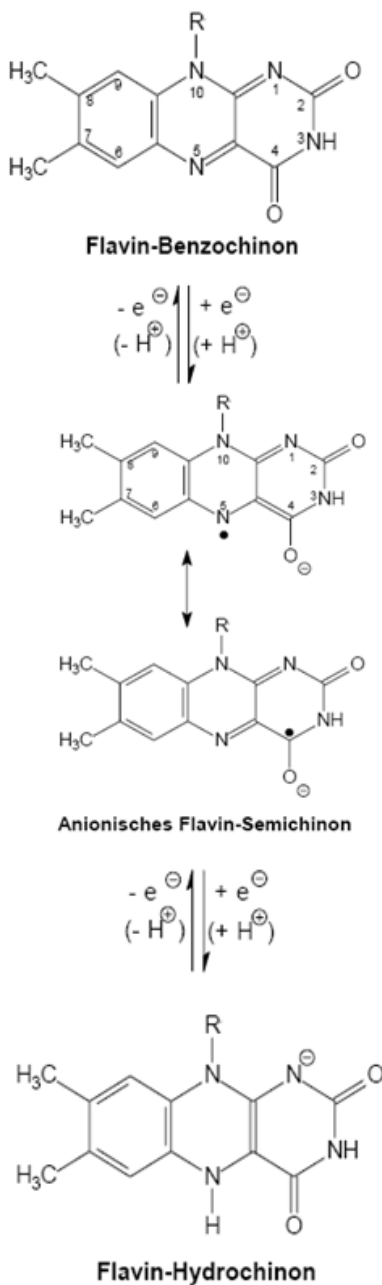


Figure 1-10. Structure and redox states of flavin isoalloxazine ring system



## 1.9 4-Hydroxybutyryl-CoA dehydratase in the 5<sup>th</sup> CO<sub>2</sub>-fixation pathway

In addition to the Calvin cycle, the reductive citric acid cycle, the 3-hydroxypropionate bicycle and the reductive acetyl-CoA pathway, a fifth pathway has been discovered for CO<sub>2</sub>-fixation in archaea, called 3-hydroxypropionate/4-hydroxybutyrate cycle (Fig. 1-11) [73, 74]. In this cycle and in the 3-hydroxypropionate cycle, CO<sub>2</sub> is fixed by acetyl-CoA and biotin-dependent acetyl-CoA carboxylase to form malonyl-CoA, which is reduced via malonate semialdehyde to 3-hydroxypropionate followed by further reduction to propionyl-CoA. Then propionyl-CoA is carboxylated to methylmalonyl-CoA, and rearranged to succinyl-CoA by coenzyme B<sub>12</sub>-dependent methylmalonyl-CoA mutase. In the bacterium *Chloroflexus aurantiacus* succinyl-CoA is converted to malyl-CoA, which is cleaved by a lyase to glyoxylate and acetyl-CoA. Again, the latter acts as the CO<sub>2</sub> acceptor molecule, whereas glyoxylate together with a second molecule of propionyl-CoA is converted to a second acetyl-CoA and to pyruvate, the final product of the 3-hydroxypropionate bicycle. Recently it has been discovered that in some archaea, such as *Sulfolobus* and *Metallosphaera*, succinyl-CoA is not converted to malyl-CoA, but instead via succinate semialdehyde and 4-hydroxybutyrate to 4-hydroxybutyryl-CoA, which is dehydrated to crotonyl-CoA by 4-hydroxybutyryl-CoA dehydratase. Crotonyl-CoA is then hydrated to 3-hydroxybutyryl-CoA and oxidized to acetoacetyl-CoA, which is cleaved to two acetyl-CoA.

4-Hydroxybutyryl-CoA dehydratase was originally considered to be restricted to the fermentative metabolism of strict anaerobic bacteria, but recently it was found to play an important role in autotrophic CO<sub>2</sub>-fixation of the aerobes *Metallosphaera sedula* and some other *Crenarchaeota*. Interestingly there are two different copies of 4-hydroxybutyryl-CoA dehydratase genes found in *M. sedula*, of which one is likely to code for the dehydratase with the iron sulfur cluster and other for a protein without the cluster, but H292 is conserved.

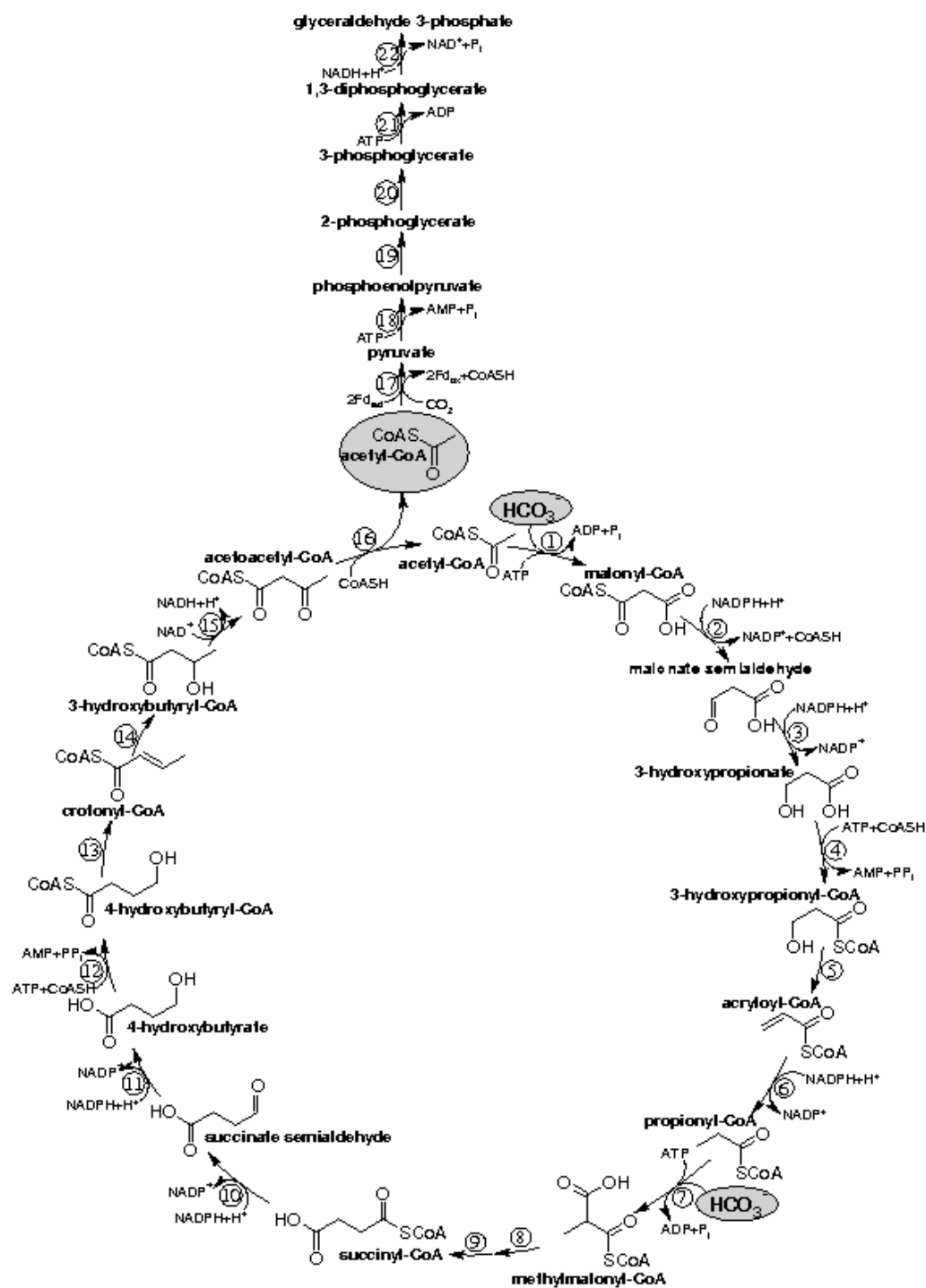


Figure 1-11. The 3-hydroxypropionate/4-hydroxybutyrate cycle

### 1.10 Goals of this work

Previous research has shown the properties of native 4-hydroxybutyryl-CoA dehydratase from *C. aminobutyricum*. However, several points in the proposed mechanism were not clarified yet. One of major problem is the role of the iron-sulfur clusters in the dehydration of 4-hydroxybutyryl-CoA to crotonyl-CoA and in the isomerization of vinylacetyl-CoA to crotonyl-CoA. Another point, the functions of the conserved residues in the active centre during the catalytic reaction was also of particular interest. Therefore, this work aimed to produce the recombinant enzyme and to increase our knowledge about catalytic reaction in detail by mutagenesis technique.

As another target, the native 4-hydroxybutyrate CoA-transferase from *C. aminobutyricum* has already been purified some time ago, but its mechanism retained still unknown. Therefore, the second purpose of this work was to obtain the recombinant CoA-transferase, which was applied for further characterization and enzyme classification. Additionally, the crystal structure of this CoA-transferase was solved and provided clear information for the reaction mechanism.

## **2. Materials and Methods**

### **2.1 Materials**

#### **2.1.1 Chemicals and reagents**

All chemicals were purchased from Sigma-Aldrich (Deisenhofen, Germany), Lancaster (Mühlheim, Germany), Fluka (Buchs, Germany) or Merck (Darmstadt, Germany) and were of the highest quality available.

The enzymes used for the molecular biology experiments were from Roche (Mannheim, Germany), MBI Fermentas GmbH (St. Leon-Rot, Germany) or Amersham (Freiburg, Germany)

#### **2.1.2 Instrument, gases and columns**

FPLC system and UV/Vis photometer (Ultrascopec 400) were from Amersham Biosciences (Freiburg, Germany). StrepTactin MacroPrep column and gravity flow StrepTactin sepharose columns were from IBA GmbH (Göttingen, Germany). N<sub>2</sub> (99.996%) and N<sub>2</sub>/H<sub>2</sub> were purchased from Messer-Griesheim (Düsseldorf, Germany).

Anoxic experiments were done in a glove box (Coy Laboratories, Ann Arbor MI, USA) providing an atmosphere of N<sub>2</sub>/H<sub>2</sub> (95%/5%). Buffers for enzyme purification were prepared by boiling and cooling under vacuum. Afterwards the buffers were flushed with nitrogen and transferred to anaerobic chamber, where 2 mM dithiothreitol was added and stirred overnight.

### 2.1.3 Bacterial strain and culture

*Clostridium aminobutyricum* (DSM 2634) was cultivated under anaerobic conditions in 100 ml serum bottles, which was used to inoculate a 10 L overnight pre-culture for the 100 L fermenter culture of the organism [26, 75].

The 1 L culture medium had the following composition,

Potassium phosphate pH 7.4	50 mM
NaHCO <sub>3</sub>	24 mM
Yeast extract	3 mg/ml
4-Aminobutyrate	97 mM
MgCl <sub>2</sub> × 6 H <sub>2</sub> O	0.20 g
FeCl <sub>3</sub> × 6 H <sub>2</sub> O	0.01 g
CaCl <sub>2</sub> × 2 H <sub>2</sub> O	0.01 g
MnSO <sub>4</sub> × H <sub>2</sub> O	1 mg
Na <sub>2</sub> MoO <sub>4</sub> × 2 H <sub>2</sub> O	1 mg
Cysteine HCl × H <sub>2</sub> O	0.50 g
Na <sub>2</sub> S <sub>2</sub> O <sub>4</sub>	0.35 g
Resazurine (Na-Salt) 0.2%	400 µl

The medium was boiled until the blue-red color of resazurine disappeared, and the air above medium was replaced by nitrogen gas.

*Escherichia coli* DH5α (F<sup>-</sup> λ<sup>-</sup> supE44 Δ(argF-lac) U169 ϕ80 ΔlacZΔM15 hsdR17 recA1 endA1 gyrA96 thi-1 relA1) (Stratagene, Heidelberg) was grown at 37 °C in LB-medium and used for gene cloning.

*Escherichia coli* BL21 CodonPlus(DE3)-RIL (B<sup>-</sup> F<sup>-</sup> *ompT* *hsdS*(r<sub>B</sub><sup>-</sup> m<sub>B</sub><sup>-</sup>) *dcm*<sup>+</sup> *Tet*<sup>r</sup> *gal* λ(DE3) *endA* Hte [*argU* *ileY* *leuW* Cam<sup>r</sup>] (Stratagene, Heidelberg) was grown at 37 °C in standard-I medium (Merck, 1.5% Pepton, 0.3% yeast extract, 100 mM NaCl and 6 mM D-Glucose) supplemented with required antibiotics, that depends on the harboured plasmid.

*Escherichia coli* BL21 CodonPlus(DE3)-GroEL contains a chaperon-plasmid, which is able to improve the gene expression. *E. coli* as a expression-system has frequently troubles to produce proteins, e.g, Inclusion-body, degradation and insolubility of proteins [76].

#### 2.1.4 Plasmids

Table 2.1 Plasmids.

Plasmid	Characteristic	Company
pASK-IBA3(+)	Amp <sup>R</sup> , P <sub>tet</sub> , <i>tet</i> <sub>R</sub> , C-terminal <i>Strep</i> -tagII	IBA, Göttingen
pASK-IBA7	Amp <sup>R</sup> , P <sub>tet</sub> , <i>tet</i> <sub>R</sub> N-terminal <i>Strep</i> -tagII	IBA, Göttingen
pACYC-Duet	Chlor <sup>R</sup> , P <sub>T7</sub> , <i>His</i> -tag, <i>S</i> -tag	Novagen, Munich

#### 2.1.5 Oligonucleotides

All the primers were synthesized by MWG Biotech (Ebersberg, Germany).

Table 2.2 Cloning primers.

Name	Nucleotide sequence ( 5' - 3' )
4HBdh-BsalIfor	ATGGTAGGTCTCAAATGTTAATGACAGCAGAACAGTACATTG
4HBdh-BsalIrev	ATGGTAGGTCTCAGCGCTTTTAATTCCAGCGATTGCCTTAGC
abfT-IBAfor	ATGGTAGGTCTCAAATGATGGATTGGAAGAAGATCTATGAAG
abfT-IBArev	ATGGTAGGTCTCAGCGCTGAATGCCGCGTTGAATCTCTTTTC
abfDMsedu1F	ATGGTACCGCGGATGGTCGTCAGAACAGGGGAGCAATATCTC
abfDMsedu1R	ATGGTAAGCGCTACTCTTGAGACCGGCCTCCTTAGCCTCTGC
DuetMS_2SacI	ATGGTAGAGCTCATGAGAAGCAAGGAGGAATTCGTG
DuetMS_2KpnI	ATGGTAGGTACCACGGTTTAGAAGGGATTTCACCAG

Table 2.3 Mutagenic primers used in 4-hydroxybutyryl-CoA dehydratase mutagenesis.

Name	Forward Primers for site directed mutagenesis
H292C	GAAAGATTTGCTGGATACTGCAGACAGTCATACGGCG
H292E	GAAAGATTTGCTGGATACGAAAGACAGTCATACGGCGG
C99A	GACAGAAGACCGCATCAGCATTCCAGAGATGTGTAG
C103A	CGCATCATGCTTCCAGAGAGCGGTAGGTATGGACGCTTTC
C299A	CAGTCATACGGCGGAGCGAAGGTTGGAGTAGG
Y296F	GATACCACAGACAGTCATTTGGCGGATGTAAGGTTGG

E257Q	CAGTTCGGCGGACAGCAGGCTTTAGTCGTATTCCG
E455Q	CTGTAGGTTACAGAACTCAGTCCATGCATGGTGCAG
R90N	GAAAAAAGGTTAAGATGCAGAACCTTCTTGGACAGAAGACCGC
Q101E	GAAGACCGCATCATGCTTCGAAAGATGTGTAGGTATGGAC
T190V	GCTAAGGCTCACCAGGTGGGTTCCATCAACTCC
K300Q	CATACGGCGGATGTCAGGTTGGAGTAGG
A460G	GAACTGAATCCATGCATGGTGGCGGTTCCCCTCAGGCTCAGAG

Table 2-4 Mutagenic primers used in 4-hydroxybutyrate CoA-transferase mutagenesis.

Name	Forward Primers for site directed mutagenesis
E238D	GGTATCCACTCTGACATGATTTCCGACGG
E238Q	CTTGGTATCCACTCTCAAATGATTTCCGACG
E238S	CCTTGGTATCCACTCTTCAATGATTTCCGACGGTG
E238A	CTTGGTATCCACTCTGCAATGATTTCCGACGG
H31S	GAGTGCTATTTGCGAGCTGTGTTGCTGAACC
H31G	GAGTGCTATTTGCGGGCTGTGTTGCTGAACC
H31A	GAGTGCTATTTGCGGCCTGTGTTGCTGAACC
H31N	GAGTGCTATTTGCGAACTGTGTTGCTGAAC
M58T	GTAACGGTTTTCACACACGGTTACCCTTGGAAAG



M58S	GTAACGGTTTCACACAGCGTTACCCTTGGAAAGG
Q213S	GAAGATGGTTCCACATTAAGCCTTGGTATCGGAGCTATTC
Q213T	GAAGATGGTTCCACATTAACCCTTGGTATCGGAGCTATTC

### 2.1.6 Media

All the media were autoclaved at 121 °C and 1 bar for 20 min.

LB medium

Trypton 10.0 g/L

Yeast extract 5.0 g/L

NaCl 5.0 g/L

Standard-I medium

Standard-I 20.0 g/L

### 2.1.7 Antibiotics

All of antibiotics was prepared and sterilized by filtration (0.2 µm).

Table 2-5. The stock solution of antibiotics.

Antibiotics	Stock	Final concentration in media
Carbenicillin	100 mg/ml H <sub>2</sub> O	50 µg/ml
Chloramphenicol	100 mg/ml 99% ethanol	50 µg/ml

### 2.1.8 Molecular biology kits

Table 2-6. Molecular biology kits

Kits	Company
Easystart PCR kit	MßP (UK)
QIAquick PCR Purification kit	Qiagen (Hiden, Germany)
QIAquick Gel Extraction kit	Qiagen (Hiden, Germany)
QIAquick Spin Miniprep kit	Qiagen (Hiden, Germany)
T4 DNA ligase	Amersham Pharmacia Biotech (Freiburg, Germany)
peqGOLD Gel Extraction kit	PEQLAQ Biotech GmbH (Erlangen, Germany)
GeneJET™ Plasmid Miniprep kit	Fermentas GmbH (St. Leon-Rot, Germany)
TOPO Walker kit	Invitrogen (Karlsruhe, Germany)
PfuUltra™ Hotstart DAN Polymerase	Stratagene
Phusion High-Fidelity DNA Polymerase kit	Finnzym

## 2.2 Molecular Biological Methods

### 2.2.1 Isolation of genomic DNA from *C. aminobutyricum*

The genomic DNA of *C. aminobutyricum* and *Metallosphaera sedula* were prepared from aerobically harvested cells.

Solutions:

Tris-sucrose-buffer	50 mM Tris/HCl pH 8.0, 25% sucrose
Tris-EDTA-buffer	50 mM Tris, 25 mM EDTA, pH 8.0
Tris-EDTA-SDS-buffer	50 mM Tris, 25 mM EDTA, pH 8.0, 1% SDS
TE-buffer	10 mM Tris/HCl pH 8.0, 1 mM EDTA

Cells (1 g) were suspended in 3 ml Tris-sucrose-buffer, which were incubated at 37 °C for 90 min with gentle shaking after adding 50 mg lysozyme. 2 ml Tris-EDTA-buffer was then added and the mixture was incubated on ice for further 15 min. After adding 5 ml 1% Tris-EDTA-SDS-buffer, 100 µg RNase und 10 mg Proteinase-K (52 units/mg, Roche), the solution was incubated at 37 °C for 3 hours. For phenol extraction, 10 ml phenol/chloroform (1:1) was added in the mixture and shaken gently. The aqueous and organic phase were separated by centrifugation at  $5,000 \times g$  for 20 min, this step was repeated twice. The aqueous phase containing the nucleic acid was transferred to a new falcon tube, which was mixed with the equal volume of chloroform/isoamylalcohol (24:1) and the protein was removed by centrifugation at  $5,000 \times g$ . The aqueous phase was subsequently dialyzed overnight in 5 L TE-buffer (10 mM Tris/HCl, 1 mM EDTA, pH 8.0) at 4 °C.

The genomic DNA was stored at 4 °C

### 2.2.2 Isolation of plasmid DNA

Plasmid DNA was isolated using QIAprep Spin Miniprep (Qiagen) oder GeneJET™ Plasmid Miniprep Kit (Fermentas).

LB medium (5 ml) with the required antibiotics was inoculated with a bacterial colony and incubated at 37 °C for overnight. The culture was transferred into an Eppendorf tube and harvested at  $13,000 \times g$  for 5 min. The pellet was resuspended in 250 µl resuspend buffer. After 2-3 times gentle shaking the solution was added with 250 µl lysis buffer and 350 µl neutralization buffer. Precipitates were removed by centrifugation and the DNA was then washed twice with wash-buffer, which was dried and redissolved in 50 µl elution buffer.

### 2.2.3 Determination of DNA concentration and purity

In order to calculate DNA concentration and purity the purified plasmid DNA was measured at the absorption of 260nm using an absorbance of 1.0 for 50 µg/ml of double-stranded DNA.

$$\text{DNA concentration (}\mu\text{g/ml)} = \Delta E_{260} \times 50 \times \text{dilution}$$

Measuring the absorbance of DNA solution at 260 nm and 280 nm was used for DNA purity. A pure sample of DNA has the 260/280 ratio at 1.8 and is relative free from protein contamination.

### 2.2.4 Agarose gel electrophoresis

#### 50 × TAE buffer

40 mM Tris	242 g
20 mM Glacial acetic acid	57.1 ml

0.5 mM EDTA pH 8.0                      100 ml 0.5 M

Fill to 1 L with H<sub>2</sub>O

### DNA loading buffer

Bromphenol blue                      0.25% (w/v)

Xylene cyanol FF                      0.25% (w/v)

Orange G                                0.25% (w/v)

Sucrose                                  40% (w/v)

Agarose powder (0.8 g) was suspended in 100 ml 1 × TAE buffer, boiled in a microwave oven until it is completely melted and the solution becomes clear. Before pouring, the solution was cooled down to about 60 °C. The agarose gel containing a sample comb was solidified at room temperature. After that the comb was removed and the gel was placed in the electrophoresis chamber, which is covered by TAE buffer. The DNA sample was mixed with the loading buffer und pipetted into the sample wells. The gel was run upon 80 volts in the beginning to allow DNA to move into the gel, and then speed up later. When the bromophenol blue has run 3/4 the length of gel, DNA fragments were stained by ethidium bromide and place on an ultraviolet transilluminator [77].

### **2.2.5 DNA extraction from agarose gel**

DNA bands of the desired size were exposed on an UV-illuminator and cuted out from gels. The extraction of DNA was performed using the QIAquick gel extraction kit or peqGOLD Gel Extraction kit following the manufactures instructions.

### **2.2.6 DNA restriction and ligation**

Restriction reaction was performed at 5 - to 20 - fold over digestion using desired restriction

enzyme and corresponding buffer. The digested fragments were analyzed with agarose gel.

To ligate the double strand DNA, T4 ligase was added in mixture of digested insert and vector, which was incubated at 22 °C for 1 - 2 hours or overnight at 16 °C. Then T4 ligase in the mixture was inactivated by heating at 65 °C for 10 min. After 30 min dialysis using Millipore-Membrane against water, the ligation mixture was transformed into host cells.

### **2.2.7 Preparation of competent *E. coli* cells for electrotransformation**

LB medium 5 ml was inoculated by a fresh *E. coli* single colony and incubated overnight at 37 °C, which was used to grow the 500 ml main culture. During the exponential phase ( $OD_{578} = 0.5 - 0.8$ ) the cells were placed on ice for 30 min, then harvested by centrifugation at  $6,000 \times g$  for 20 min in a SLA-3000 rotor at 4 °C. The pellets were washed twice with 500 ml and 250 ml ice-cold sterilized H<sub>2</sub>O, then washed once again with 10% ice-cold glycerol and centrifuged at  $5,000 \times g$  for 10 min at 4 °C. The final pellets were resuspended in 1 ml sterilized ice-cold 10% glycerol and 40 µl aliquots in thin wall 500 µl tubes, which were stored at - 80 °C.

### **2.2.8 Electrotransformation**

The plasmid was added to 40 µl competent cells on ice and transferred to a GenePulser cuvette (Bio-Rad). The GenePulser was set to 25 µF, 1.8 kV and 200 Ohm. After that the cuvette was washed using 500 µl LB medium, which is transferred to a sterile Eppendorf tube. The transformation mixture was incubated at 37 °C for 1 hour before plating on a LB agar plate containing antibiotics. The plate was incubated overnight at 37 °C [78].

### **2.2.9 PCR reaction**

The PCR reaction was performed with a thermostable DNA polymerase and desired primers.

Primers should not be self-complementary and the GC content should be kept between 40 – 60 %. In contrast to Taq-polymerase, Phusion-polymerase has lower error rate and higher fidelity [79].

The 50 µl reaction was mixed with

	Final concentration/volume
Forward primer	200 nM
Reverse primer	200 nM
dNTP	200 µM
5 × HF buffer	10 µl
Template DNA	1 ng – 1 µg
(Higher concentration for total genomic DNA; lower for plasmid)	
DNA polymerase	0.5 – 1 unit
(HF buffer: prepared PCR buffer in Phusion® High-Fidelity DNA Polymerase Kit)	

Temperature cycling of Phusion DNA polymerase

Initial denaturation	98 °C	3 min	
Denaturation	98 °C	30 s	} × 30
Annealing	45 – 65 °C	30 s	
Extension	72 °C	1 kb/30 s	
Final extension	72 °C	10 min	

#### Temperature cycling of Taq DNA polymerase

Initial denaturation	95 °C	5 min	
Denaturation	95 °C	1 min	} × 30
Annealing	45 – 65 °C	1 min	
Extension	72 °C	1 kb / 1 min	
Final extension	72 °C	10 min	

#### 2.2.10 Cloning of the genes

Before cloning into pASK-IBA3(+) or pASK-IBA7 vector, the DNA fragments of *abfD* and *abfT* were amplified with the designed primer, which contains a restriction cut site of *BsaI*. The amplified DNA and vector were digested by *BsaI* and purified by gel extraction and gel extraction kit. Before transformation into *E. coli* DH 5 $\alpha$  cells, the digested DNA and vector was ligated together by T4 ligase and dialysed for at least 30 min.

#### 2.2.11 Sequencing of the cloned genes

DNA cloned in pASK-IBA vector was sequenced with the standard IBA sequencing primers. This was performed by MWG Biotech.

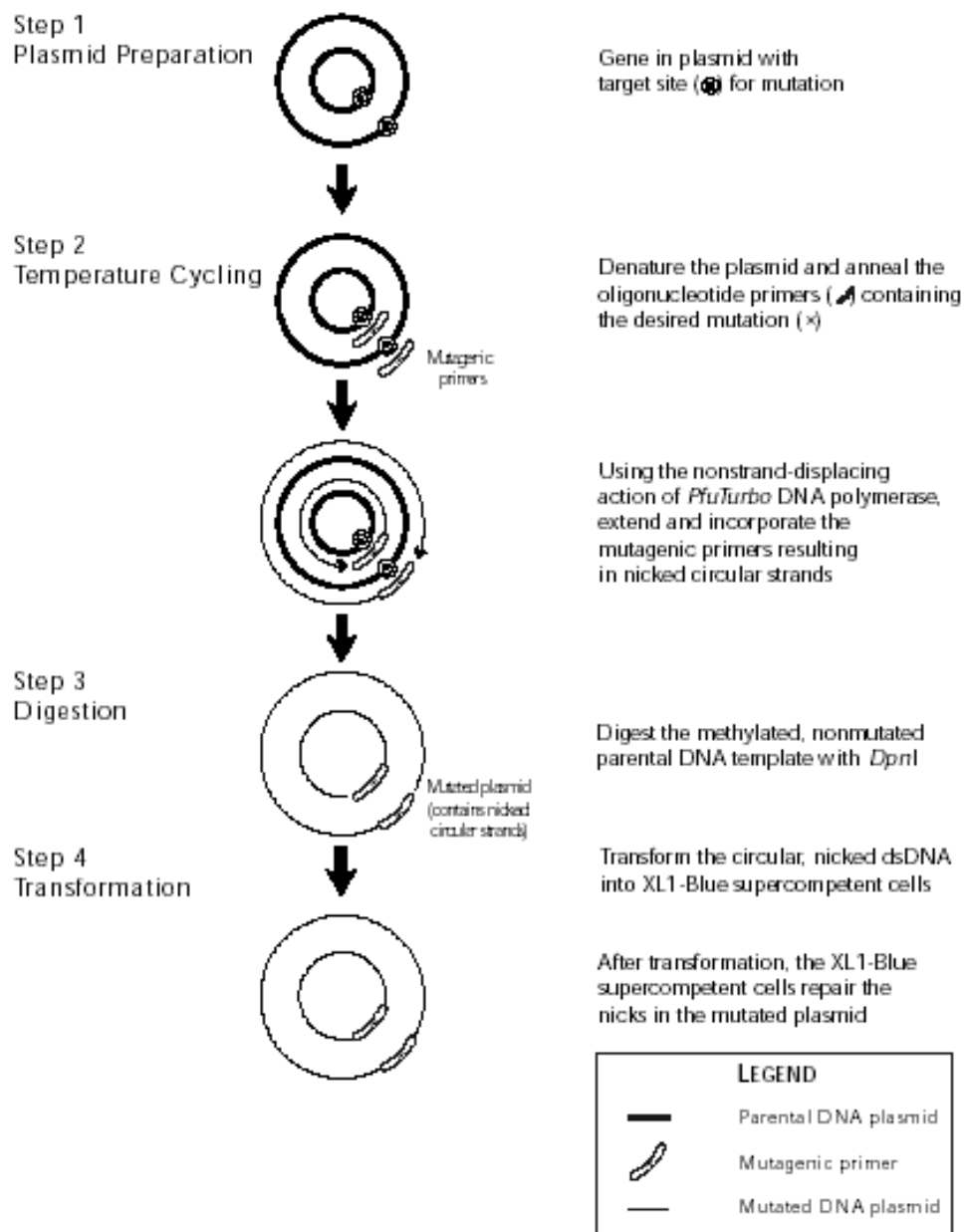
#### 2.2.12 Site directed mutagenesis

To facilitate site directed mutagenesis, two complementary primers were designed for PCR, which contains the mutated sequence flanked by 20 bases on each side. About 20 PCR cycles were performed on a relatively large amount of plasmid template to minimize the chance of expanding PCR sequence errors. For desalting, the PCR product was dialysed through a Millipore dialysis paper for 30 min, after that is was digested with *DpnI* for 1 hour at 37 °C.



Before transformation into *E. coli* DH5 $\alpha$  cells product was dialysed again. The *abfD* containing plasmids obtained from colonies were sequenced and used to transfer into the expression system – *E. coli* BL21 CodonPlus (DE3)-GroEL strain.

*DpnI* only cuts dam methylated DNA. The parental plasmid DNA will be cut to pieces while the nascent PCR DNA is left intact. All routine *E.coli* strains have an intact dam methylase system [80].



## 2.3 Biochemical methods

### 2.3.1 Gene expression in *E. coli* and protein purification

#### 2.3.1.1 Recombinant 4-hydroxybutyryl-CoA dehydratase

*E. coli* strain BL21 CodonPlus (DE3)-GroEL containing extra copies of rare *E. coli* *argU*, *ileY*, *leuU* and *proL* tRNA genes [81, 82], is able to improve the gene expression. pASK-IBA3(+) plasmid carrying *abfD* was transformed into this strain, which was grown aerobically in standard-I medium supplemented with 2 mM iron citrate, 0.27 mM riboflavin and containing carbenicillin 50 µg/ml, chloramphenicol 50 µg/ml at room temperature (20 °C – 25 °C). At an OD<sub>578</sub> of 0.5 – 0.6 the culture was induced with AHT (100 µg/l) and incubated for overnight. The cells were harvested by centrifugation at 6,000 × *g*, and cell pellets were washed with anaerobic water in an anaerobic chamber under 95% N<sub>2</sub> and 5% H<sub>2</sub>.

Transformed *E. coli* cells were suspended in 50 mM potassium phosphate, pH 7.4, 2 mM DTT and 200 mM sodium chloride. The suspension was sonicated for 3 × 8 min (Branson Sonifier, 50% duty cycle), and centrifuged at 100,000 × *g* for 1 hour at 4 °C (Ultracentrifuge, Beckman Instruments, Munich). The filtrated supernatant fluids were applied directly to previously with wash buffer (100 mM Tris-HCl pH 8.0, 150 mM NaCl and 2 mM DTT) equilibrated StrepTactin column. The StrepTactin purification system is based on the highly effective interaction between the Streptag overhang of the recombinant protein and the StrepTactin of the column [83-85]. After loading of the supernatant and washing with 50 ml wash buffer, the protein was eluted with wash buffer containing 2.5 mM desthiobiotin. The purified 4-hydroxybutyryl-CoA dehydratase was concentrated with a 100 kDa centricon and stored at – 80 °C for several months, but it was observed that even at this temperature the dehydratase activity was slowly lost. All experiments were performed in an anaerobic chamber.

### 2.3.1.2 Recombinant 4-hydroxybutyrate CoA-transferase

The *abfT*-containing pASK-IBA3(+) vector was grown aerobically at 37 °C in standard-I medium with antibiotics. At an OD<sub>578</sub> of 0.5 – 0.6 the culture was cooled to room temperature and induced with AHT (200 µg/l) and incubated for 2 hours. AbfT was also purified using StrepTactin purification system.

### 2.3.1.3 Recombinant 4-hydroxybutyryl-CoA dehydratase MS\_1 and MS\_2 from *M. sedula*

Recombinant MS\_1 from *M. sedula* was purified anaerobically using a StrepTactin column. The harvested cells were washed by deoxygenated water and suspended in 50 mM potassium phosphate buffer containing 300 mM NaCl and 1 mg DNase. The suspended cells were then opened by sonication (3 × 5 min) and centrifuged at 100,000 × g for 60 min. The supernatant was heated at 75 °C for 20 min to select the thermophile protein and then centrifuged at 10,000 × g for 15 min. The clear supernatant was filtrated and loaded on the affinity StrepTactin column. After washing with 5 column volumes of wash buffer (100 mM Tris/HCl and 150 mM NaCl) the MS\_1 protein was eluted by adding 2.5 mM desthiobiotin.

To purify the recombinant MS\_2 using Ni-Sepharose column, the harvested cells was washed previously by deoxygenated water and suspended in 20 mM Tris/HCl, pH 7.5 binding buffer containing 0.5 M NaCl and 20 mM imidazole. The cells were then opened by sonication (3 × 5min) and centrifuged at 100,000 × g for 60 min. The supernatant was heated at 75 °C for 20 min to select the thermophile protein and then centrifuged at 10,000 × g for 15 min. The clear supernatant was filtrated and loaded on the Ni-Sepharose column. After washing with 5 column volumes of wash buffer (20 mM Tris/HCl, pH 7.5, 0.5 M NaCl and 60 mM imidazole) the MS\_2 protein was eluted by elution buffer containing 20 mM Tris/HCl, pH 7.5, 0.5 M NaCl and 500 mM imidazole.

## 2.3.2 Purification of other proteins

### 2.3.2.1 Purification of 4-hydroxybutyrate CoA-transferase from *C. aminobutyricum*

All steps of CoA-transferase purification were performed aerobically at 4 °C [42].

Frozen cells of *C. aminobutyricum* 30 g were suspended in 60 ml 50 mM potassium phosphate, pH 7.0, which contains 10 mM NaCl and 0.6 mg DNase I. The cells were lysed by AMICO French Cell Press (American Instrument Company – Division of Travenol Laboratorie, Inc., Maryland, USA) at 110 MPa and centrifuged at 100,000 ×g for 1 h. The supernatant was fractionated by adding of a saturated ammonium sulfate solution (55 – 80% saturation). The second precipitate was resuspended in 22 ml 50 mM potassium phosphate with 1.5 M ammonium sulfate and was transferred to a Phenyl-Sepharose column (Pharmacia, Freiburg, Germany), which was equilibrated with 50 mM potassium phosphate containing 1.5 M ammonium sulfate. The protein was eluted using a decreasing ammonium sulfate gradient (1.5 M – 0) in 360 ml of 50 mM potassium phosphate, pH 7.0 followed by 370 ml 50 mM potassium phosphate buffer without ammonium sulfate using a flow rate of 3 ml/min. The CoA-transferase activity containing fractions were combined and concentrated (Amicon-concentrator, 10 kDa pore size, Witten, Germany).

Then the protein solution was loaded on a DEAE-Sepharcel column. After washing with the same buffer, the protein was eluted by 360 ml of a linear gradient increasing potassium phosphate, pH 6.8 from 0 to 400 mM followed by 10 ml of 1 M potassium phosphate in same buffer at a flow rate 3 ml/min. The active fractions were loaded on a Superdex 200 Hiloal 26/60 column.

Until this step, the protein solution contains still phosphotransacetylase activity. In the presence of phosphate, it results in formation of acetylphosphate and release of CoASH, which interferes the enzyme assay. Therefore, after concentration to 1 ml, the protein was loaded on a Mono Q-column (GE Healthcare), which was prior equilibrated by H<sub>2</sub>O, then washed with low salt buffer (20 mM Tris/HCl, pH 7.0) and afterwards with high salt buffer (20 mM Tris/HCl, 1 M NaCl, pH 7.0), finally using low salt buffer again. This procedure improves protein separation and binding capacity. The protein was eluted by a 100 ml gradient of 0 – 300 mM NaCl. Most of transferase

activities were observed in the 42 – 48 ml fractions, and most of phosphotransacetylase activities between 46 – 50 ml. The fractions from 42 ml to 45 ml were concentrated and frozen at - 80 °C.

### 2.3.2.2 Purification of ‘enzyme pool’ from *Acidominococcus fermentas*

The following purification steps were achieved at 4 °C under aerobic conditions [54].

Frozen cells from *A. fermentas* 25 g were suspended in 20 mM potassium phosphate, pH 7.0 with 1 mM PMSF, 5 mM MgCl<sub>2</sub> and 1 mg DNase I. The solution was lysed by French Press at 110 MPa, which was then centrifuged at 100,000 × *g* for 60 min. The pellet was used to purify the glutaconyl-CoA decarboxylase. After two ammonium sulfate precipitations (50 % and 80 %) the solution was centrifuged at 10,000 × *g* for 30 min. The pellets were suspended in 20 mM potassium phosphate, pH 7.0 and dialyzed overnight in 5 L 20 mM potassium phosphate. To remove small particles, the protein solution was filtrated with a 0.45 µm filter. The filtrate was transferred with a flow rate 3 ml/min to a DEAE-Sepharose Fast-Flow column (3 × 10 cm). The column has been washed with 100 ml 20 mM potassium phosphate, pH 7.0 with 1 M NaCl, and equilibrated with 150 ml 20 mM potassium phosphate. After loading, the column was washed with 50 ml of the same buffer and the protein was eluted by a linear 500 ml NaCl-gradient from 0 to 1 M. The enzyme pool was concentrated and frozen at – 80 °C.

### 2.3.2.3 Purification of crotonyl-CoA carboxylase/reductase

The GenoStat<sup>TM</sup> pGS-2 expression plasmid containing the gene of crotonyl-CoA carboxylase/reductase from *Rhodobacter sphaeroides* (AG Fuchs, Freiburg, Germany) was transformed into *E. coli* BL21 (DE3) and a single colony was selected for the purification of the enzyme [86, 87]. The 2 L standard-I medium with carbenicillin (50 µg/ml) was inoculated with a transformed plasmid and grown at 37 °C. When the cells reached an OD<sub>578</sub> of approximately 0.5, the culture was induced by addition of IPTG to a final concentration of 0.5 mM and grown for further 4 hours. After 15 min centrifugation at 6,000 × *g*, the harvested cells were suspended in

50 mM potassium phosphate, pH 7.0 and 1 mg DNase I and lysed by sonication on ice, which was then centrifuged at 100,000 ×g for 60 min. The supernatant was loaded onto a Ni-Sepharose Fast Flow column that washed by 20 mM Tris/HCl, pH 7.8 and again by the same buffer with 75 mM imidazole, then equilibrated with 20 mM Tris/HCl and 50 mM KCl. The crotonyl-CoA carboxylase/reductase was eluted with 20 mM Tris/HCl, pH 7.8 containing 500 mM imidazole. The enzyme was concentrated and stored at – 80 °C [87].

### **2.3.3 Determination of protein concentration**

Protein concentration was determined by the Bradford method. The assay is based on the shift of the absorbance maximum for an acidic solution of Coomassie Brilliant Blue G-250 from 465 nm to 595 nm upon binding of protein. The 50 µl protein was mixed with 950 µl 1:5 diluted Coomassie Brilliant Blue G-250 reagent using 0 – 0.2 mg/ml bovine serum albumin (BSA) as standard. After 30 min incubation in the dark at room temperature, the absorbance was measured at 595 nm [88].

### **2.3.4 Sodium dodecylsulfate-polyacrylamide gel electrophoresis (SDS-PAGE)**

According to their electrophoretic mobility the protein could be separated by SDS PAGE [89]. The gel was prepared as in table 2-7.

Table 2-7. Protocols for SDS-PAGE gel preparation

	Separating gel 12.5% (μl)	Stacking gel 8% (μl)
H <sub>2</sub> O dest.	2080	2540
Tris/HCl, pH 8.8	4500	-----
Tris/HCl, pH 6.8	-----	470
Acryl/Bisacryl.30%	5000	950
10% SDS	120	40
5% TEMED	120	40
10% APS	180	80

APS: 10% ammonium persulfate (fresh)

#### Electrophoresis running buffer

Tris	0.3% (w/v)
Glycin	1.44% (w/v)
SDS	0.1% (w/v)

#### Protein loading buffer

Tris, pH 6.8	125 mM
Glycerol	4% (w/v)
β-Mercaptoethanol	10% (w/v)
Bromophenol blue	0.1% (w/v)
DTT	10 mM

Staining solution for Coomassie Blue staining

Coomassie R 250	1.2 g
Acetic acid	200 ml
Methanol	1 L
Fill to 2 L with H <sub>2</sub> O	

Destaining solution for Coomassie Blue staining

Ethanol	50 ml
Acetic acid	70 ml
Fill to 1 L with H <sub>2</sub> O	

Prior to electrophoresis, the protein sample was mixed with protein loading buffer and incubated at 95 °C for 5 min prior to load on the gel. The electrophoresis was performed at a constant voltage between 120 – 150 volts until the tracking dye reached the bottom of the gel. Afterwards the gel was stained with Coomassie Brilliant Blue in the microwave oven for 1 -2 min and destained slowly on a shaker.

### **2.3.5 Gel-filtration**

For molecular mass determination of native enzymes, the protein solution was loaded on a HiLoad 26/60 Superdex 200 column that was prior washed by H<sub>2</sub>O and 50 mM Tris/HCl, pH 7.4. The chromatography was achieved using 50 mM Tris/HCl pH 7.4 and 150 mM NaCl with a flow rate of 0.5 ml/min.

A calibration curve was prepared by measuring the elution volumes of four standard proteins (Amersham Biosciences, Germany), aldolase from rabbit muscle (158 kDa), catalase from human serum (232 kDa), ferritin from horse spleen (440 kDa) and thyroglobulin from bovine thyroid (669 kDa). A  $K_{av}$  value (elution volume of protein/molecular mass) was calculated from the



calibration curve with standard proteins.

### 2.3.6 Enzyme activity assays

#### 2.3.6.1 4-Hydroxybutyryl-CoA dehydratase

4-Hydroxybutyryl-CoA dehydratase was assayed anaerobically in a cuvette containing 100 mM potassium phosphate, pH 7.4, 2 mM EDTA, 2 mM DTE, 2 mM  $\text{NAD}^+$ , 1 mM sodium 4-hydroxybutyrate, 0.1 mM CoASH, 0.1 mM acetyl-phosphate, 1 mM acetyl-CoA, 1.2 U 4-hydroxybutyrate CoA-transferase and 'enzyme pool' from *Acidaminococcus fermentans* (0.3 mg/ml). After 3 min incubation at room temperature, the reaction was started by adding 4-hydroxybutyryl-CoA dehydratase and the formation of NADH was measured at 340 nm using an extinction coefficient  $6.3 \text{ mM}^{-1} \cdot \text{cm}^{-1}$  [75].

#### 2.3.6.2 Vinylacetyl-CoA $\Delta$ -isomerase

Vinylacetyl-CoA  $\Delta$ -isomerase was assayed using crotonyl-CoA reductase/carboxylase from *Rhodobacter sphaeroides* in a reaction mixture with 100 mM potassium phosphate, 0.2 mM DTT, 1 mM vinylactate, 2 mM NADPH, 0.5 mM acetyl-CoA, 30 mM  $\text{KHCO}_3$  and 1.2 U 4-hydroxybutyrate CoA-transferase, 0.5 U crotonyl-CoA reductase/carboxylase. After 2 min incubation at room temperature, the reaction was started by adding the 4-hydroxybutyryl-CoA dehydratase and the formation of  $\text{NADP}^+$  was measured at 340 nm using an extinction coefficient  $6.3 \text{ mM}^{-1} \cdot \text{cm}^{-1}$ .

Vinylacetyl-CoA  $\Delta$ -isomerase could also assayed aerobically with 100 mM potassium phosphate, pH 7.4, 0.5  $\mu\text{mol}$  vinylacetyl-CoA, which was synthesized from acetyl-CoA and vinylacetic acid using 1.2 U 4-hydroxybutyrate CoA-transferase. The reaction was initiated by adding the 4-hydroxybutyryl-CoA dehydratase, and its conversion to crotonyl-CoA was followed by

measuring the increasing a absorbance at 290 nm using an extinction coefficient value  $2.2 \text{ mM}^{-1} \text{ cm}^{-1}$ .

#### **2.3.6.3 4-Hydroxybutyrate CoA-transferase**

4-Hydroxybutyrate CoA-transferase was assayed with 40 mM sodium acetate and 0.25 mM butyryl-CoA as the substrates in a cuvette containing 100 mM potassium phosphate, 0.4 mg/ml DTNB, 1 mM oxalacetate and 4 U citrate synthase. In the assay the formed acetyl-CoA was condensed with oxalacetate, thereby liberating CoASH, which reacted with DTNB to a yellow thiophenolate anion. The reaction was started by adding CoA-transferase. The initial rate was measured at 410 nm using an extinction coefficient  $14.0 \text{ mM}^{-1} \text{ cm}^{-1}$ .

4-Hydroxybutyrate CoA-transferase was also assayed with butyryl-CoA as the CoA-donor and acrylate as CoA-acceptor in a cuvette containing 100 mM potassium phosphate, pH 7.4, butyryl-CoA and acrylate. The reaction was started by adding 0.15 U of 4-hydroxybutyrate CoA-transferase. The initial rate was measured at 280 nm using an extinction coefficient  $4.2 \text{ mM}^{-1} \text{ cm}^{-1}$ .

#### **2.3.6.4 Butyryl-CoA dehydrogenase**

Butyryl-CoA dehydrogenase was assayed spectrophotometrically in a cuvette containing 50 mM potassium phosphate, 0.3 mM ferrocenium hexafluorophosphate, 0.25 mM butyryl-CoA, 5  $\mu\text{M}$  FAD. The reduction of ferrocenium was measured by adding butyryl-CoA dehydrogenase at 300 nm using an extinction coefficient  $4.3 \text{ mM}^{-1} \text{ cm}^{-1}$ .

#### **2.3.6.5 Crotonyl-CoA reductase/carboxylase**

The crotonyl-CoA reductase/carboxylase was assayed with 100 mM Tris/HCl, 0.2 mM NADPH,

0.5 mM crotonyl-CoA and 30 mM  $\text{KHCO}_3$  in a reaction. After 2 min incubation at room temperature the crotonyl-CoA reductase/carboxylase was added to initiate the reaction. Enzyme activity was measured spectrophotometrically by decreasing in absorbance at 340 nm using an extinction coefficient  $6.3 \text{ mM}^{-1}\text{cm}^{-1}$  [86, 87]

### 2.3.7 Iron protein reconstitution

In order to reconstitute sufficient iron in the active centre of 4-hydroxybutyryl-CoA dehydratase, 200 mM DTT, 100 mM  $\text{FeCl}_3$  and 30 mM  $\text{Na}_2\text{S} \cdot 9 \text{ H}_2\text{O}$  were prepared in 100 mM Tris-HCl, pH 7.4. Firstly, DTT with 5 mM final concentration was added to the enzyme solution, it was incubated at room temperature for 30 min [90]. After adding  $\text{FeCl}_3$  with 5 mol excess amount over protein and  $\text{Na}_2\text{S} \cdot 9 \text{ H}_2\text{O}$  with 10 mol excess amount over protein, the mixture was incubated again for further 90 min. To remove the precipitated iron sulfide, it was centrifuged by  $13,000 \times g$  for 5 min, and the protein solution was concentrated with a centricon. All experiments were performed at room temperature in an anaerobic chamber.

### 2.3.8 Non-heme iron determination with Ferene

Reagents:	1.0% (w/v)	HCl
	7.5% (w/v)	Ammonium acetate solution
	2.5% (w/v)	SDS
	4.0% (w/v)	Ascorbic acid (always freshly prepared)
	1.5% (w/v)	Ferene

Non-heme iron in protein was quantified with Ferene (3-(2-pyridyl)-5,6-bis (5-sulfo-2-furyl)-1,2,4-triazine, disodium salt trihydrate). For the calibration curve with iron standard a freshly prepared solutions of 0.2 mM  $(\text{NH}_4)_2\text{Fe}(\text{SO}_4)_2 \cdot 6 \text{ H}_2\text{O}$  (Mohr's salt) was used [91, 92].

Six iron standard samples (10, 20, 40 , 80, 100  $\mu$ l), 100  $\mu$ l H<sub>2</sub>O as blank and 2 diluted protein solutions were filled with H<sub>2</sub>O to an end volume of 100  $\mu$ l, which were mixed 1% HCl and incubated at 80 °C for 10 min. After cooling down to room temperature 500  $\mu$ l 7.5% ammonium acetate, 100  $\mu$ l 4% ascorbic acid, 100  $\mu$ l 2.5% SDS and 100  $\mu$ l iron chelator Ferene were sequentially added into each samples with vortexing. The Eppendorf tubes were centrifuged at  $13,000 \times g$  for 10 min. The supernatant was used for measuring the absorbance at 593 nm. The iron content of the protein solution was calculated from the calibration curve of the absorbance valued vs. [Fe<sup>2+</sup>] of the standard Mohr's salt.

### 2.3.9 Acid-labile sulfur determination

Reagents:	1.0% (w/v)	Zinc acetate (freshly prepared)
	7.0% (w/v)	Sodium hydroxide
	0.1% (w/v)	N, N'-dimethyl-p-phenylenediamine (DMPD) in 5 M HCl
	10 mM	FeCl <sub>3</sub> in 1 M HCl
	2 mM	Sulfide standard Na <sub>2</sub> S $\times$ 9 H <sub>2</sub> O in 10 mM NaOH

The iron sulfur protein is denatured in an alkaline solution containing zinc hydroxide. The released sulfide is co-precipitated with Zn(OH)<sub>2</sub> as ZnS. After acidification, H<sub>2</sub>S condenses with two molecules of DMPD to form methylene blue.

The crystals of Na<sub>2</sub>S  $\times$  9 H<sub>2</sub>O (about 0.5 g) was added rapidly to a 1 L volumetric flask containing 10 mM NaOH, which has been purged with nitrogen. The flask was closed immediately and stirred magnetically. The absorbance of diluted stock solution vs the sulfide concentration was used to calculate the sulfide content of enzyme.

Five sulfide standard (5 – 50  $\mu$ M), two blanks, 2 protein samples and 2 protein samples with sulfide standard additions were transferred in Eppendorf tubes and filled to 200  $\mu$ l with distilled

water. 600  $\mu$ l 1% zinc acetate and then 50  $\mu$ l 7% NaOH were added and mixed carefully. After incubation at room temperature for 15 min the tubes were centrifuged for several seconds to minimize the loss of sulfide. DMPD solution was added and mixed. When zinc hydroxide and sulfide precipitates were completely dissolved, 150  $\mu$ l 10 mM FeCl<sub>3</sub> was rapidly added. The Eppendorf tubes were closed immediately, and vortexed for 30 seconds and then incubated at room temperature for 20 min. The mixture was centrifuged at  $9,000 \times g$  for 10 min before measuring the absorbance at 670 nm against water

### **Iodimetric determination of the sulfide standard**

The gravimetric preparation of a sulfide standards using Na<sub>2</sub>S  $\times$  9 H<sub>2</sub>O is inaccurate because of the hygroscopic nature of the compound leading to overestimation of the sulfide amount in protein. So an accurate amount of iodine (I<sub>2</sub>) is partly reduced with a know volume of sulfide standard solution. The remaining amount of I<sub>2</sub> could be determined by titration with sodium thiosulfate, and the sulfide concentration of Na<sub>2</sub>S solution is calculated by subtraction.

Sodium thiosulfate (Na<sub>2</sub>S<sub>2</sub>O<sub>3</sub>) 45 mM (accurate amount)

Iodine solution I<sub>2</sub>      40 mM in 50 ml 300 mM KI

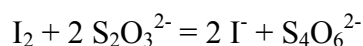
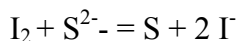
Soluble starch          0.35 g/70 ml H<sub>2</sub>O (boiled and cooled down under continuous stirring)

In 100 ml Erlenmeyer flask 25 ml water, 5 ml iodine solution and 1 ml 1M sulfuric acid (H<sub>2</sub>SO<sub>4</sub>) were mixed on a white sheet of paper using a magnetic stirrer and titrated with sodium thiosulfate until the solution turned almost colorless. Then 0.5 ml indicator solution (Soluble starch) was added for further titration with sodium thiosulfate until the blue color disappeared, and the volume of sodium thiosulfate was read from the buret.

After the accurate amount of iodine was determined, the same amount of iodine was partly reduced with 25 ml sulfide standard and the remaining iodine was titrated by sodium thiosulfate.

The determination was repeated at least 3 times and values were used to calculate the exact concentration of the sulfide standard.

#### Stoichimometry



#### 2.3.10 Flavin determination by UV-Vis

For flavin determination of 4-hydroxybutyryl-CoA dehydratase, the protein solution was denatured at 80 °C for 10 min and centrifuged at 10,000 × g for 5 min. The supernatant was used to measure the flavin content spectroscopically. The flavin amount was calculated using an extinction coefficient 11.3 mM<sup>-1</sup>.cm<sup>-1</sup> at 445 nm [53].

#### 2.3.11 MALDI-TOF Mass Spectrometry

The mass spectrometry analysis of the CoA derivatives was achieved with **Matrix Assisted Laser Desorption Ionisation Time Of Flight Mass Spectrometry** (MALDI-TOF MS). The samples were measured in a Voyager Spectrometer DE-RP (Applied Biosystem). Before measurement the sample was embedded in a low molecular mass, UV-absorbing matrix, namely 3-hydroxy- $\alpha$ -cyanocinnamonic acid or 4-hydroxy- $\alpha$ -cyanocinnamonic acid [93]. When the matrix is hit by a laser beam it transfers enough energy to the sample for forming the molecular ions. The ions are accelerated and allowed to drift through the high vacuum Time-of-Flight analyzer. They separate the CoA derivatives according to their mass-to-charge ratios and the ion abundance as a function of time is measured by the detector.

### **2.3.12 EPR Spectroscopy**

X-band of EPR spectra were obtained with a Bruker ESP-300E EPR spectrometer equipped with an ER-4116 dual mode cavity and an Oxford Instrument ESR-900 helium-flow cryostat with an ITC4 temperature controller.

To prepare the samples for EPR spectroscopy, suitable activity tests were performed to confirm functionality of the enzymes. In an anaerobic glove box (atmosphere of 95 % N<sub>2</sub> and 5 % H<sub>2</sub>) ca 200 µl of the reaction mixture were transferred to ERP-tubes. Anaerobic tubing was placed over the end of each EPR tube and closed. Then the EPR tubes were removed from the glove box and immediately frozen in liquid nitrogen prior analysis by EPR spectroscopy.

## **2.4 Chemical synthesis**

### **2.4.1 Acetyl-CoA, butyryl-CoA and crotonyl-CoA synthesis by anhydride**

To synthesize the CoA-ester, acetyl-CoA, butyryl-CoA, crotonyl-CoA and glutaryl-CoA, 50 mg free CoASH (60.9 µmol) was added in 2 ml 1 M NaHCO<sub>3</sub> and 7 ml H<sub>2</sub>O, which was mixed with 11 µl corresponding anhydride in 1.5 ml acetonitrile. After 15 min incubation at room temperature, the reaction was stopped by acidifying using 1 M HCl to a pH 1.5 – 2, and loaded on a C18 Sep-Pak<sup>TM</sup> column (Waters, USA), which was previously washed by 5 ml methanol and equilibrated by 10 ml 0.1% trifluoroacetic acid. The column was washed with 5 column volume of 0.1% trifluoroacetic acid and the CoA-ester was eluted by 5 ml 1% trifluoroacetic acid and 50% acetonitrile. After lyophilisation the mass of the synthesized CoA-ester was confirmed by MALDI-TOF mass spectroscopy.

#### **2.4.2 CoA-esters synthesis by 4-hydroxybutyryl-CoA transferase**

To synthesize the CoA-ester, 4-hydroxybutyryl-CoA and vinylacetyl-CoA, 4-hydroxybutyrate sodium salt and vinylacetate were incubated with 2.5  $\mu\text{mol}$  acetyl-CoA and 5 U 4-hydroxybutyrate CoA-transferase in 1 ml 100 mM potassium phosphate, pH 7.4 for at least 30 min at 37 °C. The product 4-hydroxybutyryl-CoA was loaded on a C18 Sep-Pak<sup>TM</sup> column and purified as in 2.4.1.

#### **2.4.3 4-Hydroxyvaleryl-CoA synthesis**

(*R,S*)- $\gamma$ -valerolactone as substrate was mixed with 10% excess amount of NaOH. After adjustment of the solution to pH 9.0, the mixture was incubated at 60 °C for 1 hour. During this period, the valerolactone is cleaved to 4-hydroxypentanoate. For further experiments it is necessary to adjust pH to neutral. The resulting 4-hydroxypentanoate was converted to 4-hydroxyvaleryl-CoA by incubation with 4-hydroxybutyrate CoA-transferase at room temperature for 30 min. The CoA ester was purified as in 2.4.1.



### 3. Results

#### 3.1 The recombinant 4-hydroxybutyryl-CoA dehydratase AbfD in *E. coli*

##### 3.1.1 Sequence analysis of AbfD

The gene of *abfD* from *C. aminobutyricum* is composed of 1473 base pairs encoding for 490 amino acids with a calculated molecular mass of 54.509 kDa. Comparison of the AbfD amino acid sequence with sequences in the databank revealed high levels of identity, including the same enzymes from *C. kluyveri*, *Porphyromonas gingivalis* and *Fusobacterium sp.*, several dehydratase/isomerases participating in gamma aminobutyrate metabolism and also two putative 4-hydroxyphenylacetate 3-hydroxylases from *Archaeoglobus fulgidus* and a marine gamma proteobacterium. As shown in Fig 3-1, more than 50% of the amino acid sequences were identical in all 16 different species. All of them contain the iron sulfur cluster coordination motif, CX<sub>3</sub>CX...HisX<sub>6</sub>C (Fig 3-1) [46]. The first two cysteine residues are from the N-terminus, while the histidine residue and the third cysteine residue are from the C-terminus. Other residues located in the active centre are the highly conserved T190, Y296, E455 and E257. Furthermore, some residues, which were not located in the active centre of the enzyme, such as K300, A460 and R90, were also revealed to be highly conserved in all sequences.

Some homologous sequences that are termed as vinylacetyl-CoA isomerase or 4-hydroxyphenylacetate 3-hydroxylase contain the iron sulfur cluster coordination motif and thus are actually 4-hydroxybutyryl-CoA dehydratases, since this motif can be considered as a signature for AbfD.

## Results

Table 3-1. Comparison of AbfD amino sequence from *C. aminobutyricum* with sequences in the database.

AbfD homologues	Sources	Length /amino acids	Identities (%)
AbfD	<i>C. aminobutyricum</i>	490	100
$\gamma$ -Aminobutyrate metabolism dehydratase/isomerase	<i>C. difficile</i>	489	83
$\gamma$ -Aminobutyrate metabolism dehydratase/isomerase	<i>Acidaminococcus sp. D21</i>	494	78
4-Hydroxybutyryl-CoA dehydratase	<i>Porphyromonas gingivalis</i>	486	75
Vinylacetyl-CoA $\Delta$ -isomerase	<i>C. beijerinckii</i>	484	75
$\gamma$ -Aminobutyrate metabolism dehydratase/Isomerase	<i>Porphyromonas endodontalis</i>	512	72
AbfD	<i>C. kluyveri</i>	484	72
4-Hydroxybutyryl-CoA dehydratase/vinylacetyl-CoA isomerase	<i>Fusobacterium sp.</i>	486	70
Vinylacetyl-CoA $\Delta$ -isomerase	<i>Thermosinus carboxydivorans</i>	495	70
Vinylacetyl-CoA $\Delta$ -isomerase	<i>Desulfatibacillum alkenivorans</i>	484	64
$\gamma$ -Aminobutyrate metabolism dehydratase/isomerase	<i>Carboxydotherrnus hydrogenofomans</i>	491	59
Vinylacetyl-CoA $\Delta$ -isomerase	<i>Geobacter metallireducens</i>	483	57
4-Hydroxybutyryl-CoA dehydratase	<i>Cenarchaeum symbiosum</i>	507	57
4-Hydroxyphenylacetate-3-hydroxylase	<i>Archaeoglobus fulgidus</i>	500	56
4-Hydroxyphenylacetate-3-hydroxylase	Marine gamma proteobacterium	513	53
$\gamma$ -Aminobutyrate metabolism dehydratase/isomerase	<i>Plesiocystic pacifica</i>	536	52

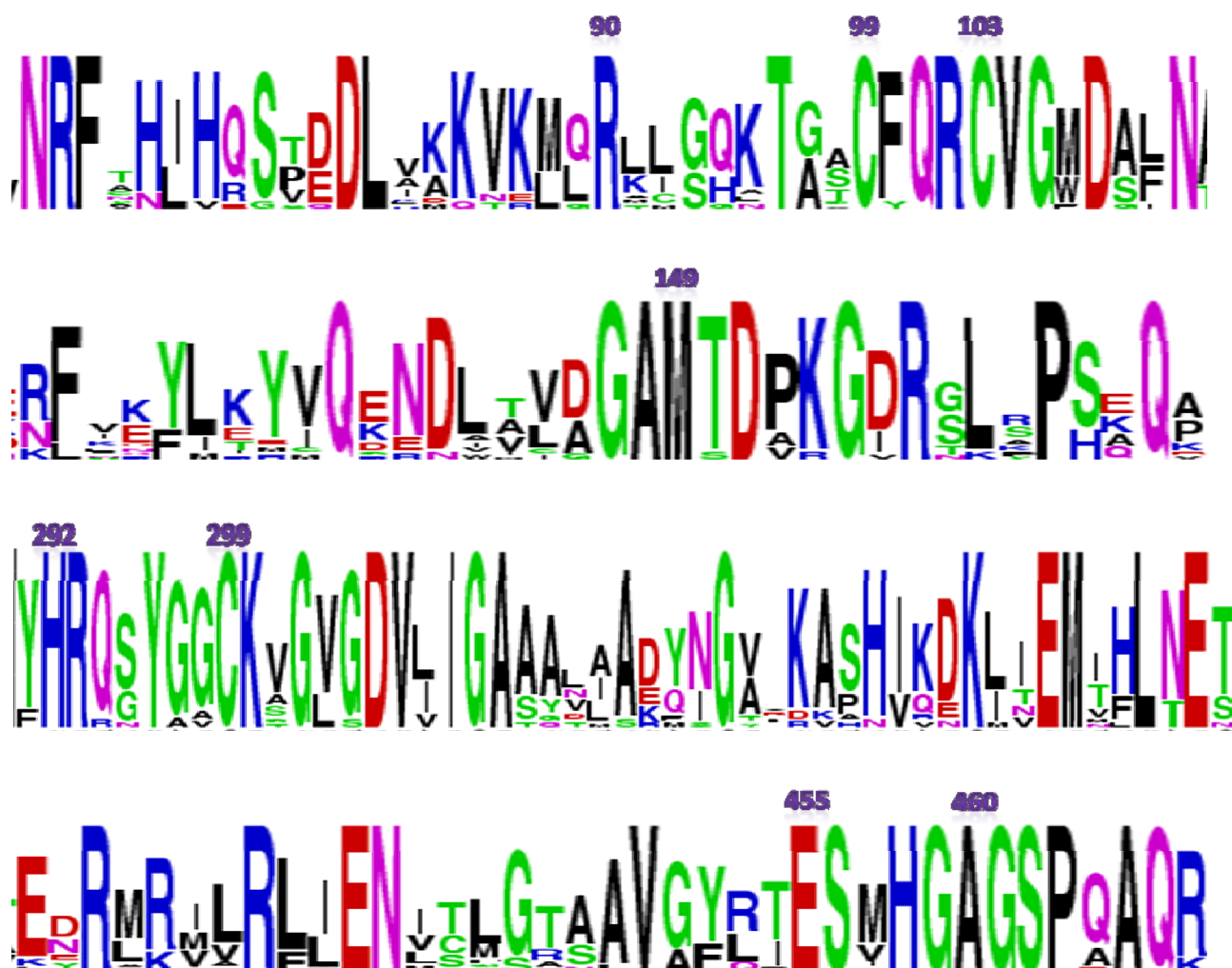


Figure 3-1. Multiple alignment of AbfD amino acid sequence with sequences of other highly similar protein [94].

The amino acids are colored according to their chemical properties. **violet**: hydrophilic, polar and uncharged; **blue**: hydrophilic, polar, and positively charged; **red**: hydrophilic, polar and negatively charged; **green**: polar and neutral; **black**: hydrophobic and unpolar.

### 3.1.2 Cloning and expression of *abfD* in *E.coli*

The gene *abfD* encoding 4-hydroxybutyryl-CoA dehydratase was amplified using Phusion DNA polymerase and "Easystart PCR Mix". After digestion by *BsaI*, the PCR products were subsequently ligated into a pASK-IBA3(+) vector. The *abfD* containing competent *E. coli* BL21 CodonPlus-GroEL cells [95] were grown in standard-I medium with 2 mM Fe-citrate and 0.27 mM riboflavin as cofactor sources at room temperature. At an OD<sub>578</sub> of 0.5 – 0.6 the culture was induced with AHT (100 µg/L) and incubated for overnight.

In the *E. coli* system, iron sulfur proteins usually are not produced in their proper folding form. All attempts to express the *abfD* gene in *E. coli* BL21 stain yielded large proportions of insoluble protein. The formation of insoluble protein or inclusion bodies was attributed to inappropriate protein-protein interactions due to the lack of proper polypeptide folding. Therefore, the expression conditions were changed to improve the solubility of the recombinant AbfD in *E. coli*. Different methods were used, for example, the incubation temperature was decreased, the concentration of AHT was lowered and iron, sulfur and riboflavin were added to the medium. Investigations on the solubility of recombinant AbfD in *E. coli* hosts have shown that a carefully controlled cell growth was required to obtain high yields of the recombinant protein in active form. A growth at 37 °C resulted in a large amount of inclusion bodies. The identified crucial parameters for a successful *abfD* expression were growth temperature, inducer concentration, cofactor concentration in the medium, coexpression of the chaperon genes *groEL* and maintenance of the exponential phase through the production phase.

### 3.1.3 Purification of the recombinant AbfD

The heterologous expression of pASK-IBA(3+) carrying *abfD* resulted in the production of recombinant protein, which was C-terminally fused to a Streptag for affinity purification on StrepTactin column. The purification procedure was performed anaerobically in an anoxic glove chamber.

The cells were harvested, resuspended and opened by sonication. After ultracentrifuging at  $100,000 \times g$  for 1 h at 4 °C, the brown supernatant, which indicated the formation of an iron sulfur cluster, was loaded on a 5 ml StrepTactin column and the protein was eluted using 2.5 mM desthiobiotin in Tris/HCl buffer. The protein sample was then stored at -80 °C.

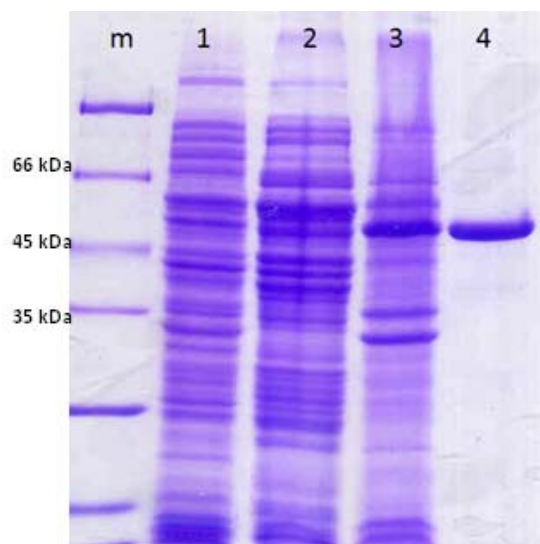


Figure 3-2. SDS-PAGE of purified recombinant 4-hydroxybutyryl-CoA dehydratase.

m, molecular mass marker; 1, cell free extract before induction; 2, pellet after sonication and ultracentrifugation; 3, supernatant after sonication and ultracentrifugation; 4, purified recombinant 4-hydroxybutyryl-CoA dehydratase.

### 3.1.4 Physical and chemical characterization of the recombinant protein

#### Molecular mass determination

According to SDS-PAGE (Fig. 3-2), the AbfD monomer revealed a mass of about 54 kDa. The quaternary structure of holoenzyme was determined by gel filtration chromatography, which separated the proteins based on their mass. As standards, aldolase, catalase, ferritin and thyroglobin were loaded individually onto a Superdex 60 column with a flowrate of 0.5 ml/min.

A calibration curve was made with their elution volume parameters and used for the determination molecular mass of recombinant AbfD. The apparent molecular mass of the recombinant AbfD amounts to ca. 230 kDa (Fig. 3-3). Therefore, a homotetrameric structure appears to be most likely, which confirmed the molecular properties of native AbfD from *C. aminobutyricum* [45].

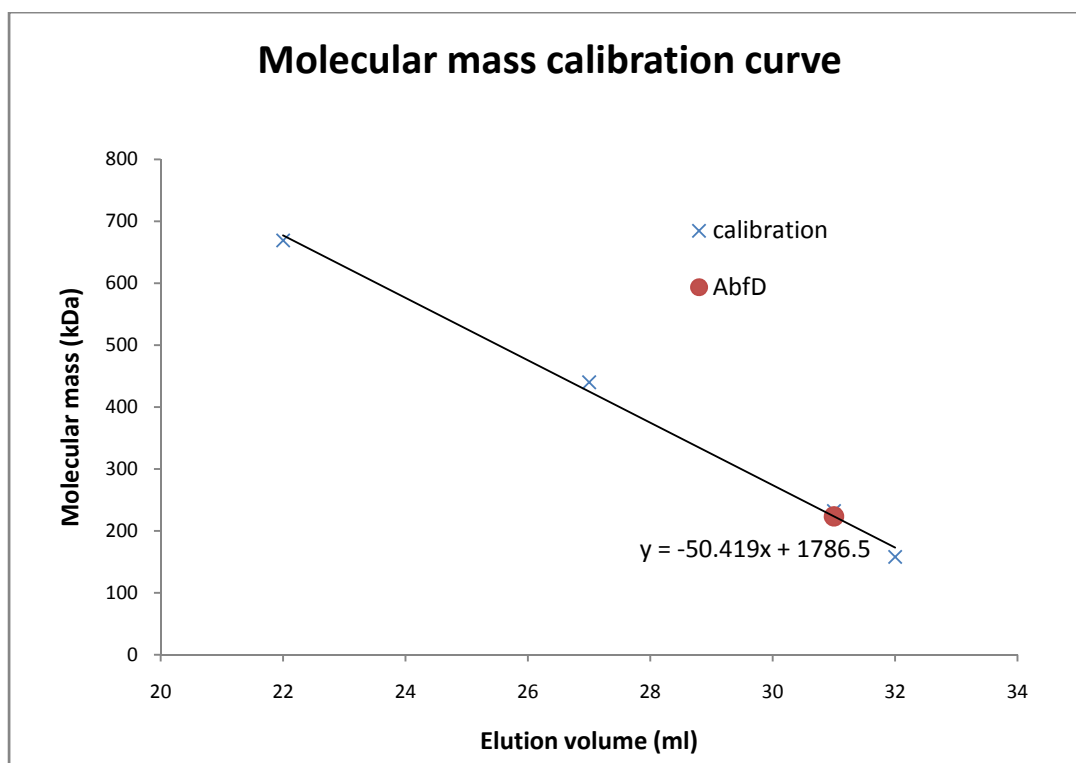


Figure 3-3. Calibration curve of molecular mass determination.

#### Specific activity and cofactor determination

AbfD was assayed spectrophotometrically with 4-hydroxybutyrate CoA-transferase (AbfT) and the 'enzyme pool' from *A. fermentans*, which is an enzyme mixture containing crotonase, 3-hydroxybutyryl-CoA dehydrogenase, thiolase and phosphate acetyltransferase [108]. The produced NADH was measured at 340 nm on the spectrophotometer. The obtained specific

activity of recombinant AbfD (0.5 mg/ml) was calculated to be about 2.2 U/mg, this corresponds to the value of native AbfD from *C. aminobutyricum* (Tab. 3-2) [52].

In order to compare the properties of the native enzyme with those of the recombinant enzyme, the cofactor contents were quantified. Non-heme iron from recombinant AbfD was determined with Ferene as 11.8 mol iron per mol homotetrameric enzyme. As evidence from previous results, *E. coli* cannot offer optimal conditions for the iron sulfur cluster assembly compared to *C. aminobutyricum*, and therefore an iron reconstitution technique was used to improve the iron stoichiometry of the enzyme. After incubation of recombinant AbfD with iron(III) chloride and sodium sulfide for 2 h, the iron content increased to 14.8 mol/mol enzyme and the specific activity to 4.5 U/mg. The FAD content was determined spectrophotometrically. The result indicated that the homotetrameric enzyme consists of  $4.4 \pm 0.2$  mol FAD per mol enzyme as expected.

Table 3-2. Comparison of recombinant AbfD properties with native enzyme

	Spec. activity (U/mg)	Iron content (mol/mol protein)	Flavin content (mol/mol protein)	Structure
AbfD from <i>C.aminobutyricum</i> (Irfan Çinkaya)	2 – 16.7	12.0 – 13.4	4	tetramer
AbfD from <i>E.coli</i>	$2.2 \pm 0.3$	$11.8 \pm 0.1$	$4.4 \pm 0.2$	tetramer
AbfD after iron reconstitution	$4.5 \pm 0.3$	14.8	n.d	tetramer

n.d: not determined

### MALDI-TOF mass spectrometry

It was used to analyze the organic molecules during the dehydration reaction. 4-Hydroxybutyryl-CoA as substrate, which was synthesized using CoA-transferase, 4-hydroxybutyrate and acetyl-CoA, incubated with active AbfD in D<sub>2</sub>O for 30 min. After purification of the reaction mixture

using a SepPak<sup>TM</sup> hydrophobic column, the products were identified by MALDI-TOF. In comparison with control (Fig 3-4, 1), the peak at 854 Da (4-hydroxybutyryl-CoA) dropped down and a peak at 839 Da revealed the production of crotonyl-CoA. The theoretical mass of crotonyl-CoA amounts 836 Da, which was shifted to 839 Da (Fig 3-4, 2), as protons were deuterium-exchanged during dehydration procedure. The peaks at 857 Da and 858 Da could be considered as 4-hydroxybutyryl-CoA carrying three or four deuterium atoms. Due to its instability, only slight peaks could be observed.

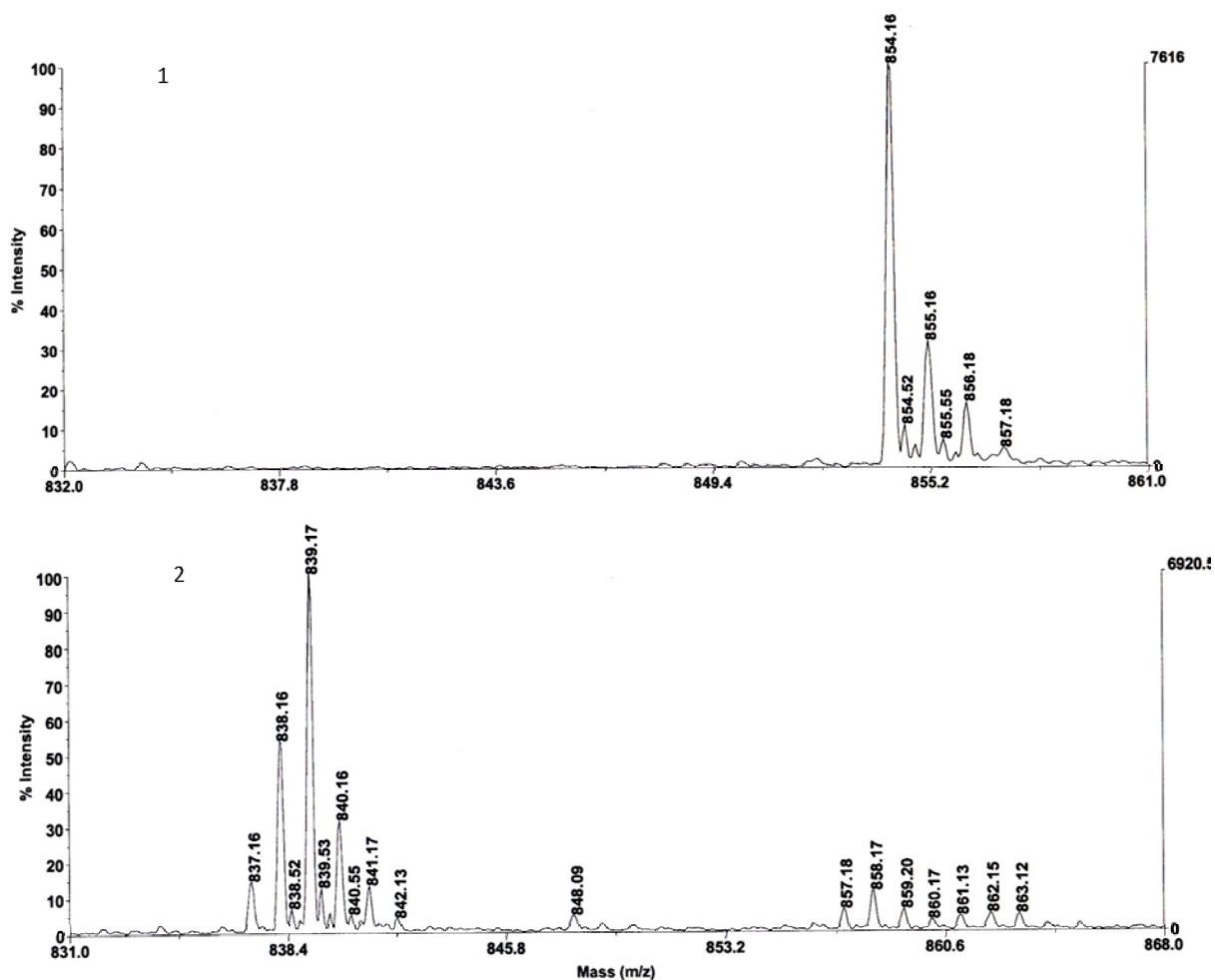


Figure 3-4. MALDI TOF mass spectrometry using 4-hydroxybutyryl-CoA as substrate.

1, Synthesized 4-hydroxybutyryl-CoA (854 Da) in D<sub>2</sub>O as control; 2, 4-Hydroxybutyryl-CoA was incubated anaerobically with purified AbfD in D<sub>2</sub>O.



To characterize the reverse reaction of AbfD, crotonyl-CoA was incubated with AbfD in D<sub>2</sub>O for 30 min. The mixture was purified with the same column as described below. Different to the control (Fig 3-5, 1), with active AbfD treated sample revealed that the peak of crotonyl-CoA (836 Da) was shifted to 839 Da (Fig. 3-5, 2), which was due to the proton-exchange by deuterium atoms. Unexpectedly, the mass spectrometry indicated an unclear peak corresponding to 4-hydroxybutyryl-CoA (854 Da). It is likely to attribute to the instability of 4-hydroxybutyryl-CoA, it could cleave to free CoA and 4-hydroxybutyrate or reconstruct to lactone.

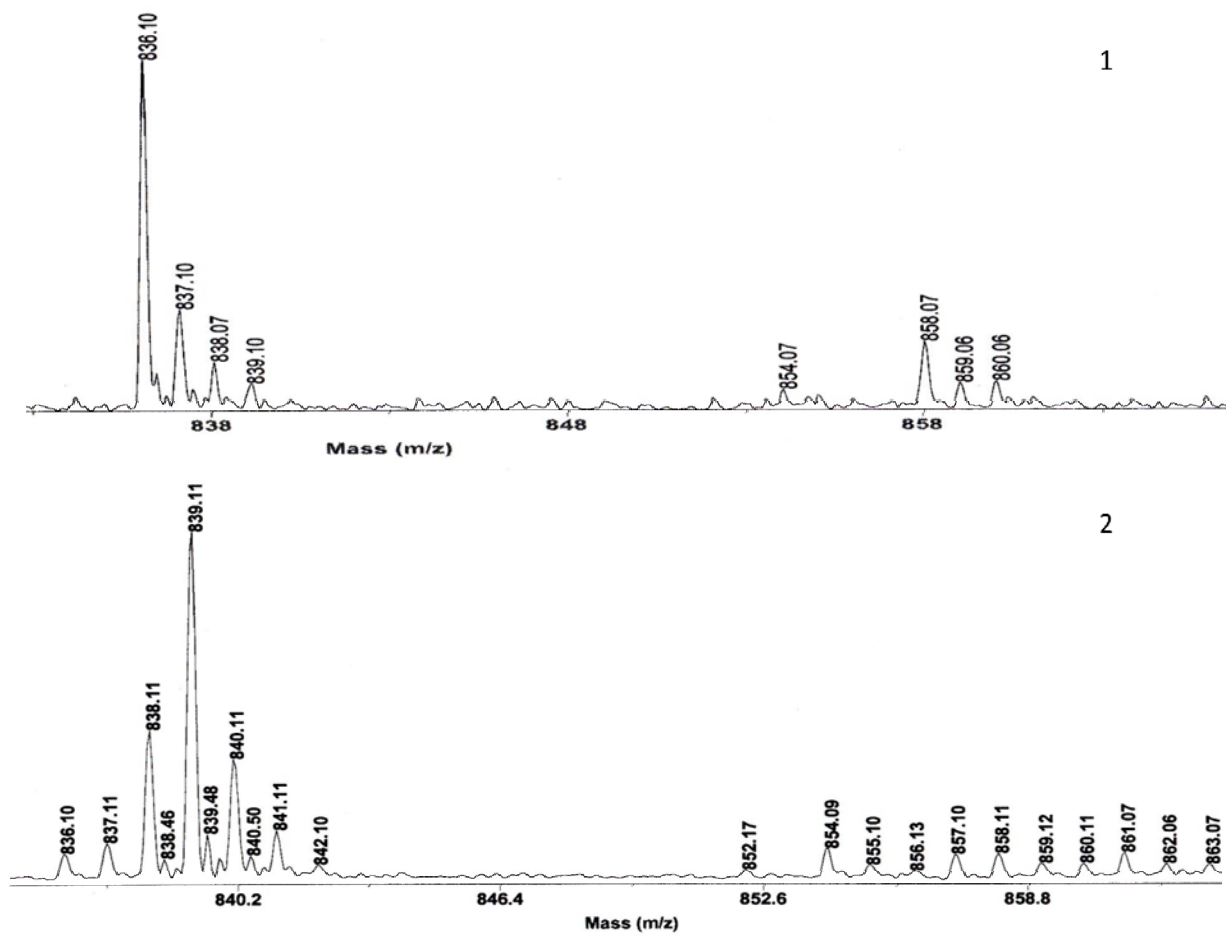


Figure 3-5. MALDI TOF mass spectrometry using crotonyl-CoA as substrate.

1, Synthesized crotonyl-CoA (836 Da) in D<sub>2</sub>O as control. 2, Crotonyl-CoA was incubated anaerobically with purified AbfD in D<sub>2</sub>O.

### Inactivation by air

As an oxygen sensitive enzyme in anaerobic microorganisms, it was shown previously that AbfD lost the dehydratase activity very quickly at room temperature during exposure to air, within 5 hours dehydratase activity disappeared completely. The native AbfDs from *C. aminobutyricum* became completely inactive within 70 min of being exposed to aerobic conditions. It has been also observed that exposure to air bleached the dark brown color. This could be an indication that the protein lost the essential iron. However, the yellow color was intensified, indicating that the flavin in the protein was still present.

### Butyryl-CoA dehydrogenase activity

A fold similar to that seen in the AbfD crystal structure was found in FAD-containing medium chain acyl-CoA dehydrogenase (MCAD) from pig liver, which catalyzes the reversible oxidation of an acyl-CoA derivative to form the  $\alpha,\beta$  double bond in the corresponding enoyl-CoA, although the amino sequence of these enzymes showed just 16 % identity. Because the non-activated  $\beta$ -hydrogen has to be removed by butyryl-CoA dehydrogenase in a way analogous to the reaction catalyzed by AbfD, the dehydrogenase activity was tested using the purified active dehydratase or the inactivated enzyme by air. However, there was no dehydrogenase activity detectable. EPR spectroscopy has been also applied to detect the FAD radical of the oxidized AbfD as a hypothetical dehydrogenase. Compared to the sample without adding butyryl-CoA, no difference of flavin signal in EPR spectra was found, as shown in Fig 3-6,

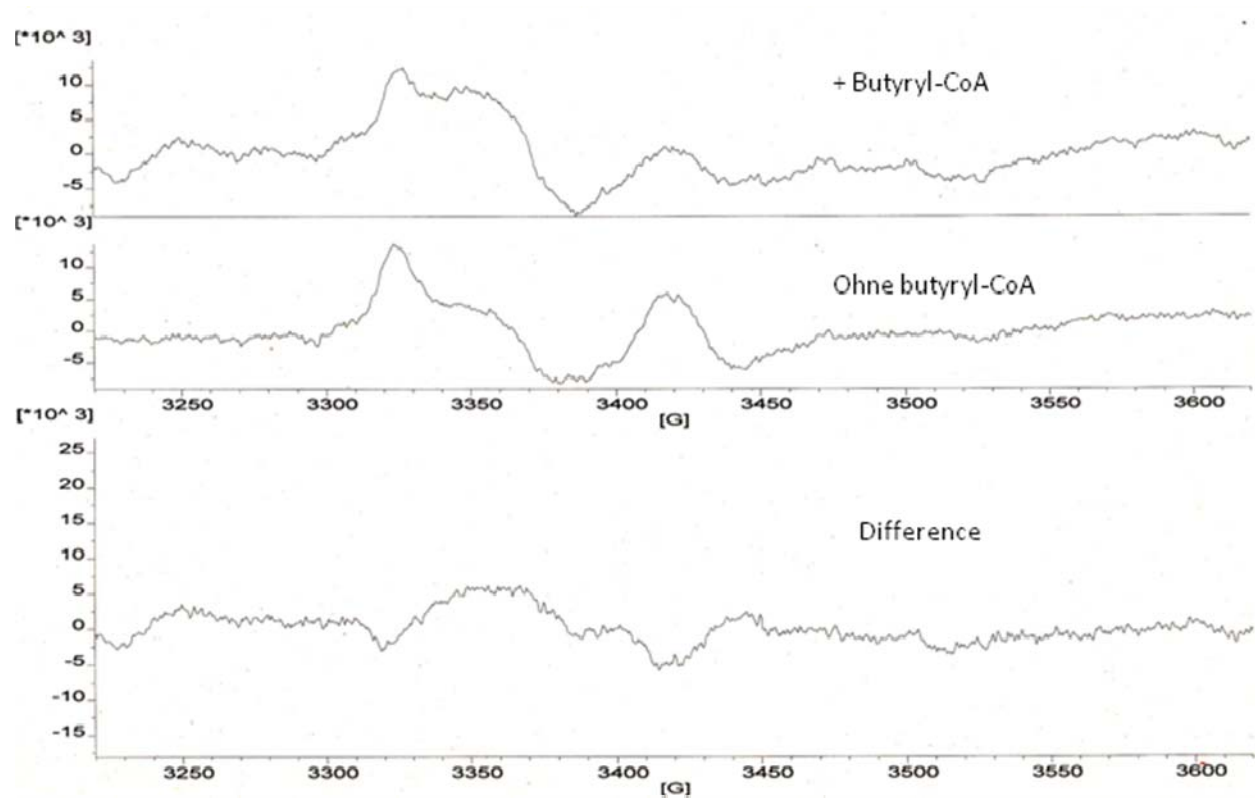


Figure 3-6. EPR spectra of inactivated AbfD by air at 77 K using butyryl-CoA as substrate.

#### Test using 4-hydroxypentanoate as inhibitor

4-Hydroxypentanoate, acts probably as an interesting inhibitor, was synthesized by incubating (*R,S*)- $\gamma$ -valerolactone and sodium hydroxide at 60 °C. After adding acetyl-CoA and AbfT in the synthesized 4-hydroxypentanoate, the products were detected by MALDI-TOF mass spectroscopy. The presence of 4-hydroxyvaleryl-CoA was inferred from the peak of 869 Da (Fig. 3-7). The resulting CoA ester was mixed with AbfD in potassium phosphate, and the products measured directly with a photometer at 290 nm. Obviously, no activity was observed. As shown in Fig 3-8, in order to detect the competition effect between 4-hydroxybutyrate and 4-hydroxypentanoate, the coupled assay of AbfD was initiated by adding 4-hydroxybutyrate as substrate. After mixing with 4-hydroxypentanoate there was no variation of the reaction rate, which proved that the CoA ester derivate of 4-hydroxypentanoate acted not as an inhibitor of AbfD.

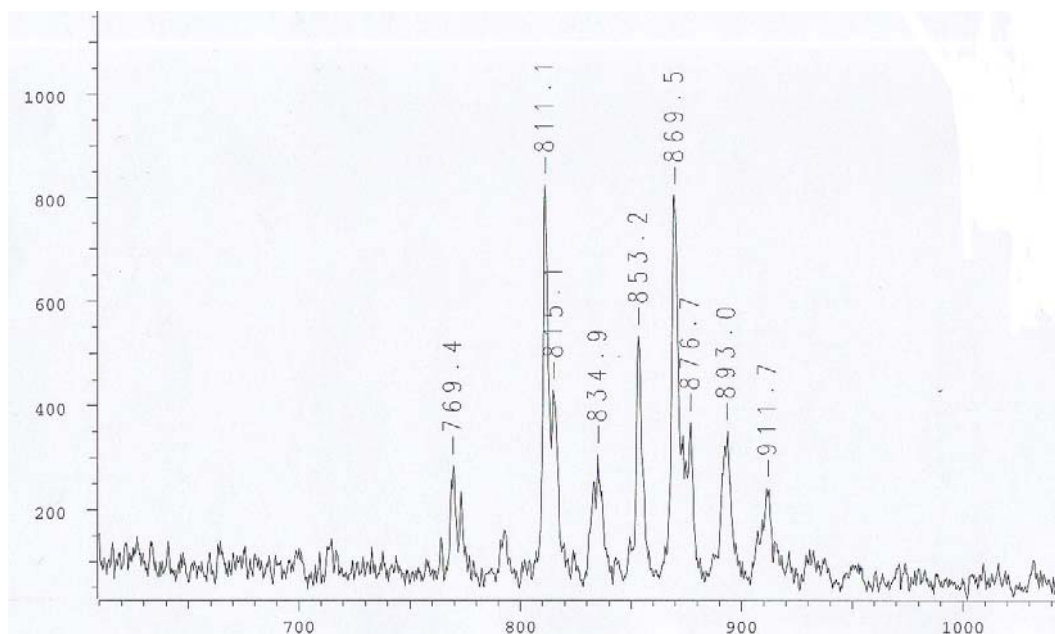


Figure 3-7. MALDI-TOF mass spectrum showing the peak at 869 Da corresponding to 4-hydroxyvaleryl-CoA.

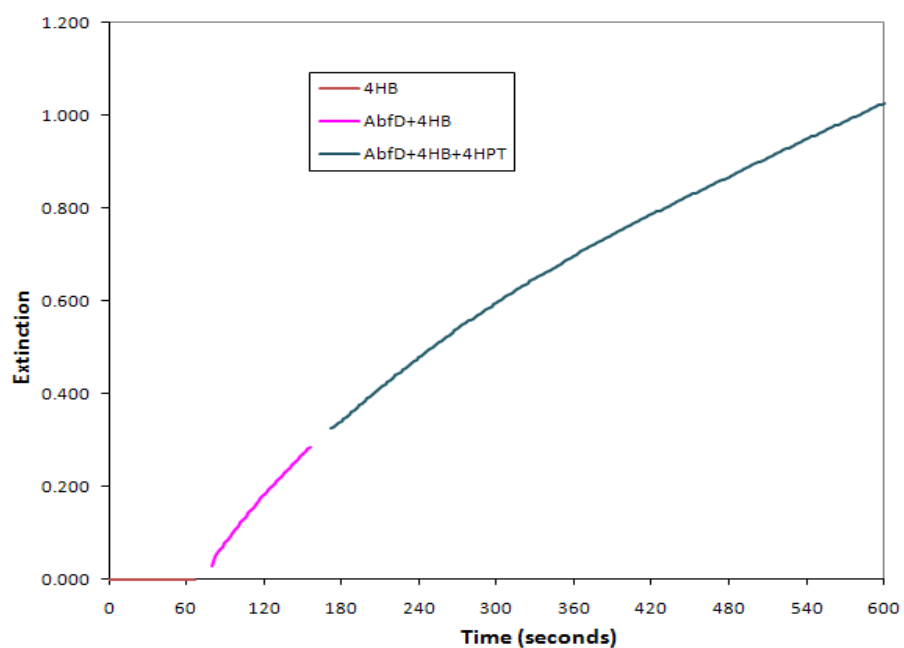


Figure 3-8. Inhibition test of AbfD using 4-hydroxypentanoyl-CoA.

### 3.1.5 Vinylacetyl-CoA $\Delta$ -isomerase

In previous publications it was reported that AbfD also exhibited vinylacetyl-CoA  $\Delta$ -isomerase activity, which catalyzes the conversion of vinylacetyl-CoA to crotonyl-CoA [33, 52, 96]. The isomerase specific activity of AbfD was measured using the same assay as that of dehydratase, in which vinylacetate was mixed in the reaction mixture instead of 4-hydroxybutyrate. However, a clear activity was observed without adding the dehydratase/isomerase sample. An explanation for this could be that the vinylacetate was converted to vinylacetyl-CoA by CoA-transferase and the produced CoA ester could be isomerized by an enzyme from the *A. fermentas* 'enzyme pool'. Consequently, a new assay using crotonyl-CoA reductase/carboxylase from *Rhodobacter sphaeroides* was devised to determine the isomerase activity. During this assay vinylacetyl-CoA was generated by CoA-transferase from vinylacetate and acetyl-CoA, and then it was isomerized to crotonyl-CoA by AbfD. The product crotonyl-CoA is then converted to ethylmalonyl-CoA upon adding crotonyl-CoA reductase/carboxylase. The disappearance of NADPH was measured on the spectrophotometer. The specific activity was calculated to be about 18.5 U/mg. Upon exposure to air the activity decreased very quickly in the first 3-4 hours, then dropped slowly to 10 % of the initial value in 24 hours, whereas the dehydratase activity was lost completely within 5 hours as shown in Fig 3-9.

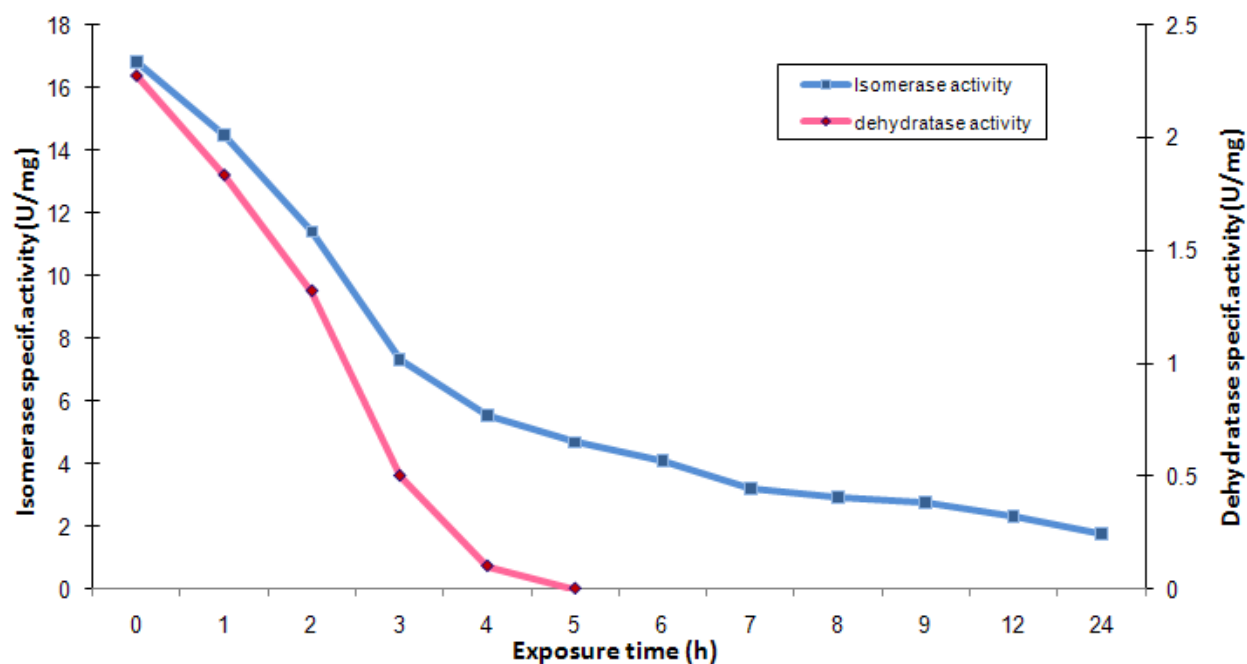


Figure 3-9. The variation of dehydratase and isomerase activity after exposure to air. 4-Hydroxybutyryl-CoA dehydratase activity is colored in red, vinylacetyl-CoA isomerase in blue.

The isomerization procedure was also determined by MALDI-TOF mass spectrometry (Fig 3-10). In comparison with control (Fig.3-10.1), after incubation of vinylacetyl-CoA with active AbfD in D<sub>2</sub>O for 30 min, the molecular mass of crotonyl-CoA (836 Da) increased by 1 Da to 837 Da, as a hydrogen atom in the product was replaced by deuterium. When the by air inactivated AbfD was added (Fig 3-10, 3), the product crotonyl-CoA was also labeled, but the response was not so strong as compared with active AbfD in the reaction.

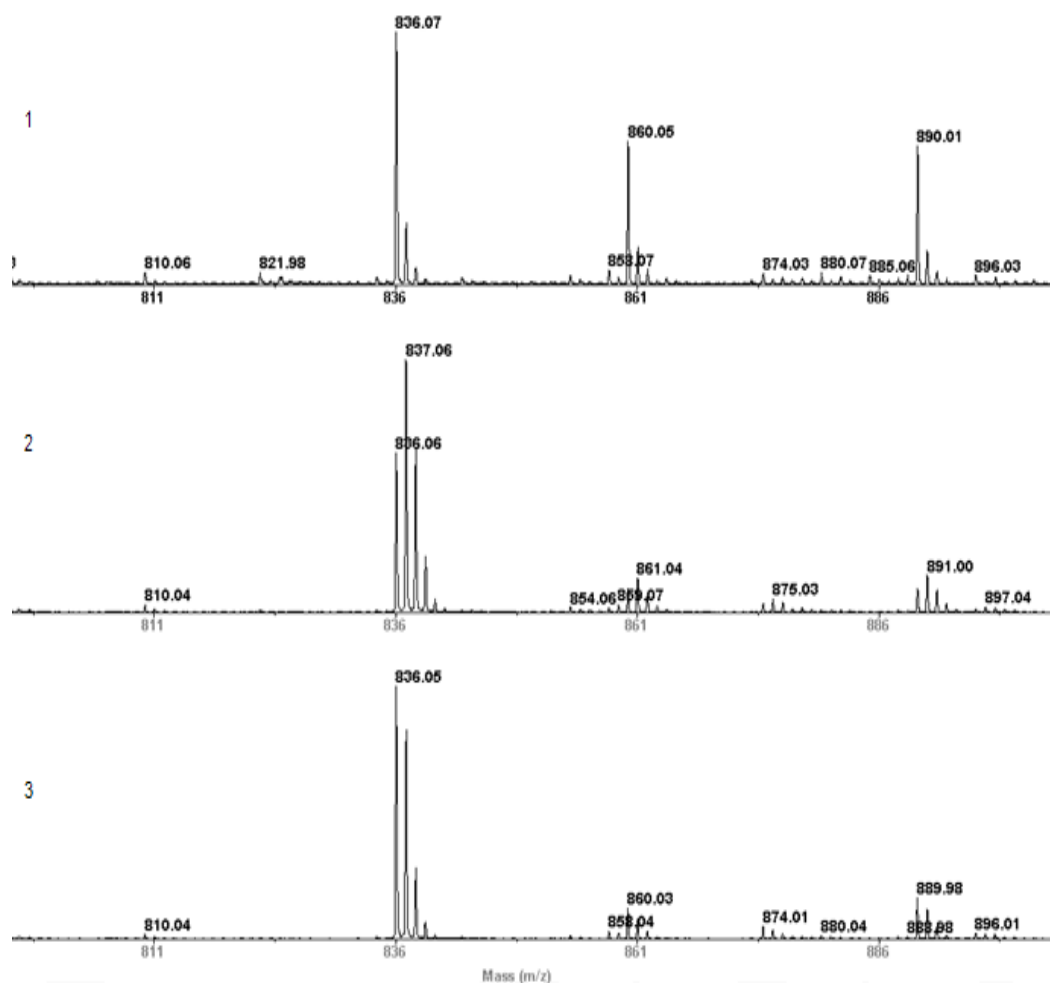


Figure 3-10. MALDI-TOF mass spectrometry using vinylacetyl-CoA as substrate.

1. Vinylacetyl-CoA in D<sub>2</sub>O as control, which was synthesized with vinylacetate and acetyl-CoA by 4-hydroxybutyrate CoA-transferase.
2. Vinylacetyl-CoA reacted with purified 4-hydroxybutyryl-CoA dehydratase/isomerase (1 mg/ml) under anaerobic condition in D<sub>2</sub>O, incubated at room temperature for 30 min.
3. Vinylacetyl-CoA reacted with oxidized 4-hydroxybutyryl-CoA dehydratase/isomerase (1 mg/ml) in D<sub>2</sub>O, which was performed by incubation under aerobic condition for 5 h. The reaction mixture was incubated at room temperature for 30 min.

### 3.1.6 Mutagenesis of 4-hydroxybutyryl-CoA dehydratase

The crystal structure and active site architecture of AbfD shows a narrow substrate binding channel in the active site, which is formed by the surface of the  $[4\text{Fe-4S}]^{2+}$  cluster, FAD and several conserved residues from both monomers. The iron atoms of the  $[4\text{Fe-4S}]^{2+}$  cluster are covalently bound to each monomer of the protein by three Cys-residues (99, 103 and 299) and one H292 residue. Between the two monomers there are some residues, which go deep into the active center, such as Y296, E257 and E455. In comparison with other 4-hydroxybutyryl-CoA dehydratases from 17 different species, it was revealed that also many highly conserved residues were not located in the active centre. To uncover the functions of these conserved residues during the catalytic reaction, these amino acids were replaced by site-directed mutagenesis, which were then produced, purified under the same conditions as the recombinant wild type. The purified mutants were analyzed by SDS-PAGE (Fig 3-12). Their specific activity, cofactor amounts and structure were also characterized (Tab 3-3).

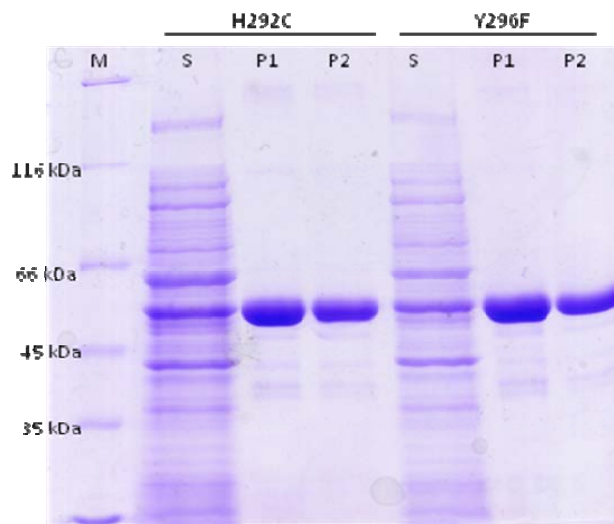


Figure 3-11. SDS-PAGE of purified H292C and Y296F mutants as examples.

M, molecular mass marker; S, supernatant after sonication, P1 and P2, purified protein in different fractions.



The mutation that weakens the building of the iron sulfur clusters yielded an enzyme without dehydratase activity and less cofactor, for example C99, C103, C299 and H292 mutants. And their structures were degraded to dimers, or even monomers, which could be due to the destruction of the iron sulfur cluster. The mutants of three highly conserved residues, such as Y296, E455, E257 and A460, which are located in the substrate binding channel, exhibited negligible or unmeasurable dehydratase activity. The Y296F mutant contains only 0.7% detectable activity in comparison with wild type dehydratase, and A460 replaced by glycine shows 2%. Several conserved residues, which are not involved in the active centre but probably also participated in catalytic reaction, were also mutated and analyzed. All of these showed a homotetrameric structure, with high iron and flavin contents and specific activities between 0.02–0.2 U/mg.

Table 3-3. Characterization of mutants.

	Specific activity (U/mg)	Iron/tetramer (mol/mol)	FAD/tetramer (mol/mol)	Structure
Wild type	$2.2 \pm 0.3$	$11.8 \pm 0.1$	$4.4 \pm 0.2$	tetramer
Wild type <sup>R</sup>	$4.5 \pm 0.2$	14.8	n.d.	n.d.
H292C	< 0.005	$8.1 \pm 0.1$	$3.1 \pm 0.1$	tetramer, dimer
H292C <sup>R</sup>	< 0.005	11.5	n.d.	n.d.
H292E	< 0.005	$7.8 \pm 0.2$	2.9	tetramer
C299A	< 0.005	$7.7 \pm 0.2$	3.0	tetra-, di- and monomer
C103A	< 0.005	8.0	2.7	tetra-, di- and monomer
C99A	< 0.005	7.7	3.2	tetra-, di- and monomer
Y296F	0.03	$11.0 \pm 0.2$	$4.4 \pm 0.2$	tetramer

## Results

Y296F <sup>R</sup>	0.03	13.8	n.d.	n.d.
E455Q	< 0.005	10.2 ± 0.2	3.8 ± 0.1	tetramer
E455Q <sup>R</sup>	< 0.005	12.2	n.d.	n.d.
E257Q	< 0.005	11.0 ± 0.1	3.5	tetramer
A460G	0.09	10.3	3.5	tetramer
Q101E	0.2	13.1	3.2	tetramer
T190V	0.02	10.6	2.9	tetramer
K300Q	0.2	13.6	3.4	tetramer

Wild type: the recombinant AbfD produced in *E. coli*,

<sup>R</sup>: the protein sample treated by iron reconstitution,

n.d: not determined

Furthermore, because the iron sulfur clusters are not chemically stable, some samples were treated by iron reconstituted using iron chloride and sodium sulfide. As shown in Fig 3-12, the specific activity of the wild type increased two fold to 4.5 U/mg, which was caused by an increase in the iron content in the enzyme. However the experiments indicated also that the mutant activities were unchanged after iron reconstitution. When the iron content after reconstitution was compared with that before (Fig 3-13), all sample were found to contain more iron. However this did not lead to enhancement of enzyme activity.

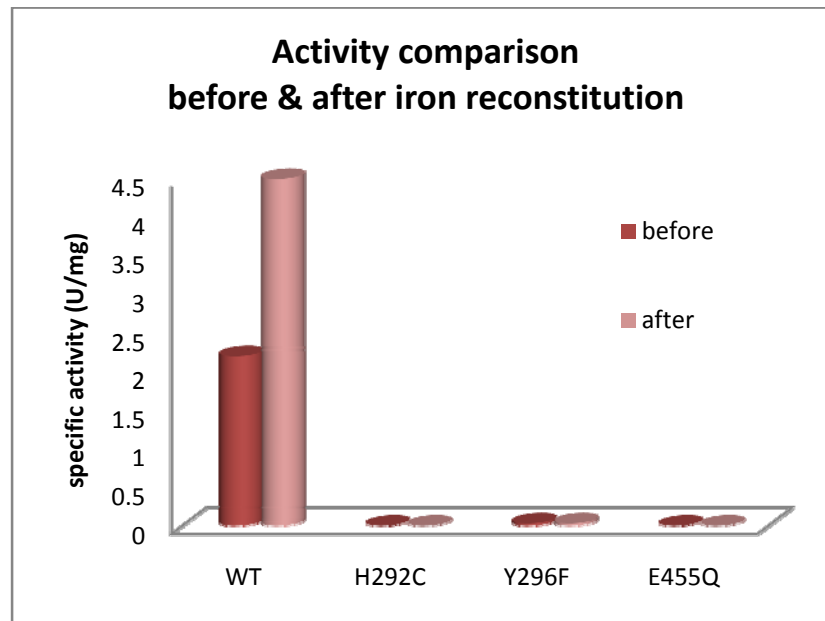


Figure 3-12. Specific activity comparison with the sample before and after iron reconstitution.

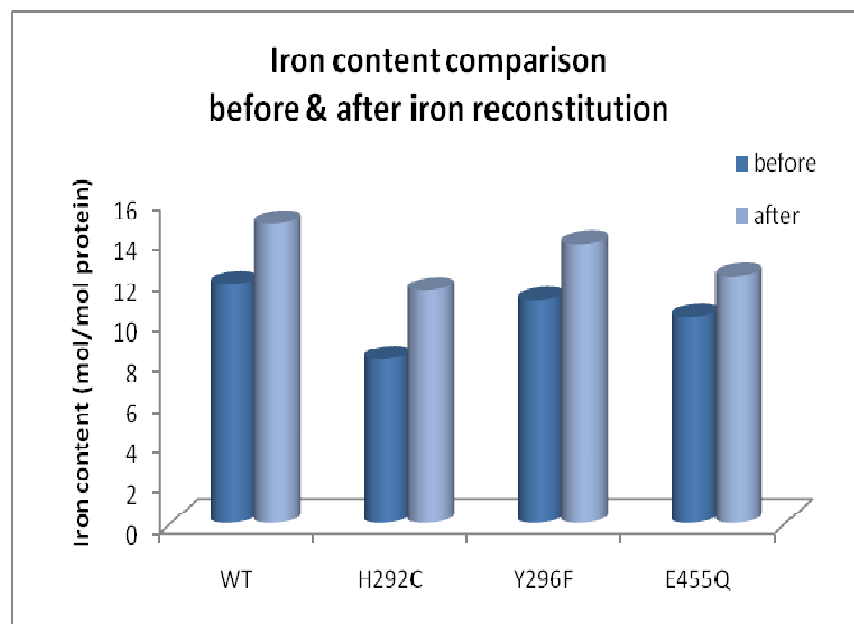


Figure 3-13. Iron content comparison with the sample before and after iron reconstitution.

In order to detect the function of conserved amino acids during the isomerization procedure, the isomerase activities of all mutants were determined and compared with the wild type (Table 3-4). E257, Y296 mutants showed a high isomerase specific activity, and even E257 contains almost same activity as wild type protein, which was retained even after incubation with oxygen. H292E and C99A mutants showed lowest isomerase specific activity and completely lost activity after incubation with oxygen. Both of H292 and C99 residues were located at the side close to the active centre. In comparison, the isomerase activities of C103 and C299 mutants were relative higher. This could be considered a consequence of the fact that these residues are located at the upper side of iron sulfur cluster, further from the active centre.

Table 3-4. Comparison of vinylacetyl-CoA  $\Delta$ -isomerase specific activity before and after 24 h exposure to air.

	Vinylacetyl-CoA $\Delta$ -isomerase activity (U/mg)	
	Purified enzyme	Enzyme after exposure to air
Wild type	18.5	1.7 $\pm$ 0.2
H292C	2.1	0
Y296F	9.6	4.4
E455Q	1.3	1.0
E257Q	17.0	17.0
H292E	0.2	0
C299A	14.0	14.0
C103A	3.1	1.8
C99A	0.25	0

### 3.2 The recombinant 4-hydroxybutyrate CoA-transferase AbfT in *E. coli*

#### 3.2.1 Sequence analysis of AbfT

AbfT is also involved in the 4-aminobutyrate fermentation pathway of *C. aminobutyricum*, which catalyzes the activation of 4-hydroxybutyrate to 4-hydroxybutyryl-CoA. The gene *abfT* coding 4-hydroxybutyrate CoA-transferase contains 438 amino acids. The protein has been characterized as a homodimeric enzyme, each monomer with a molecular mass of 54 kDa. Comparing the amino acid sequence of *abfT* with other 4-hydroxybutyrate CoA-transferases in the data bank revealed a high level of identity (ca. 60%) to 4-hydroxybutyrate CoA-transferase of *C. difficile*, *C. kluyveri* and *C. beijerinckii* exists. Other CoA-transferases from various microorganisms including *Anaerofustis caccae*, *Prophyromonas gingivalis*, *P. unenonis*, *P. endodontalis* *Fusobacterium nucleatum*, *F. sp*, *C. tetani* indicated an identity between 45% - 50% to AbfT.

```

Sequence      -----MDWKKIYEDRTCTADEAVKSIKSGDRVLFAHCVAEPPVLVEAMVANAAAYKNV 53
Q9RM86_CLOAM  -----MDWKKIYEDRTCTADEAVKSIKSGDRVLFAHCVAEPPVLVEAMVANAAAYKNV 53
Q185L2_CLOD6 -----MSWQELYQSKLCSATEAVKQIKNGD TVVFACVGEPPALVEAMIEAENAEQYKDV 53
A6LV90_CLOB8 ----MSKISWKDLYKSKVVTADEAVRKIKSNDRVVTGHACGEPKEIIDAMVRNKDLYENV 56
CAT2_CLOK5    -----MEWEEIYKEKLVTAEKAVSKIENHSRVVFAHAVGEPVDLVNALVKNKDNYIGL 53
BOM9J7_9FIRM MMRDKKDKPWKAERYEKLVSADAEVSHIRSGQRIVFSAAGESLVLSDALVRNRALFENV 60
B2RIP9_PORG3 -----MKDVLAEYASRIVSAEEAVKHINKGERVALSHAAGVPQSCVDALVQQADLFQNV 54
Q7P6F4_FUSNV -----MGNWKERYESKLCTSDEAIKKIAGVKRIIFEHACGESALLTEALMKNKELFKKT 54
C3WS57_9FUSO -----MGNWKERYESKLCTSDEAIKKIAGVKRIIFEHACGESALLTEALMKNKELFKKT 54
C3JA15_9PORP -----MEEYKSKVVSQAIRAIRAIKNGDSVVLSHAAGAPQLISRALADNYQNYQDV 50
              * . : : : * : * . . : * . . : * : : :

Sequence      TVSHMVTLGKGEYSKPEYKENFTFEGWFTSPSTRGSI AEGHGQFVPVFFHEVPSLIRKD- 112
Q9RM86_CLOAM  TVSHMVTLGKGEYSKPEYKENFTFEGWFTSPSTRGSI AEGHGQFVPVFFHEVPSLIRKD- 112
Q185L2_CLOD6  EIKHVMVSLGSGGYTAGMEAHFRVNP MFVSGNVRKAIENG DGDFTPAFFHEVPKLLREK- 112
A6LV90_CLOB8  EIVHVMVMGKSEYCKPEMAVNF RHNSIFAGGTTREAI F DGRADFTPCFFSEVPKMFREG- 115
CAT2_CLOK5    EIVHVMAMGKGEYTKEGMQRHF RHNA LFVGGCTRD AVNSGRADYTPCFFYEVP SLFKKE- 112
BOM9J7_9FIRM  EIVHVMVAMGA AKYCEPGMEKHFRHNSFFLGASTRKA AKEGRADVTPVYFSEVP ELFRTT- 119
B2RIP9_PORG3  EIYHMLCLGEGKYMAPEMAPHF RHITNFVGGNSRK AVEENRADFIPVFFYEVP SMIRKD- 113
Q7P6F4_FUSNV  EIIHLVAMGKGEYAKEENSEYFRHNA LFVGGTTREAA NSSYGDYTPSFFFEMPKL FKKG- 114
C3WS57_9FUSO  EIIHLVAMGKGEYAKEENSEYFRHNA LFAGGTTREAA NSSYGDYTPSFFFEMPKL FKKG- 114
C3JA15_9PORP  KIFHMLVLGDAPYCAPEMEGHFRHVTNFVGGNTRQALADGRADFIPLFFYQVPRMFENG- 109
              : * : : * : . *          *          * .      * : . . : * : * : * : :

Sequence      IFHVDVFMVMVSPPDHNGFCCVGVSSDYTMQAIKSAKIVLAEVNDQVPVVGDTFVHVSE 172
Q9RM86_CLOAM  IFHVDVFMVMVSPPDHNGFCCVGVSSDYTMQAIKSAKIVLAEVNDQVPVVGDTFVHVSE 172
Q185L2_CLOD6  RLKCDVVL AQVTPPDEHGYCSLGTSVDYTYEAIKTARTVIVQVNDQFPTYG-EV VHVSE 171
A6LV90_CLOB8  TLPVDVALVQLSV PDEHGYCSFGVSN DYTKPAEAAKIVIAELNEKMPRTLGD SFIHVSD 175
CAT2_CLOK5    RLPVDVALIQVSE PDKYGYCSFGVSN DYTKPAESA KLVIAEVNKNMPRTLGD SFIHVSD 172
BOM9J7_9FIRM  -LPVDVAVFLNLSPDEHGYCSFGISVDYSKPAAMEAELVIAQINPSMPTLGD SFIHISD 178
B2RIP9_PORG3  ILHIDVAIVQLSMPDENG YCSFGVSCDY SKPAESAHLVIGEINRQMPYVHGDNLHIHISK 173
Q7P6F4_FUSNV  VLNPDVTIIQVSY PDEHGYCSYGISCDYTKCAEENSNI V I AQVNKFMPTLGNCFIHIDS 174
C3WS57_9FUSO  VLNPDVTIIQVSY PDEHGYCSYGISCDYTKCAEENSNI V I AQVNKFMPTLGNCFIHIDS 174
C3JA15_9PORP  AIPVDVAVVHVSEPN EEGYCSYGVS CDYTKPAERA KVVIAEMNKQMPFVHGDNLHIH VSK 169
              : * . . : : * : . * : * * : * : . : * : * : * : * : * :

```

## Results

```

Sequence      IDK F V E T S H P L P E I G L P K I G E V E A A I G K H C A S L I E D G S T L Q L G I G A I P D A V L S Q L K D K K H 232
Q9RM86_CLOAM  IDK F V E T S H P L P E I G L P K I G E V E A A I G K H C A S L I E D G S T L Q L G I G A I P D A V L S Q L K D K K H 232
Q185L2_CLOD6  F D Y I V E K S Q P L F E L Q P A K I G E V E E A I G K N C A S L I E D G S T L Q L G I G G I P D A V M L F L T D K K D 231
A6LV90_CLOB8  I D Y I V E T S N D I I E L K P P K I G E V E K A I G E N C A K L I E D G S T L Q L G I G A I P D A V L L F L K G K K D 235
CAT2_CLOK5    I D Y I V E A S H P L L E L Q P P K L G D V E K A I G E N C A S L I E D G A T L Q L G I G A I P D A V L L F L K N K K N 232
BOM9J7_9FIRM  I D Y I V E A D T P L I E L P P A G I S E V E R A I G K N C A S L I E D G D T L Q L G I G A I P D A V L G F L K E K K D 238
B2RIP9_PORG3  L D Y I V M A D Y P I Y S L A K P K I G E V E E A I G R N C A E L I E D G A T L Q L G I G A I P D A A L L F L K D K K D 233
Q7P6F4_FUSNV  I D Y I V E Q A T P I I E L K I P V I G E I E K R I G E H C A S L I D D G A T L Q L G I G A I P D A V L S F L R H K K D 234
C3WS57_9FUSO  I D Y I V E Q A T P I I E L K I P V I G E I E K R I G E H C S S L I D D G A T L Q L G I G A I P D A V L S F L R H K K D 234
C3JA15_9PORP  L D Y I V E A D Y P L Y E I A L P T I G D V E K A I G D N V A H L V Q D G D T L Q L G I G A I P D A V L L F L K D K K D 229
               : * : *      : . : . : : * * : : * : * * * * * * . * * * .

Sequence      L G I H S E M I S D G V V D L Y E A G V I D C S Q K S I D K G K M A I T F L M G T K R L Y D F A A N N P K V E L K P V D 292
Q9RM86_CLOAM  L G I H S E M I S D G V V D L Y E A G V I D C S Q K S I D K G K M A I T F L M G T K R L Y D F A A N N P K V E L K P V D 292
Q185L2_CLOD6  L G I H S E M I S D G T L A L Y E K G V I N G K Y K N F D K E K M T V T F L M G T K K L Y D F A N N N P A V E V K P V D 291
A6LV90_CLOB8  L G I H S E M I S D G V V E L I E A G V I T N K A K T L H P G K S V V T F L M G T K R L Y D Y V N G N P S V A M Y P V D 295
CAT2_CLOK5    L G I H S E M I S D G V M E L V K A G V I N N K K K T L H P G K I V V T F L M G T K K L Y D F V N N N P M V E T Y S V D 292
BOM9J7_9FIRM  L G I H S E M I S D G I V E L Y E A G V I T N R R K S L H A G K S I V T F L M G T R K L Y D F A D N N P A V E L H P V D 298
B2RIP9_PORG3  L G I H T E M F S D G V V E L V R S G V I T G K K K T L H P G K M V A T F L M G S E D V Y H F I D K N P D V E L Y P V D 293
Q7P6F4_FUSNV  L G I H S E M I S D G V V D L V N L G V I T N K R K N I N V G K S I V S F L M G T R K L Y D Y I D N N P E I E L H P V D 294
C3WS57_9FUSO  L G I H S E M I S D G V V D L V N L G V I T N K R K N I N V G K S I V S F L M G T R K L Y D Y I D N N P E I E L H P V D 294
C3JA15_9PORP  L G I H T E M F S D G V L E L V R A G V I T G K K K E I D N G K L T A T F L M G S R D L Y D F V N N N P D V R L A P V N 289
               * * * : * : * * : * . * * *      * : . *      : * * * : . : * :      * * :      . * :

Sequence      Y I N H P S V V A Q C S K M V C I N A C L Q V D F M G Q I V S D S I G T K Q F S G V G G Q V D F V R G A S M S I D K G K 352
Q9RM86_CLOAM  Y I N H P S V V A Q C S K M V C I N A C L Q V D F M G Q I V S D S I G T K Q F S G V G G Q V D F V R G A S M S I D K G K 352
Q185L2_CLOD6  Y V N H P A I I M K Q H K M V S I N S A I Q V D L M G Q V V A E A M G L R Q F S G V G G Q V D F I R G V S M G E D G K - 350
A6LV90_CLOB8  Y V N N P C V I A E N Y K M V S I N S C I Q V D L M G Q V A A D T I G L K Q F S G V G G Q V D F V R G A A M A K G G K - 354
CAT2_CLOK5    Y V N N P L V I M K N D N M V S I N S C V Q V D L M G Q V C S E S I G L K Q I S G V G G Q V D F I R G A N L S K G G K - 351
BOM9J7_9FIRM  Y V N D P Y V I A Q N E R L V S V N S C V Q V D L M G Q V V S A S V G R R Q I S G V G G Q V D F V R G A N M S R G G K - 357
B2RIP9_PORG3  Y V N D P R V I A Q N D N M V S I N S C I E I D L M G Q V V S E C I G S K Q F S G T G G Q V D Y V R G A S W S K N G K - 352
Q7P6F4_FUSNV  Y V N N P F I I A Q N D N M I S I N S A I Q V D L M G Q V N A E S I G S K Q F S G T G G Q V D F V R G A A M S K G G K - 353
C3WS57_9FUSO  Y V N N P F I I A Q N D N M I S I N S A I Q V D L M G Q V N A E S I G S K Q F S G T G G Q V D F V R G A A M S K G G K - 353
C3JA15_9PORP  W V N D P V T V M N F D R M V S I N S C I E V D L M G Q V A S E T I G Y K Q F S G T G G Q V D Y V R G A S M S G H G V - 348
               : : * . *      : :      . : : : : * : : : : * : * * :      : * : * : * * . * * * : : * .      .      *

Sequence      K A I I A M P S V A K K K D G S M I S K I V P F I D H G A A V T T S R N D A D Y V V T E Y G I A E M K G K S L Q D R A R 412
Q9RM86_CLOAM  K A I I A M P S V A K K K D G S M I S K I V P F I D H G A A V T T S R N D A D Y V V T E Y G I A E M K G K S L Q D R A R 412
Q185L2_CLOD6  - A I I A M P S I T T K K D G T V I S K I V S I V D E G A P I T T S R N D V D Y I V T E Y G I A E L K G K S L R E R A R 409
A6LV90_CLOB8  - S I I A M P S T A S K G K - - - L S R I V P I L D E G A T V T T S R N D I H Y V V T E F G I A E L K G K T L K E R A K 410
CAT2_CLOK5    - A I I A I P S T A G K G K - - - V S R I T P L L D T G A A V T T S R N E V D Y V V T E Y G V A H L K G K T L R N R A R 407
BOM9J7_9FIRM  - S I M A M P S T A A E G R - - - I S K I V P V I G E G A A V T T S R Y D A D Y I V T E Y G T A R L K G E T L R N R A R 413
B2RIP9_PORG3  - S I M A I P S T A K N G T - - - A S R I V P I I A E G A A V T T L R N E V D Y V V T E Y G I A Q L K G K S L R Q R A E 408
Q7P6F4_FUSNV  - S I I A L P S T A A K G T - - - I S K I V F T L D E G A A V T T S R N D V D Y I V T E Y G I A H L K G K S L R E R A K 409
C3WS57_9FUSO  - S I I A L P S T A A K G T - - - I S K I V F T L D E G A A V T T S R N D V D Y I V T E Y G I A H L K G K S L R E R A K 409
C3JA15_9PORP  - S I M A M P S T A A K G K - - - V S R I V P L L A E G A A V T T S R N D V D Y V V T E F G A A K L K G K S L R E R A E 404
               : * : * : * *      : :      * : . *      : * * : * * *      : * : * * : * * : * * : * : * : * : * .

Sequence      A L I N I A H P D F K D E L K A E F E K R F N A A F - - - - 438
Q9RM86_CLOAM  A L I N I A H P D F K D E L K A E F E K R F N A A F - - - - 438
Q185L2_CLOD6  N L I N I A H P S V R E S L A V E F E K R F K E K Y - - - - 435
A6LV90_CLOB8  A L I N V A H P D F R D A L I K E W E K R F K V K F - - - - 436
CAT2_CLOK5    A L I N I A H P K F R E S L M N E F K K R F - - - - - - 429
BOM9J7_9FIRM  K L I R I A H P D F R R M L A E E Y E K R F R E A W S D D E 443
B2RIP9_PORG3  A L I A I A H P D F R E E L T E H L R K R F G - - - - - - 431
Q7P6F4_FUSNV  A L I E I A H P D F R E E L T K K A V G K F G T L - - - - 434
C3WS57_9FUSO  A L I E I A H P D F R E E L T K K A V G K F G T L - - - - 434
C3JA15_9PORP  A L I S I A H P D F R P Q L L E E F N K R F P S K - - - - 429
               * * : * * * . :      *      .      : *

```

Figure 3-14. Homology analysis of AbfT from *C. aminobutyricum*.

It has also been concluded in previous research that E324 in propionate CoA-transferase from *C. propionicum* [97, 98] and  $\beta$ E54 in glutaconate CoA-transferase from *A. fermentas* [39] act as covalent-catalytic residues in the active centre. A mechanism was proposed in which the glutamate residue acts as a nucleophile and attacks the carbonyl group of the CoA-ester substrate, which causes release of the CoA group. The amino acid alignment revealed only two conserved glutamates, E195 and E238, in the gene *abfT*. Furthermore, compared to two known 4-hydroxybutyrate CoA-transferase structure from *Shewanella oneidensis* and *P. gingivalis* suggested that E238 was the most likely candidate for the formation of the enzyme CoA thioester. As evidence of this, E238 was mutated and analyzed in chapter 3.2.4.

### 3.2.2 Cloning and expression of *abfT* in *E.coli*

The *abfT*-gene encoding 4-hydroxybutyrate CoA-transferase was amplified by PCR using Phusion DNA polymerase and primers containing restriction enzyme cut sites. The PCR product and the pASK-IBA3 (+) plasmid were digested by restriction enzymes and ligated with one another. The products were then transformed into an *E. coli* DH5 $\alpha$  strain. The DNA sequences of four clones were analyzed by *XbaI* and *PstI* (Fig. 3-15). The digestion by *XbaI* showed one band (4.5 kb) and by *PstI* showed two bands (3.8 kb and 700 bp), as expected.

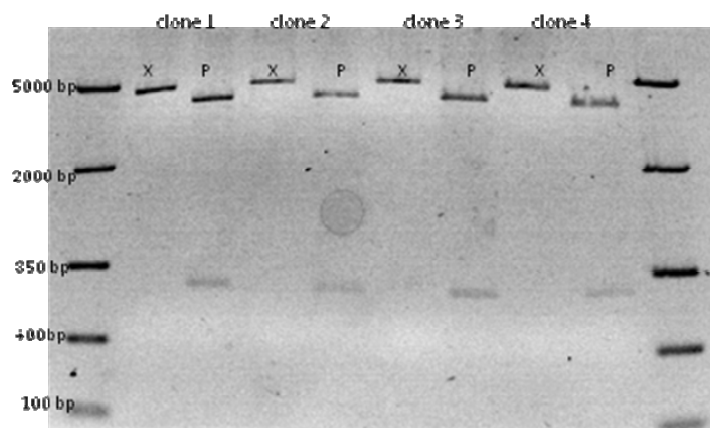


Figure 3-15. Restriction analysis of the clone in pASK-IBA3(+).

X: the sample was digested by *XbaI*; P: the sample was digested by *PstI*.

Before transformation and expression in *E. coli* BL21CodonPlus strain, the gene was sequenced. The results revealed that eight nucleotides in the database were inaccurate (Tab. 3-5), which caused three amino acid errors (Table 3-6).

Table 3-5. The corrected eight nucleotides of *abfT*.

Nucleotide position*	Old data (wrong)	New data(corrected)
3406	G	a
3530	A	g
3532	T	a
3562	G	a
3871	A	g
3884	A	c
4005	G	a
4012	G	a

\* The position in the gene cluster of 4-hydroxybutyrate dehydration.

Table 3-6. New corrected amino acids of AbfT in database

Amino acid position	Old data (wrong)	New data(corrected)
172	N	E
290	T	P
330	R	Q

([http://www.ncbi.nlm.nih.gov/nuccore/188032705?ordinalpos=1&itool=EntrezSystem2.PEntrez.Sequence.Sequence\\_ResultsPanel.Sequence\\_RVDocSum](http://www.ncbi.nlm.nih.gov/nuccore/188032705?ordinalpos=1&itool=EntrezSystem2.PEntrez.Sequence.Sequence_ResultsPanel.Sequence_RVDocSum))



The *abfT* gene in pASK-IBA3(+) was expressed in standard-I medium with carbenicillin and chloramphenicol. To improve the yield of the protein, the expression was tested at different temperature (37 °C, 30 °C and room temperature) and induced by AHT 200 µg/L. As shown in Fig 3-16 and 3-17, a carefully controlled growth was required to obtain high yield purification of the recombinant protein. At 37 °C and 30 °C no obvious expression was detectable, but at room temperature the SDS-PAGE exhibited an efficient expression in *E. coli* strain.

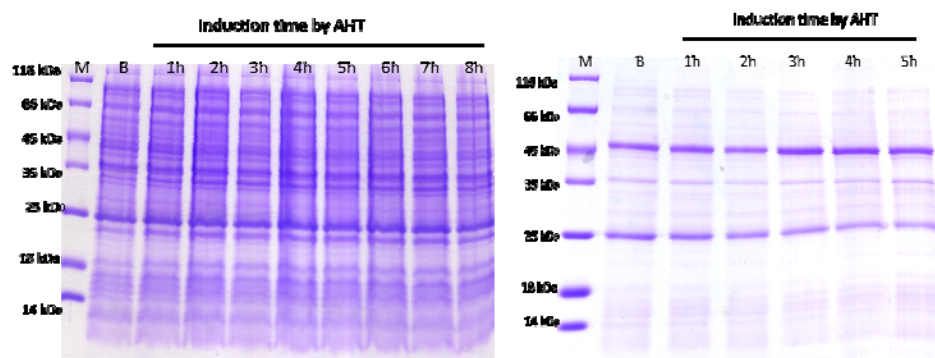


Figure 3-16. Test of *abfT* expression condition at 37 °C 30 °C. M, molecular mass marker; B, cell free extract before induction; 1-8 h, cell free extract with different induction time.

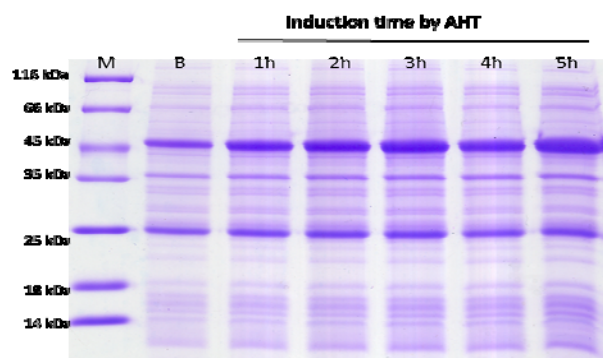


Figure 3-17. Test of *abfT* expression condition at room temperature (22-25 °C)

### 3.2.3 Protein purification and analysis

The protein purification was performed under aerobic conditions with a StrepTactin column. The eluted AbfT were stored at  $-80^{\circ}\text{C}$  without loss of activity for several months and analyzed by SDS-PAGE (Fig 3-18).

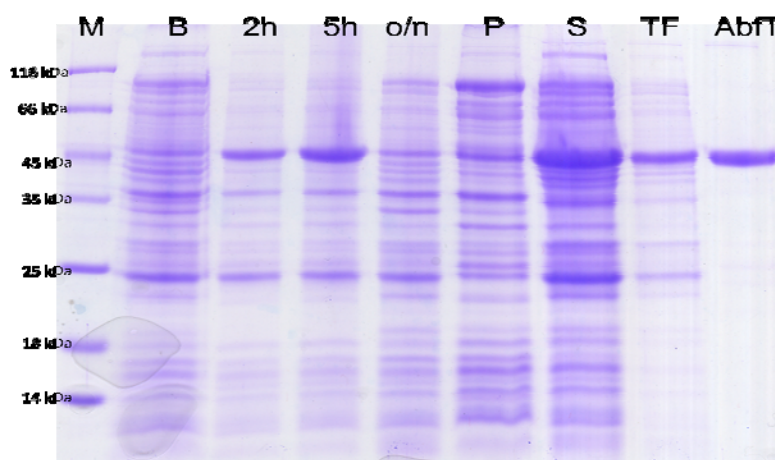


Figure 3-18. SDS-PAGE of recombinant AbfT purification in *E. coli*.

M, molecular mass marker; B, cell free extract before induction; 2h, 5h and o/n, cell free extract after induction for 2, 5 h and overnight; P and S, pellet and supernatant after sonication and ultracentrifugation; TF, flow through from Strep-Taction column; AbfT, purified recombinant 4-hydroxybutyrate CoA-transferase.

#### Enzymatic properties and substrate specificity

The purified protein revealed a specific activity of 170–181 U/mg using butyryl-CoA as substrate instead of 4-hydroxybutyryl-CoA, due to the instability of the latter. It is a colorless enzyme, which indicates no additional cofactor in the protein, such as an iron-sulfur cluster. In order to ascertain the substrate specificity of the enzyme the activity was measured with a different CoA-donor (Tab. 3-7). The highest activity of the CoA-transferase was obtained by adding butyryl-CoA in the enzyme assay, followed by propionyl-CoA (142 U/mg), vinylacetyl-CoA (96 U/mg)

and 4-hydroxybutyryl-CoA (41 U/mg). The activity was undetectable with *trans*-crotonyl-CoA as the CoA-donor. The instability and ease of degradation of 4-hydroxybutyryl-CoA could lead to apparently reduced CoA-transferase activity.

### 3.2.4 Mutagenesis in the active site of 4-hydroxybutyrate CoA-transferase

#### Determination of glutamate residue coordinated with CoAS-moiety of acyl-CoA substrate

Glutaconate CoA-transferase from *A. fermentas* and propionate CoA-transferase from *C. propionicum*, both contain a highly conserved glutamate residue ( $\beta$ E54 and E324, respectively) in the active centre. This acts as a nucleophile to attack the thioester carbonyl. The amino acid sequence alignment of 4-hydroxybutyrate CoA-transferase exhibited two conserved glutamate residues, E195 and E238 (Fig. 3-13, colored in red). In order to verify our hypothesis, E238 as the most likely candidate for the formation of the enzyme-CoA thioester intermediate was mutated to glutamine, alanine, serine and aspartate. After purification with affinity chromatography, the activities of the mutants were measured and compared to that of the wild type. The yields of purified mutants E238Q, E238A and E238S were 41 – 67% of that of wild type, except E238D that showed a very low expression rate (2%). Interestingly, only this E238D mutant retained a remarkable CoA-transferase activity (30 – 35 U/mg, 20% of the wild type), the specific activities of other mutants were negligible (0.04 – 0.05%) or not measurable. It has been found in glutaconate CoA-transferase from *A. fermentas* that the single amino acid replacement  $\beta$ E54D resulted in a reduced CoA-transferase activity and an appearance of acyl-CoA hydrolase activity. According to this, the acyl-CoA hydrolase of these three mutants were also assayed. Unfortunately, all of them indicated no acyl-CoA hydrolase activity (Tab. 3-7).

Table 3-7. Specific activities of E238 mutants in comparison to the wild type.

	Obtained protein concentration (mg/ml)	Specific activity of CoA-transferase (U/mg)	Activity relative to that of wt (%)	Specific activity of acyl-CoA hydrolase (U/mg)
Wild type	2.7	170-181	100	0
E238Q	1.1	0.07	0.04	0
E238D	0.1	30-35	20	0
E238A	1.4	0.1	0.05	0
E238S	1.8	0	0	0

The substrate specificity of E238D mutant was same as that of wild type. With butyryl-CoA as the CoA-donor, the E238D mutant exhibited the highest activity, which is 20% of the wild type activity. Almost all of the substrate specificity showed a reduced activity to 17 - 20%. However, using 4-hydroxybutyryl-CoA the activity decreased to 11%. This is likely to be due to the degradation of 4-hydroxybutyryl-CoA under storage (Tab. 3-8).

Table 3-8. Specific activities' comparison using different CoA-donors.

CoA esters	Wild type specific activity (U/mg)	E238D specific activity (U/mg)
Vinylacetyl-CoA	96	16.3 (17%)
Crotonyl-CoA	0	0
Propionyl-CoA	142	24 (17%)
4-Hydroxybutyryl-CoA	41	4.5 (11%)
Butyryl-CoA	181	35 (20 %)

### 3.2.5 Crystal structure analysis

The produced recombinant CoA-transferase *abfT* in 50 mM Tris/HCl, pH 7.0 and 200 mM 200 NaCl was sent for crystallization (Group of A. Messerschmidt, MPI of Biochemistry).

The crystal structure revealed a homodimeric protein, which consists of subunits A and B. Both molecules are built up by seven parallel  $\beta$ -sheets flanked by  $\alpha$ -helices on both sides of the sheet (Fig 3-19). Subunit A has two  $\alpha$ -helices at the N-terminus, and subunit B has an additional antiparallel  $\beta$ -strand at the C-terminal end of the sheet and two  $\alpha$ -helices at the C-terminus.

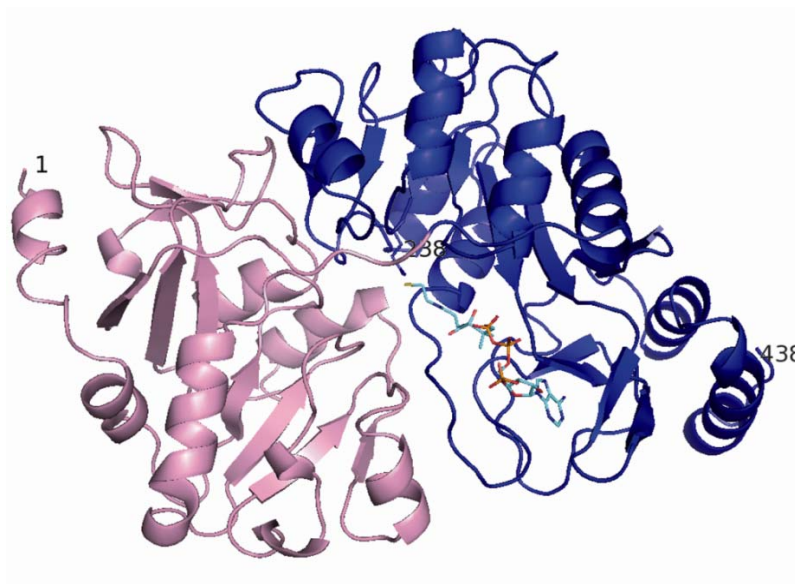


Figure 3-19. Crystal structure of homodimer AbfT from *C. aminobutyricum*.

Subunit A and B are colored in pink and blue

The active site is a narrow channel between A and B subunits which extends to the glutamate residue 238 in the active site. It was studied by crystallization with a spermidine in the active site (Fig 3-20, left). The electron density map showed that the amino group of spermidine builds a salt bridge with the carboxyl group of E238. The putative binding pocket for the 4-hydroxybutyrate substrate is filled with several water molecules.

Interestingly, two pockets can be seen in the crystal structure (Fig 3-20, right). They are situated at the both side of the active site E238. The left pocket with H31 at the bottom refers to the binding site for either the acetyl-CoA or the acyl-CoA and the right pocket with Q213 at the bottom could represent the co-substrate binding site. However, this pocket is rather broad and little characteristic for specific binding of 4-hydroxybutyryl-CoA. To confirm this hypothesis, the substrate binding pockets were studied using site directed mutagenesis in next chapter.

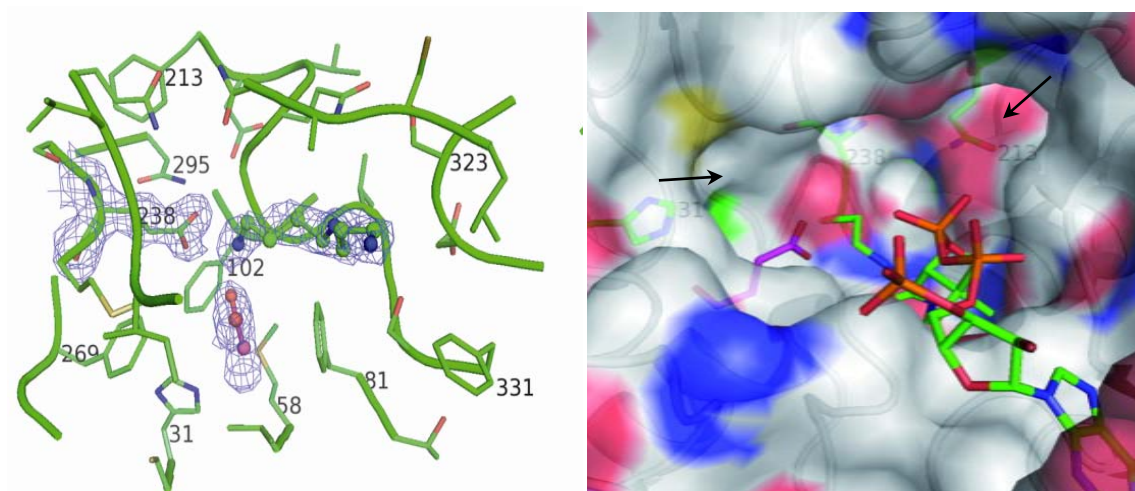


Figure 3-20. Active site of AbfT from *C. aminobutyricum*.

Left: the active site occupied by spermidine (blue) and water molecules. In addition, an acetate molecule (red) was manually docked into the active site. Right: the surface of active site including the glutamyl-CoA as bound in AbfT from *S. oneidensis*.

### Determination of substrate binding pocket using mutagenesis

The successful expression of *abfT* in *E. coli* facilitated the possibility to analyze the functions of conserved amino acid residues by site directed mutagenesis. The residues, which were deduced from the 3D structure to be important for the substrate binding, were studied by mutagenesis. The yields of mutants and their activities were measured and compared as stated in Table 3-9.

To determine the roles of H31 in the substrate binding pocket, it was replaced by several amino acids. H31S and H31G exhibited 2% of that of wild type and inactive, respectively, while H31A and H31N mutants had activities of 71% and 183%, respectively. However, their activities decreased significantly during storage at – 20 °C. The mutants M58S and M58T were constructed, in order to examine the influence of a hydrophilic group close to the imidazole ring in H31. Both of them showed reduced activities (15% and 40% of wild type activity, respectively). In contrast to the H31 mutants, the M58 mutants retained stability during storage at – 20 °C with no activity loss after 24 hours. Other investigated residues were the conserved Q213 (Fig 3-13). It was replaced by serine and also by threonine, in order to find its roles as hydrogen bonding forming residue in a putative separate co-substrate binding site. Both mutants were found to be inactive. Furthermore three double mutants H31A/D139A, H31A/S137A and H31A/M58S were made to ascertain the reason that H31A has relative higher activity than expected. All of them indicated the specific activities of 60%, 6% and 3%, respectively. As for the H31 mutants, the activities of these three double mutants exhibited instability during storage at – 20 °C.

## Results

Table 3-9. Yields and specific activities of the AbfT mutants.

Mutants	Protein concentration (mg/ml)	Specific activity (U/mg)	Specific activity relative to that of wt (%)	Specific activity after 24 h storage at - 20 °C (U/mg)
Wild type	2.7	170 - 181	100%	160
H31S	0.04	3.0	2%	2.2
H31G	0.14	0.5	0	0.5
H31N	0.8	320	183%	137
H31A	0.2	125	71%	8
M58S	4.2	27	15%	30
M58T	1.7	70	40%	68
Q213S	0.1	≤ 1.0	0	≤ 1.0
Q213T	0.13	≤ 0.5	0	≤ 0.5
Double Mutants				
H31A/D139A	1.0	105	60%	2
H31A/S137A	0.02	10	6%	< 0.5
H31A/M58S	4.0	5	3%	< 0.5



### Crystal structure of AbfT & butyryl-CoA complex

The crystal structure of enzyme-butyryl-CoA complex has been determined at a resolution of 2.6 Å. The butyryl-group of substrate is located in an approximate *syn*-conformation in the left-hand pocket (H31 at the bottom) of the enzyme, which has been identified in the previous chapter. Unexpectedly, butyryl-CoA was not observed to react with the active site glutamate (Figure 3-21). However, the binding of butyryl-CoA with enzyme causes a flip of the active site loop (residues 215-219) from an open conformation in the apo-form to a closed conformation in the enzyme-substrate complex. This conformation change is likely characteristic for all family I CoA-transferase.

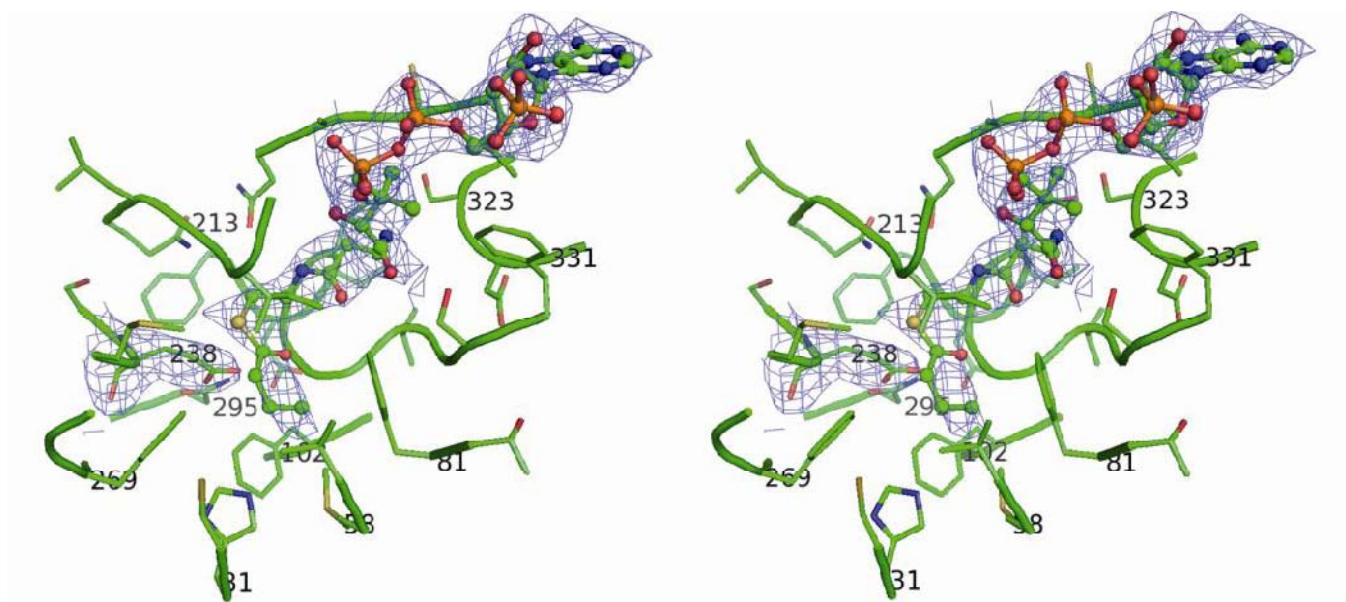


Figure 3-21. Stereo view of butyryl-CoA as substrate in the active centre.

The protein sequence and the structure of AbfT revealed a similarity to that of the  $\alpha$ -subunit of the family II enzyme – citrate lyase, which does not form the enzyme-CoA thioester intermediate in its catalytic pathway. To uncover the existence of this glutamyl-CoA thioester, three different methods were applied: reduction by sodium borohydride ( $\text{NaBH}_4$ ) to the inactive alcohol, mechanism based fragmentation of the peptide chain by heating at 70 °C and the kinetic determination.

### Inactivation of AbfD by sodium borohydride or hydroxylamine

In the case of CoA-transferase family I, the reaction proceeds via a ping-pong mechanism, involving the formation of a glutamyl-CoA thioester intermediate, which could be reduced by  $\text{NaBH}_4$  or cleaved by hydroxylamine [99-101]. The treatment with  $\text{NaBH}_4$  results in the reduction of the glutamyl-CoA thioester to the corresponding alcohol, whereas hydroxylamine could cleave the thioester bond generating a hydroxamate and free CoA.

Therefore, purified AbfT 600  $\mu\text{g}$  was incubated with 2 mM butyryl-CoA for 5 – 20 min, and then treated with 20 mM  $\text{NaBH}_4$  or 200 mM hydroxylamine. The enzyme in the absence of butyryl-CoA acts as control. The results exhibited that CoA-transferase treated with butyryl-CoA was inactivated almost completely by  $\text{NaBH}_4$  (0.7% residual activity), whereas in the absence of butyryl-CoA the activity of AbfT was hardly affected (Fig. 3-22). Surprisingly, longer incubation with  $\text{NaBH}_4$  reactivated the enzyme to a small extent. Similar results have been observed with all of family I and III CoA-transferases.

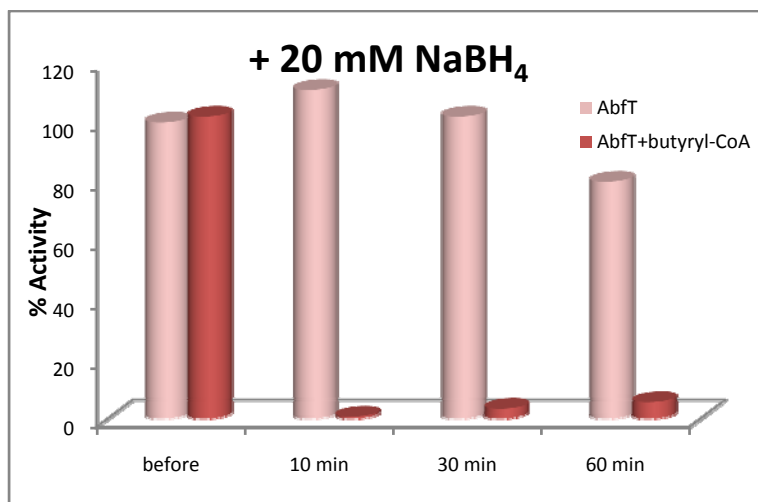


Figure 3-22. Inactivation of 4-hydroxybutyrate CoA-transferase by  $\text{NaBH}_4$  in the presence or absence of butyryl-CoA. Light red bars are in the absence of butyryl-CoA and dark red bars are in the presence of butyryl-CoA.

However, incubation of the enzyme with 200 mM hydroxylamine did not result in inactivation of CoA-transferase (Fig. 3-23). In order to ascertain the function of hydroxylamine on CoA thioester intermediate of family I CoA-transferase, glutaconate CoA-transferase as a well studied CoA-transferase was also treated by hydroxylamine. After 10 min 77% activity was retained as shown in 4-hydroxybutyrate CoA-transferase. In comparison to prior publications, only the thioester intermediates of propionate CoA-transferase (family I) and 2-hydroxyisocaproate CoA-transferase (family III) are known to react with hydroxylamine.

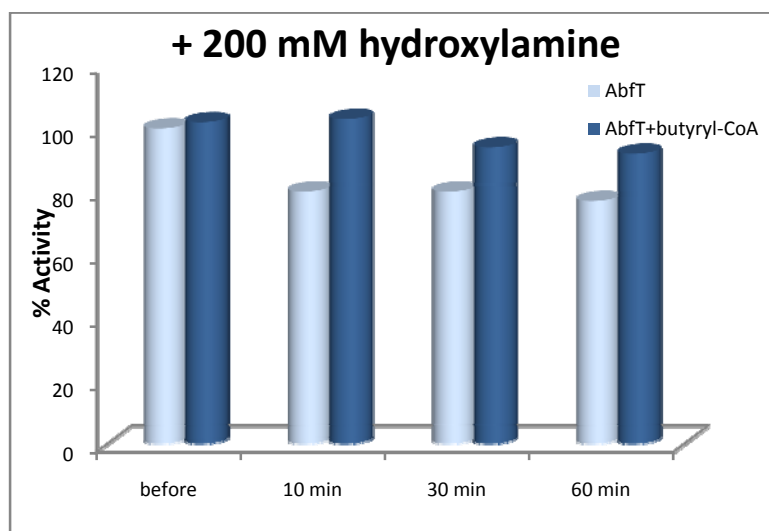


Figure 3-23. Inactivation of 4-hydroxybutyrate CoA-transferase by hydroxylamine in the presence or absence of butyryl-CoA. Light bars are in the absence of butyryl-CoA and dark bars are in the presence of butyryl-CoA.

#### Mechanism-based fragmentation of the peptide chain

In a previous publication it has been shown that the glutamyl-CoA thioester intermediate from succinyl-CoA: 3-keto acid CoA transferase in pig heart was susceptible to fragmentation at 70 °C [102]. To ascertain the existence of this intermediate from 4-hydroxybutyrate CoA-transferase, AbfT was incubated with 2 mM butyryl-CoA at room temperature for 5 – 20 min. Afterwards, the protein solution was heated at 70 °C up to 1 hour. The protein components were identified by gel electrophoresis.

The protein sequence of AbfT possesses 438 amino acids, and the protein molecular mass was calculated to be about 48 kDa. The active-site glutamyl residue is located at residue 238. Therefore, fragments of 23 kDa and 25 kDa were expected. The results were shown in Fig. 3-24, which revealed a small but significant cleavage to a fragment about 24 kDa, but only when the enzyme-CoA thioester intermediate was formed. AbfT in the absence of butyryl-CoA could not fragment. Furthermore, to ascertain that the thioester is generated from the active site E238, the inactive E238A was also treated in the same way. As expected, no small fragment could be observed. The detection of only one peptide probably is due to lack of separation.

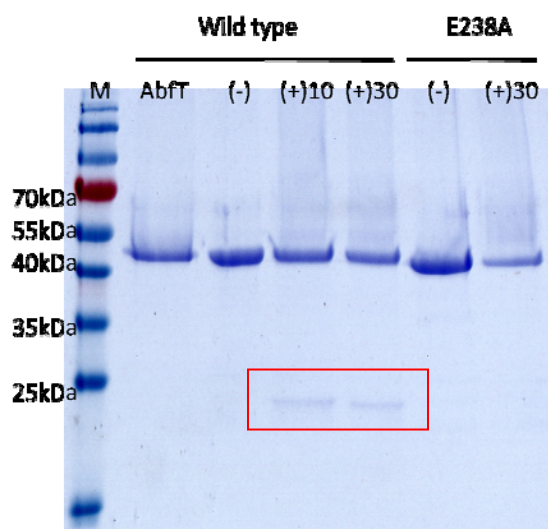
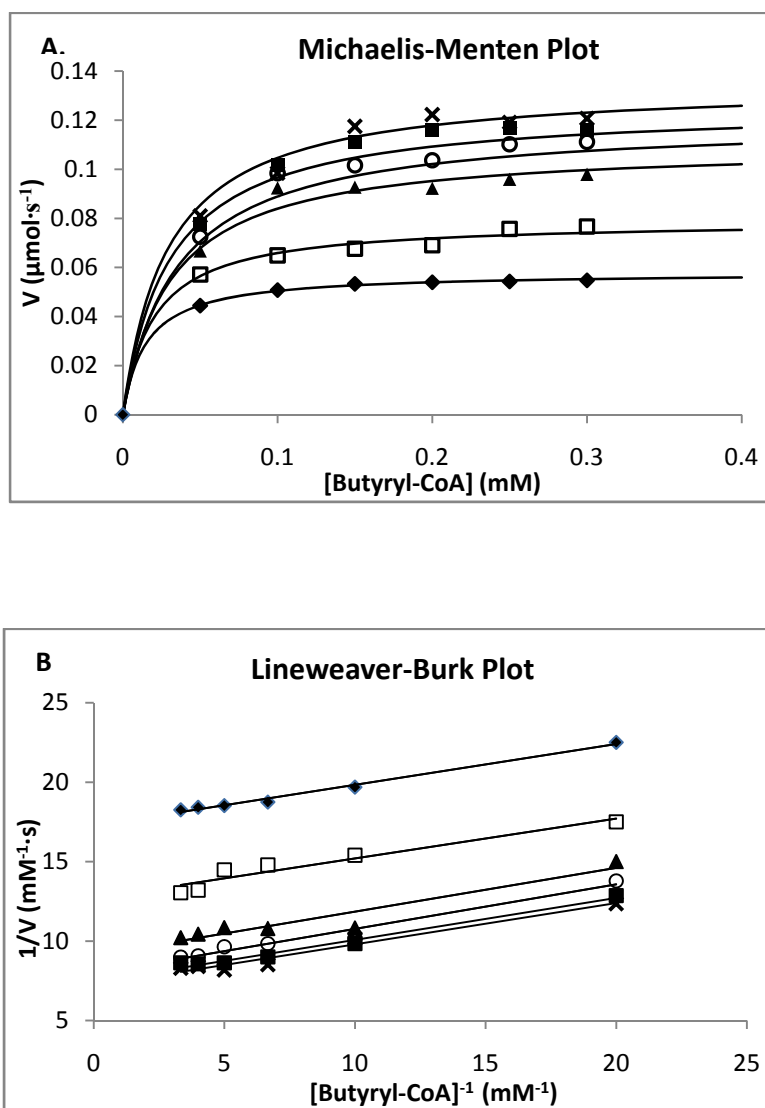


Figure 2-24. The mechanism-based fragmentation of CoA-thioester intermediate during CoA-transfer. AbfT, purified enzyme; AbfT (-), in the absence of butyryl-CoA and the protein was heated for 1 h at 70 °C; 10 and 30 min, the incubation time at 70 °C.

### Kinetics of 4-hydroxybutyrate CoA-transferase

Routinely, AbfT activity was assayed by a coupled assay, in which butyryl-CoA reacts with acetate to produce butyrate and acetyl-CoA. The formation of acetyl-CoA could be monitored by citrate synthesis, whereby the liberated CoASH was detected with DTNB. Using this coupled assay, no reliable  $K_m$  values for butyryl-CoA and acetate could be determined. In order to obtain

accurate mechanistic information on 4-hydroxybutyrate CoA-transferase from *C. aminobutyricum*, the reaction mixture contained butyryl-CoA, acrylate as substrate and 0.15 U CoA-transferase. The appropriate butyryl-CoA concentration ranges were chosen to be 0.05 – 0.3 mM, and acrylate varied between 5 – 30 mM. The activity was measured directly at 280 nm. As shown in the double reciprocal plots of Fig. 3-25 and 3-26, the data exhibited parallel lines.



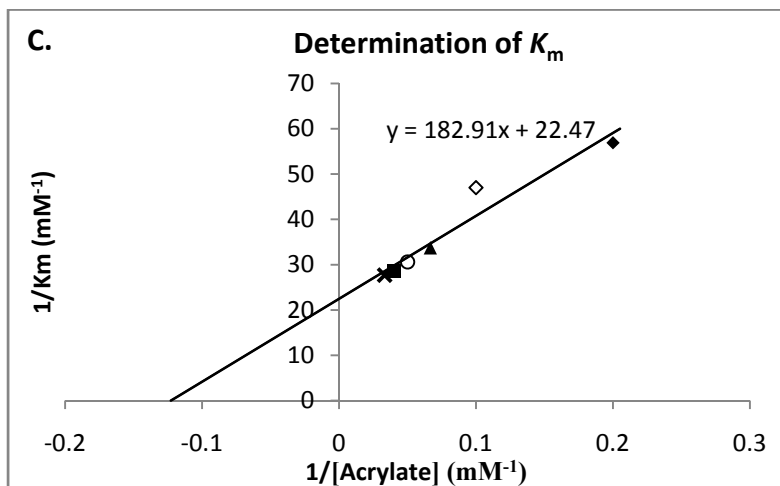


Figure 3-25. Kinetics of 4-hydroxybutyrate CoA-transferase.  $K_m$  for butyryl-CoA was determined at 5 mM ( $\blacklozenge$ ), 10 mM ( $\diamond$ ), 15 mM ( $\blacktriangle$ ), 20 mM ( $\Delta$ ) 25 mM ( $\blacksquare$ ) and 30 mM ( $\times$ ) acrylate. A. Michaelis-Menten plot; B. Lineweaver-Burk plot; C. determination of  $K_m$  for butyryl-CoA at saturating acrylate concentration.

The  $K_m$  for butyryl-CoA increased with rising concentrations of acrylate until saturation state (Fig. 3-25). To determine the apparent  $K_m$  values for butyryl-CoA, a curve using  $1/K_m$  as X-axis and  $1/[\text{butyryl-CoA}]$  as Y-axis was made.  $K_m$  for butyryl-CoA at saturating acrylate was calculated to be  $0.06 \pm 0.01$  mM,  $V_{\max}$  to be 0.13 U/mg (Tab. 3-10). The parallel lines suggests that reaction proceeds via a ping-pong mechanism, by which butyryl-CoA as substrate forms the enzyme-CoA thioester and the generated butyrate is released before the second substrate acrylate enters the catalytic pathway.

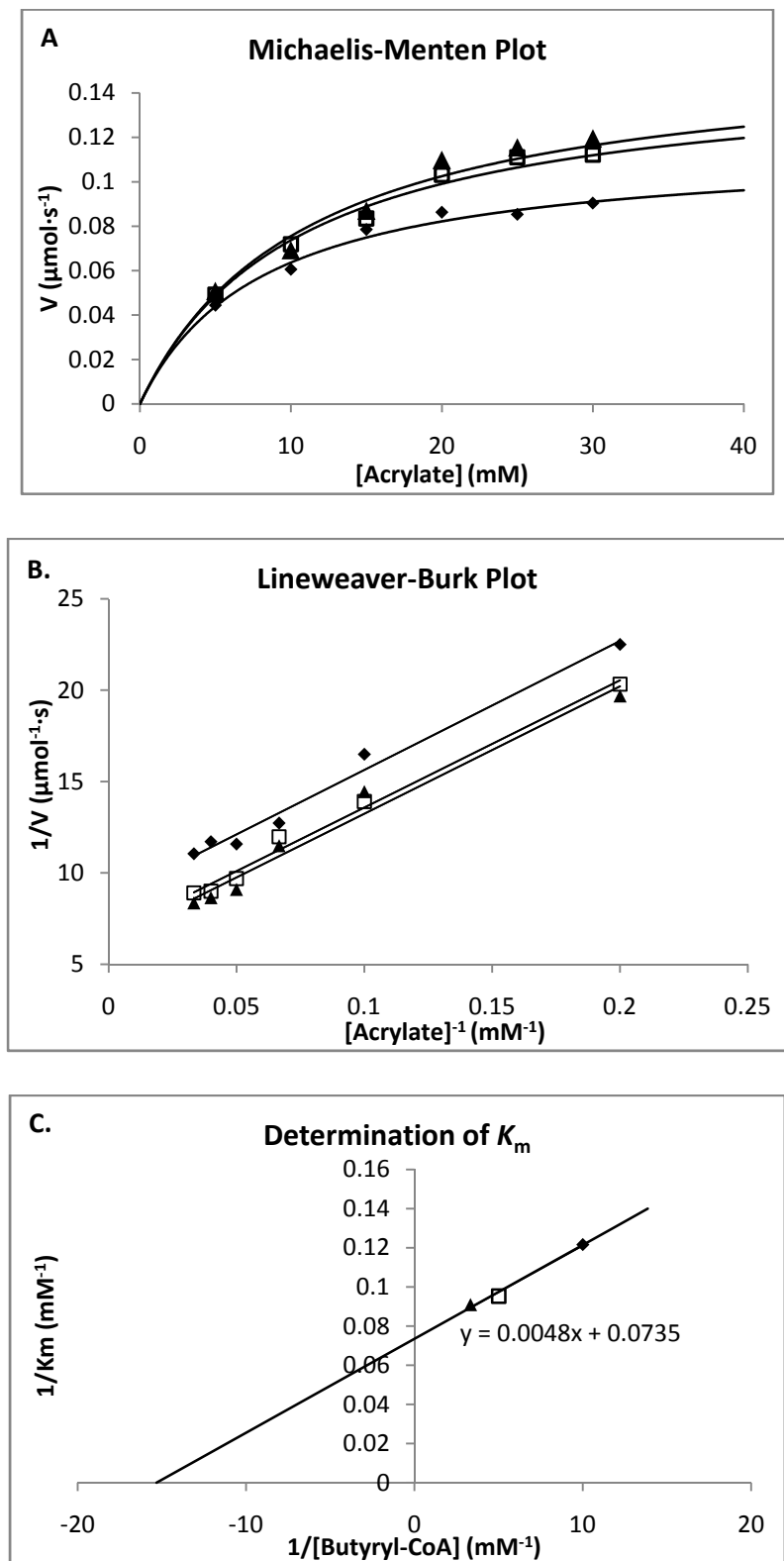


Figure 3-26. Kinetics of 4-hydroxybutyrate CoA-transferase.  $K_m$  for acrylate was determined at 0.1 mM ( $\blacklozenge$ ), 0.2 mM ( $\square$ ) and 0.3 mM ( $\blacktriangle$ ) butyryl-CoA. A. Michaelis-

Menten plot; B. Lineweaver-Burk plot; C. determination of  $K_m$  for acrylate at saturating butyryl-CoA concentration.

The data using acrylate as substrate gave at saturating butyryl-CoA  $K_m = 15 \pm 2$  mM,  $V_{max} = 0.16$  U/mg (Tab. 3-10). Although acrylate is not an optimal substrate as compared to 4-hydroxybutyryl-CoA, the lines clearly favor a ping-pong mechanism (Fig. 3-26).

Table 3-10. Summary of  $K_m$  and  $V_{max}$  under saturation conditions.

Substrate	Cosubstrate	$K_m$ (mM)	$V_{max}$ ( $\mu$ mol/min/mg)
Butyryl-CoA	Acrylate	$0.06 \pm 0.01$	0.13
Acrylate	Butyryl-CoA	$15 \pm 2$	0.16

### 3.3 4-Hydroxybutyryl-CoA dehydratase in CO<sub>2</sub>-fixation

Recently a new CO<sub>2</sub>-fixation pathway was found in *Achaea*, namely the 3-hydroxypropionate/4-hydroxybutyrate pathway. The genome of autotrophic *Metallosphaera sedula* unexpectedly showed two different copies of 4-hydroxybutyryl-CoA dehydratase, namely, MS\_1 and MS\_2. This part of the project aims to detect the functions of these two copies through the cloning of their genes in plasmids and analysis of purified recombinant proteins.

#### 3.3.1 Cloning and expression of two different 4-hydroxybutyryl-CoA dehydratases from *M. sedula*

The genes encoding two copies of 4-hydroxybutyryl-CoA dehydratase (MS\_1 and MS\_2) from *M. sedula* were amplified by Phusion-polymerase and desired primers containing restriction cut sites. The PCR products of *ms\_1* were digested and ligated into a pASK-IBA3(+) vector and



*ms\_2* into a pACYCDuet vector. Before sequencing, the clones were analyzed by using restriction enzymes (Fig. 3-27). The in IBA3 (+) ligated MS\_1 gene was digested by *Xba*I and *Xba*I/*Eco*37III, and MS\_2 in pACYCDuet by *Kpn*I and *Kpn*I/*Sac*I.

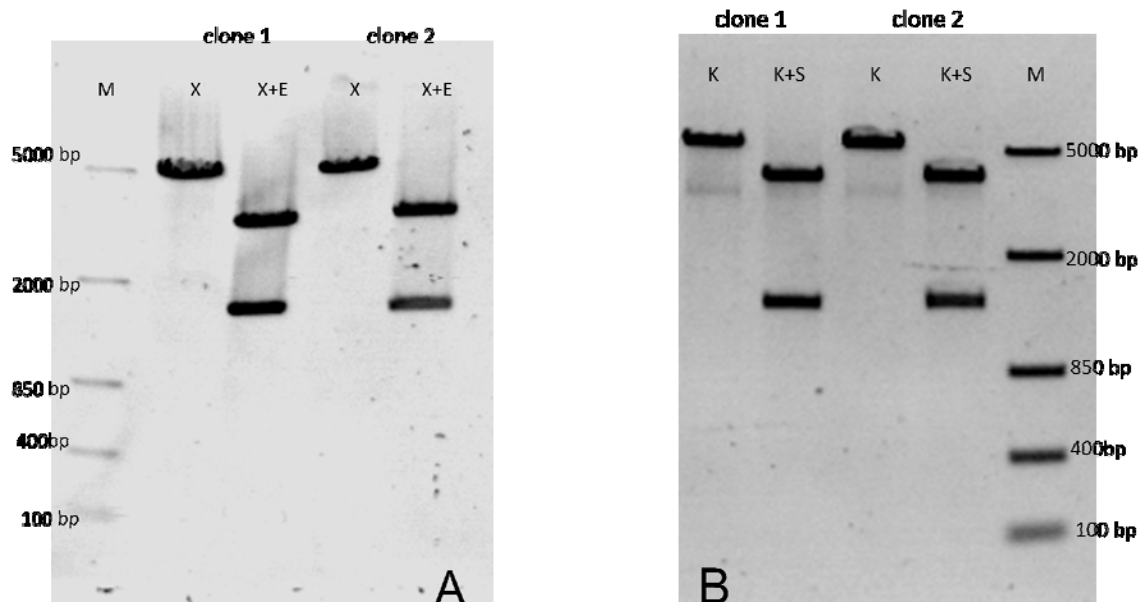


Figure 3-27. Restriction analysis of MS\_1 and MS\_2 from *M. sedula*.

X: digested with *Xba*I, X+E: digested with *Xba*I/*Eco*37III, K: digested with *Kpn*I, K + S: digested with *Kpn*I/*Sac*I.

After successful ligation in pASK-IBA3(+) and pACYC-Duet1 and transformation into *E. coli* BL21 CodonPlus-GroEL, the gene encoding MS\_1 was expressed in standard-I medium supplemented with 2 mM iron citrate, 0.27 mM riboflavin and antibiotics, and the gene of MS\_2 was expressed in same medium without iron citrate. The cells were grown aerobically at room temperature and induced by adding AHT (100µg/l) (*ms\_1* in pASK-IBA3(+)) and 1mM IPTG (*ms\_2* in pACYC-Duet1).

### 3.3.2 Protein purification

Recombinant MS\_1 from *M. sedula* was purified using a StrepTactin column. As shown in Figure 3-28, the resulting protein was checked for purity using SDS-PAGE and Coomassie staining after affinity purification. As expected, the protein found to have a molecular mass of ca. 55 kDa. Unfortunately, purified MS\_1 did not show 4-hydroxybutyryl-CoA dehydratase activity and revealed a low vinylacetyl-CoA  $\Delta$ -isomerase activity (2-3 U/mg), although the enzyme revealed a brown color.

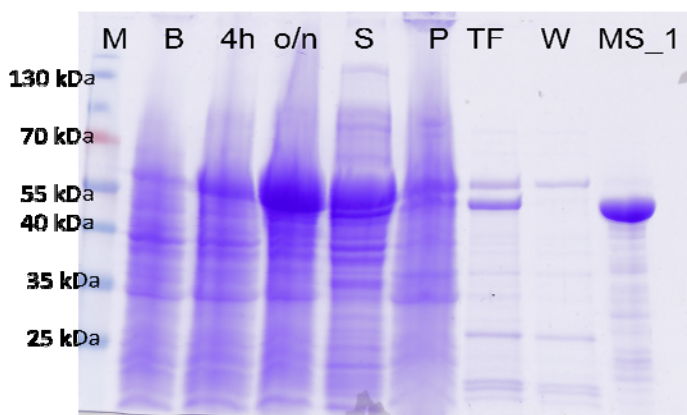


Figure 3-28. SDS-PAGE of recombinant MS\_1 purification.

M, molecular mass marker; B, cell free extract before induction; 4h and o/n, cell free extract after induction for 4 h and overnight; P and S, pellet and supernatant after sonication and ultracentrifugation; TF, flow through from StrepTaction column; W, flow through during column washing; MS\_1, purified recombinant 4-hydroxybutyryl-CoA dehydratase from *M. sedula*.

Up to now the gene expression of MS\_2 in *E. coli* host cells seems unsuccessful; there was no obviously expressed band on SDS-PAGE. It is hoped that further improvements can be made in this direction.

## 4. Discussion

### 4.1 4-Hydroxybutyryl-CoA dehydratase

#### 4.1.1 Recombinant 4-hydroxybutyryl-CoA dehydratase

In contrast to common dehydratases, some anaerobic organisms possess special dehydratases, which catalyze the removal of protons from non-activated  $\beta$ - or  $\gamma$ -carbons of 2-, 4- or 5-hydroxyacyl-CoA derivatives. An example is 4-hydroxybutyryl-CoA dehydratase from *C. aminobutyricum* which converts 4-hydroxybutyryl-CoA to crotonyl-CoA most likely via a ketyl radical intermediate. For the purpose of elucidating its catalytic mechanism, the recombinant protein was produced for biochemical studies.

To produce the soluble dehydratase in *E. coli*, a strong promoter *tet* and chaperones were used. Consequently, a new host cell, namely *E. coli* BL21-GroEL, was applied in this work. It contains extra copies of rare *E. coli* tRNA genes, *argU*, *ileY*, *leuU*, *proL*, and an additional gene for the molecular chaperone GroEL, which will be co-expressed during fusion protein production. It improves the appropriate folding of the proteins and avoids their self-association [103-105].

Moreover, without addition of cofactor sources, such as iron citrate and riboflavin in the nutrient medium for *E. coli* growth, no functional and active protein was detectable. Furthermore, the concentration of the cofactor sources could also influence the enzyme activity. Too low amounts cannot offer enough cofactor for protein assembly in its active form, and too high cofactor concentrations in the medium may be toxic for the bacteria or prevent growth. Therefore, the cofactor sources at optimal concentrations are also an important parameter to produce fully active enzyme.

Aside from these, the gene expression was tried under different conditions with varying inducer concentrations in order to increase the protein yield. The experiments showed that carefully controlled growth of the recombinant *E. coli* strains and a lower inducer concentration are

necessary for the production of high quality enzymes. Remarkably more soluble protein that is soluble was produced at low temperature 15 – 25 °C during a longer growth time. The protein solubility can also be improved by adding lower and moderate amounts of the inducer AHT (50 – 100 µg/l).

Growth of *E. coli* BL21-GroEL cells under aerobic and anaerobic conditions resulted in no differences of protein amount and solubility. Both conditions yielded the same active enzyme, in spite of the sensitivity of the dehydratase towards molecular oxygen. In order to yield sufficient cells and to improve the work efficiency, the host cells were grown aerobically, but the protein purification was performed under strict anaerobic conditions. With the help of the StrepTactin affinity chromatography, the produced fusion protein AbfD could be purified easily.

The successful production and purification of AbfD from *E. coli* offered the possibility to characterize the recombinant protein. The recombinant AbfD revealed to be a 232 kDa homotetramer with a subunit molecular mass of 56 kDa, containing  $11.8 \pm 0.1$  mol Fe and  $4.4 \pm 0.2$  mol FAD per homotetramer. In comparison to the theoretical value of cofactors, 16 mol Fe and 4 mol FAD per tetramer, the level of cofactors in the recombinant protein are relatively low. However, this is not surprising, since *E. coli* probably cannot offer the optimal environment for gene expression as *C. aminobutyricum*. Another possibility is that purification by StrepTactin column may also routinely decrease the content of iron and sulfide, which results in fewer cofactors in the recombinant protein.

The specific activity was calculated to be around  $2.2 \pm 0.3$  U/mg using 4-hydroxybutyrate and acetyl-CoA as substrates. Interestingly, reconstitution with iron and sulfide doubled the dehydratase specific activity to 4.5 U/mg. Aside from this, the measurable iron amount in the protein also increased close to the optimal value, 16 mol Fe per mol homotetramer. This indicated that the iron content plays a key role for dehydratase activity.

Like other iron containing proteins, AbfD is oxygen sensitive and unstable under aerobic conditions. Incubation of the dehydratase under air at room temperature resulted in rapid decrease of specific activity, which was completely lost in 5 hours. Even after storage at –20 °C or –80 °C a reduced activity was observed. Additionally, the inactivation of dehydratase by oxygen could not be reversed under reconstitution conditions.

The crystal structure of AbfD without substrate has been solved six years ago [46]. Interestingly, a structure similar to AbfD has been found in the FAD-containing medium chain acyl-CoA dehydrogenase (MCAD) from pig liver, which catalyzes the reversible oxidation of an acyl-CoA derivative to generate the  $\alpha$ ,  $\beta$ -double bond in the corresponding enoyl-CoA. The AbfD and MCAD monomers revealed a highly similar fold (Fig 4-1, left), whereas the two enzymes showed only 16% amino acid sequence identity. The related structures suggested, however, a similar substrate binding mode for the respective substrates (Fig 4-1, right). Using MCAD as a model, in AbfD 4-hydroxybutyryl-CoA with its hydroxyacyl part has been located between the two prosthetic groups as a sandwich and fixed by two hydrogen bonds between its CoA-thiol ester carbonyl group and both the 2'-OH of FAD and A460 of the polypeptide backbone [46, 106]. Both enzymes, MCAD and AbfD, have to remove one proton from the non-activated  $\beta$ -position. However, in contrast to anaerobic dehydratase from *C. aminobutyricum*, the aerobic flavoprotein MCAD is devoid of an iron sulfur cluster. It has been assumed that AbfD could contain butyryl-CoA dehydrogenase activity, but none was measurable using active and air-inactivated recombinant AbfD. The EPR spectral analysis and MALDI-TOF mass spectrometry exhibited also no evidences that AbfD could act as a butyryl-CoA dehydrogenase.

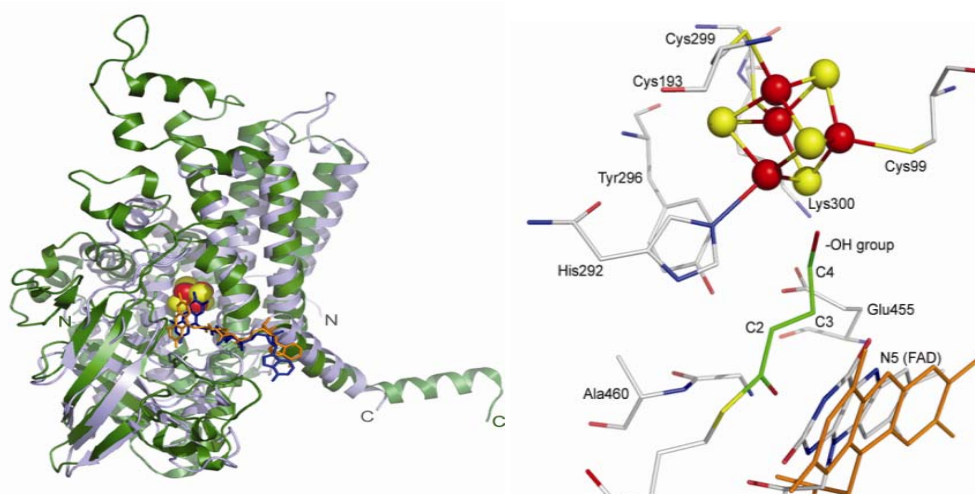


Figure 4-1. Stereo view of the structures of AbfD and medium chain acyl dehydrogenase from pig liver. Left, monomer structure of both enzymes, N and C termini of the polypeptide chains are labeled; Right, substrate binding mode of both enzymes, FAD from dehydrogenase is colored in orange.

4-Hydroxypentanoyl-CoA as a probable substrate or inhibitor for AbfD was measured using the standard enzyme assay, in which 4-hydroxybutyrate was replaced by 4-hydroxypentanoate. It neither acted as substrate nor inhibited the activity observed with 4-hydroxybutyrate. MALDI-TOF mass spectrometry indicated the successful synthesis of 4-hydroxypentanoyl-CoA by AbfT. This result showed that AbfT can use 4-hydroxypentanoate as substrate. The crystal structure suggested that the methyl group of 4-hydroxypentanoyl-CoA did not fit into the active centre.

#### 4.1.2 Mutagenesis of 4-hydroxybutyryl-CoA dehydratase

The successful expression and characterization of recombinant AbfD offered the possibility to study the most important amino acid residues involved in the catalytic mechanism by site-directed mutagenesis. The crystal structure and active site architecture of native has been already solved as shown in chapter 1.4. All highly conserved residues located in the active centre were mutated.

The iron atoms of the  $[4\text{Fe-4S}]^{2+}$  cluster of each monomer are covalently bound to the protein by three cysteine residues, C99, 103, 299 and one H292 residue. Accordingly, the mutants C99A, C103A, C299A and H292C and H292E contain only 50% of iron and 75% of FAD compared with the wild type protein, which led to the inactivation of the recombinant protein. It demonstrated that the histidine and cysteine residues are crucial for the integrity of the iron sulfur cluster as a functional prosthetic group. These mutants also resulted in the structural degradation of the tetramer to dimers and monomers. These results indicated that the iron sulfur cluster is also necessary for the stability of the whole enzyme. In many iron sulfur cluster containing proteins, only cysteine residues coordinate the iron atoms. Therefore, H292 was mutated to cysteine or glutamate in order to uncover the role of the histidine residue. As expected, both mutants showed no dehydratase activity. Hence, it was proposed that H292 acts as a base to abstract the 2*Re*-proton of 4-hydroxybutyryl-CoA, and the now uncoordinated Fe atom functions as Lewis acid to eliminate the hydroxyl group. Therefore, the replacement of H292 by cysteine could stabilize the cluster, but inactivate the enzyme. However, the H292C mutant destabilized the cluster and inactivated the enzyme. Perhaps the distance is too long for the cysteine residue to attach to the

iron-sulfur cluster. The inactive H292E mutant shows that glutamate cannot replace histidine as a base.

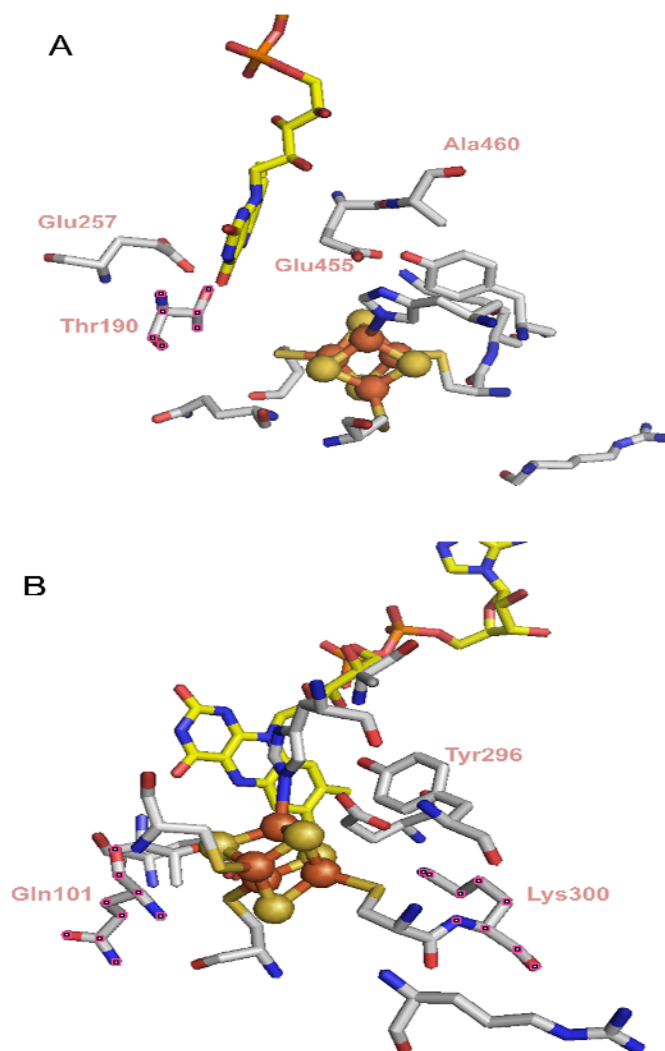


Figure 4-2. Active centre architecture.

A: stereo view from side; B: stereo view from upper.

Aside from this, mutants of three residues located in the active centre, Y296F, E455Q and E257Q were generated, whereas only Y296F retained 0.7% dehydratase activity. Both glutamate mutants completely lost activity, although they contain similar cofactor amounts and maintained a homotetrameric structure as the wild type protein. It was postulated that upon substrate binding in

the active site, the electron transfer could proceed via Y296, which is in hydrogen bonding distance to E455. In addition, E455 is at hydrogen bonding distance to K300 (Fig 4-2), which together with Y296 belongs to the helix coordinating the  $[4\text{Fe-4S}]^{2+}$  cluster. Moreover, E455 is ideally positioned to add a proton at the C4-position of substrates, either 4-hydroxybutyryl-CoA or vinylacetyl-CoA. E257, as another highly conserved residue among all known 4-hydroxybutyryl-CoA dehydratases, is located on the *Si*-side of the FAD isoalloxazine ring, and has a strong interaction at hydrogen bonding distance between its carboxyl group and the hydroxyl group of T190. A replacement of T190 by valine resulted in an over 99% drop-off of specific activity. It was considered that T190V may alter the redox potential of flavin and be involved in the stability of flavin in cooperation with E257. The structure modelling of 4-hydroxybutyryl-CoA as substrate in the active centre of the dehydratase indicated that the CoA-thiol ester carbonyl group is at hydrogen bonding distance to the 2'-OH of FAD and the backbone amide of A460. The replacement of alanine by glycine caused a reduced activity (2% residual activity). Because glycine is much more conformational flexible, the substrate cannot be held in the appropriate position. Besides this, Q101 is located in the N-terminal domain and anchors the loop with C99 and C103 to the middle domain via interactions at hydrogen bonding distance with N194, and Q101 also helps to fix C103 through interactions at hydrogen bonding distance between its main chain and the carbonyl group of C103. The same interaction occurs also between C99 and Q101. The exchange of this conserved Q101 to glutamate may not much influence this network of interactions, and thereby Q101E retained about 10 % dehydratase activity.

#### 4.1.3 Vinylacetyl-CoA $\Delta$ -isomerase

AbfD possesses also vinylacetyl-CoA  $\Delta$ -isomerase activity, which catalyzes the irreversible isomerization of vinylacetyl-CoA to crotonyl-CoA. The specific activity as an isomerase was calculated to be 18 U/mg, which could not be improved by iron reconstitution. Upon exposure to air, the dehydratase activity was completely lost in 5 hours. However, the isomerase was more stable, after 24 hours 10% activity retained without further loss within several days and weeks.



In order to investigate the difference in mechanism between dehydratase and isomerase, a few mutants, which were likely to be important, were measured using an isomerase assay. Remarkably, only H292E and C99A (0.2 and 0.25 U/mg, respectively) mutants revealed very low isomerase activities, which disappeared after incubation under aerobic conditions, whereas C103A and C299A carried more activity (3.1 and 14 U/mg, respectively) that persisted under air (1.8 and 14 U/mg). As shown in figure 4-3, the Fe atoms coordinated to H292 and C99 are located closed to the substrate-binding channel, whereas the Fe atoms coordinated to C103 and C299 are located further from the active centre. Thus, the results show that the isomerase does not require the iron sulfur cluster as functional prosthetic group, although the H292 and C99 residues play an important role for isomerase.

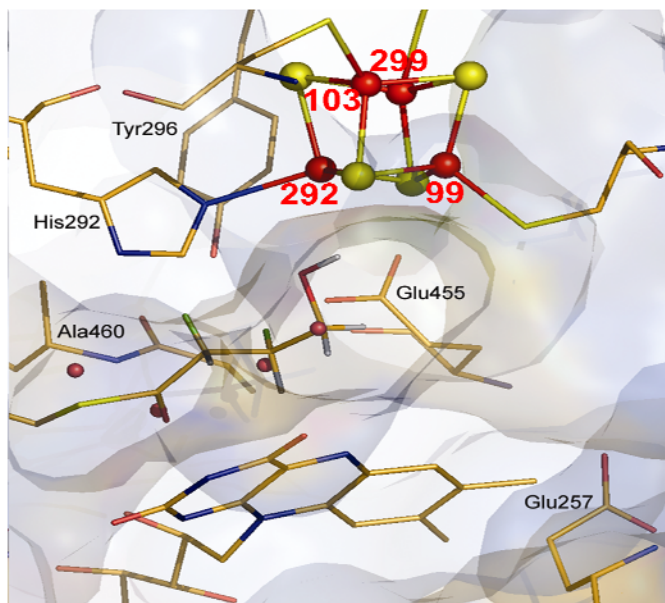


Figure 4-3. Fe atom positions in the stereo view of crystal structure.

The isomerase activity of E257Q, E455Q and Y296F mutants were also tested. The E257Q mutant exhibited an isomerase activity almost as high as that of the wild type protein (17 U/mg). It was unexpected that even upon exposure to air the mutant did not lose any isomerase activity. This confirms that E257 as well as FAD are not involved in the catalytic reaction. The Y296F mutant exhibited relatively high isomerase activity (9.4 U/mg, 52%), and after exposure to air the activity decreased to 4.4 U/mg (24%). Probably there is no electron transfer via Y296 during

isomerisation. Interestingly, the mutant E455Q revealed a low isomerase activity (1.3 U/mg, 7%). Most likely E455 plays a role in proton translocation, therefore, the displacement of glutamate residue by glutamine interferes with the proton transport during catalytic reaction. All of these results supposed that H292 could abstract the 2*Re*-proton of vinylacetyl-CoA as a base, whereas C99 helps the histidine residue to dock at the appropriate position.

#### 4.1.4 Proposed AbfD mechanism via a ketyl radical

A fully active recombinant AbfD requires the assembly of cofactors in the protein, such as FAD and the iron sulfur cluster. Iron sulfur clusters are often discussed as cofactors, and have been found in a variety of metalloproteins. They play a role in oxidation-reduction reactions, radical generation, and act as sulfur donors for biosyntheses [61-63]. The long distance between Fe<sub>1</sub> atom and Nε<sub>2</sub> of H292 (2.4 Å) suggested the tuning of the electronic and bonding properties of Fe<sub>1</sub>, which is ideally positioned to interact with the hydroxyl group of the substrate [46]. In presence of the substrate, the redox potential of the [4Fe-4S]<sup>2+</sup> cluster is increased by ca. 200 mV [53], which indicates alternation of the cluster environment and direct interaction between cluster and substrate. In addition, H292 is located at 3 Å distance to 2*Re*-proton (modelled), which makes this residue ideally positioned to abstract this proton as a catalytic base. The replacement of H292 by C or E abolished the AbfD activities, impeding the removal of 2*Re*-proton from substrate. Furthermore, H292 has a similar structural position as the active base in MCAD. Therefore, we proposed that in the first step of the dehydratase mechanism, the substrate 4-hydroxybutyryl-CoA enters the binding channel between the two prosthetic groups and consequently displaces the H292 residue from the Fe<sub>1</sub> atom. While the Fe atom acts as a Lewis acid to attach the hydroxyl group of the substrate, the released H292 residue acts as the base to abstract the 2*Re*-proton yielding the enolate.

The modeled distance between N5 of FAD and the 3*Si*-proton is ≈ 3 Å, which facilitates the removal of the 3*Si*-proton from the substrate. Two residues, E257 and T190, which are thought to participate in the stabilization of FAD according to the crystal structure, were replaced by Q and V. The mutants showed either none (E257Q) or only negligible activity (0.4 % in T190V

compared to that in the wild type). So in the next step an enoxy radical is generated by one electron oxidation using FAD forming the semiquinone anion, for which the 3*Si*-proton is acidified from  $pK$  40 to  $pK$  14 [7]. Now the flavin semiquinone anion as a base removes this proton to yield a neutral semiquinone  $FADH^\bullet$  and a ketyl radical. The released hydroxyl group attached to the  $[4Fe-4S]^{2+}$  cluster interacts with the removed 2*Re*-proton at H292 to form the water molecule. Now the flavin semiquinone reduces the dioxygen radical to the dienolate, whereby the initial quinone form of FAD is regenerated.

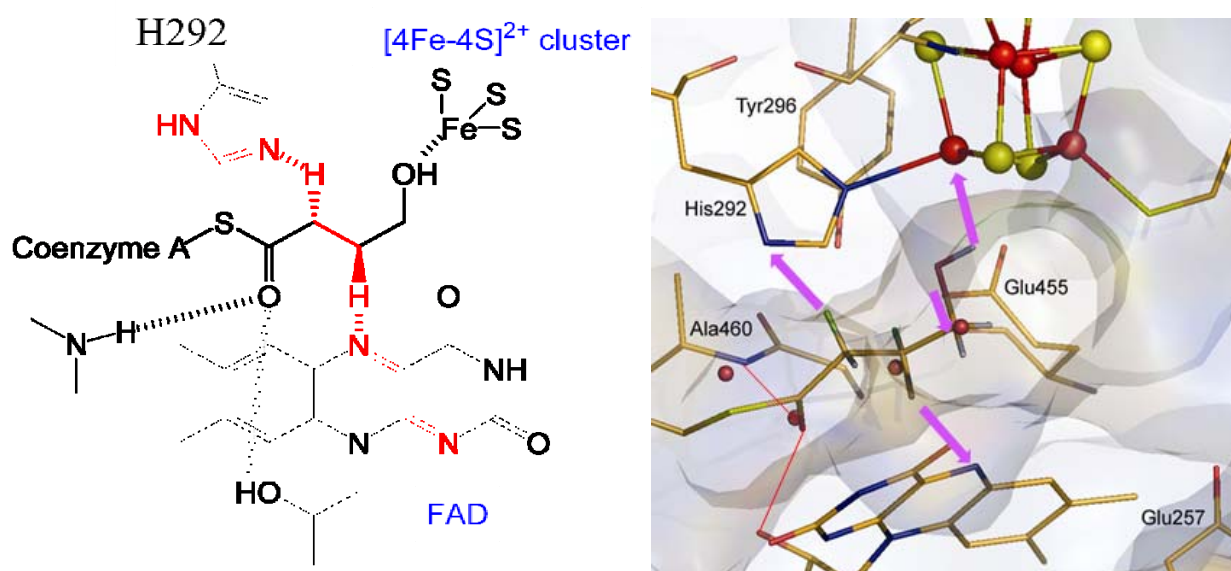


Figure 4-4. Proposed substrate binding during dehydration process.

E455 as a further highly conserved residue in all 4-hydroxybutyryl-CoA dehydratase is ideally positioned to add a proton at the C4-position with retention of configuration [57]. The substitution of glutamate's carboxylate by glutamine's amide suppresses the proton transfer from E455 to C4 of the substrate, which lead to the disappearance of the dehydratase activity. Therefore, in the final step, E455 transports a proton to C4 of the formed dienolate producing the end product crotonyl-CoA (Fig. 4-4).

Another goal of my work was to uncover the mechanism of AbfD as vinylacetyl-CoA  $\Delta$ -isomerase. The replacement of E257 by Q did not abolish the isomerase activity (92% residual activity); even after incubation with air, the mutant retained the identical isomerase activity. This indicates that FAD is not involved in the isomerization, because E257 is most likely responsible for the stability of the flavin [46]. The isomerase activity of H292E was diminished by about 99%, which confirmed the function of H292 as the base to remove the 2*Re*-proton not only from 4-hydroxybutyryl-CoA during dehydration, but also from vinylacetyl-CoA during isomerization (Fig. 4-5).

Now, it becomes logical that AbfD retained 10% of isomerase activity upon exposure to air in 24 hours, whereas it as dehydratase is completely inactivated by air within 5 hours. Because it was deduced that the released H292 from the destroyed iron sulfur cluster by air abstracts the  $\alpha$ -proton from vinylacetyl-CoA, resulting in the formation of a dienolate. Then, the dienolate is protonated by adding a proton by E455 at the C4-position to generate the end product crotonyl-CoA. The whole reaction does not require the  $[4\text{Fe-4S}]^{2+}$  cluster and FAD as cofactors. Following the breakage of the  $[4\text{Fe-4S}]^{2+}$  cluster by oxygen, however, the spatial configuration of the active site could be effected or changed, which leads to the slowly decreasing isomerase activity.

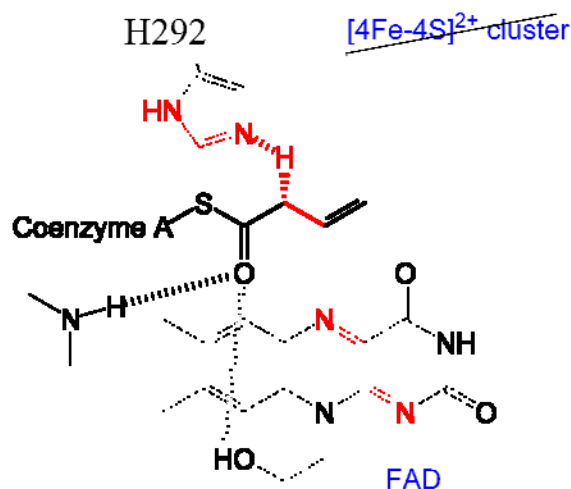


Figure 4-5. Proposed substrate binding during isomerization process.

## 4.2 4-Hydroxybutyrate CoA-transferase

4-Hydroxybutyrate CoA-transferase (AbfT) is involved in the fermentation of 4-aminobutyrate to ammonia, butyrate and acetate in *C. aminobutyricum*. The native enzyme has been purified and characterized several years ago, but the mechanism was not elucidated. In this chapter the gene *abfT* was cloned and the recombinant protein was purified and analyzed.

### 4.2.1 Recombinant 4-hydroxybutyrate CoA-transferase

The *abfT* gene encoding CoA-transferase was ligated into a pASK-IBA(+) vector, which is a vector designed for high level expression and purification of recombinant Strep-tag fusion proteins. After sequencing, three amino acid errors were corrected. Since AbfT is an oxygen-insensitive protein and requires no additional cofactor for catalytic reactions, the gene expression in *E. coli* BL21 strain was more effective than that of the oxygen sensitive AbfD. However, a carefully controlled growth was also required for a successful expression, and the expression exhibited a highest level at room temperature.

The molecular mass of the colorless recombinant AbfT with a C-terminal Streptag was calculated to be about  $2 \times 49$  kDa. The activity was measured at 412 nm using citrate synthase, oxaloacetate and DTNB, revealing a high specific activity between 170 – 181 U/mg with butyryl-CoA and acetate as substrate. Because the synthesized 4-hydroxybutyryl-CoA was unstable and degraded during storage, the specific activity with it as substrate amounts only to 41 U/mg, much less than observed previously [42]. Using propionyl-CoA, vinylacetyl-CoA and (*E*)-crotonyl-CoA as substrates the specific activities were 142, 96 and 0 U/mg, respectively). Compared to the native enzyme, the recombinant AbfT exhibited much higher specific activities with all tested CoA esters.

The kinetics of the recombinant AbfT are shown in Fig. 3-19 with butyryl-CoA as the substrate at different concentrations, double-reciprocal plots gave the parallel lines indicating a ping pong

mechanism. This demonstrates that AbfT belongs to family I of CoA-transferases. In family I the reaction proceeds via a ping pong mechanism, involving a glutamate residue in the enzyme acting as acceptor of covalently bound intermediates. This family contains CoA-transferases for 3-oxoacids, short chain fatty acids and glutaconate. The mechanism of CoA-transferase family I has been well studied as shown in Fig.4-6. Negative charged substrates, such as glutaconate, propionate and 4-hydroxybutyrate, are attached by the positive charges at the entrance of the active site. The carboxylate anion of the enzyme's glutamate residues attacks the carbonyl carbon of the substrate R1-CO-CoA to generate a mixed anhydride. Then the negative charged free CoA reacts with the carbonyl carbon of glutamate resulting in the displacement of the first product, R1-carboxylate. Subsequently, the substrate R2-carboxylate enters the reaction, and through a second mixed anhydride the CoA-group is transferred to yield R2-carboxylate. The whole catalytic cycle consists of four subsequent nucleophilic attacks on electrophilic carbonyl groups, alternately by carboxylate and thio anions.

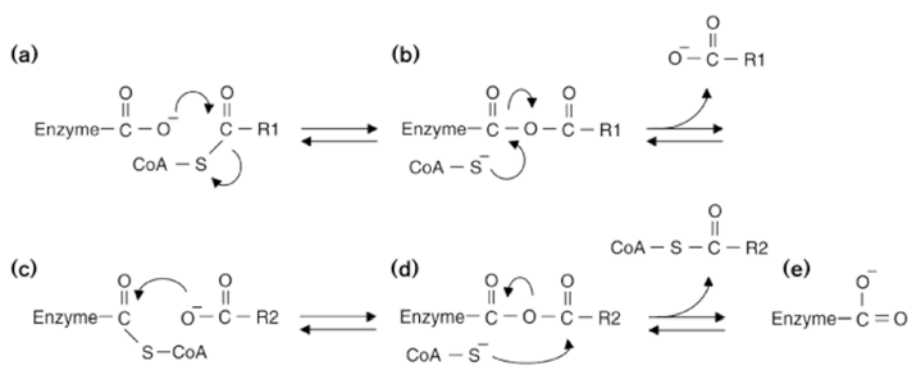


Figure 4-6. The reaction mechanism of CoA-transferases of family I.

The amino acid sequence of AbfT was compared to other CoA-transferases from various microorganisms including *Anaerofustis caccae*, *Prophyromonas gingivalis*, *P. unenonis*, *P. endodontalis*, *Fusobacterium nucleatum*, *Fusobacterium. sp.*, *Clostridium. tetani*, all of which revealed a high level of identity between 60 – 45%. As expected, a highly conserved glutamate residue has been recognized, which is located within a so-called EM-SDG motif. However, this

characteristic motif is found only in 4-hydroxybutyrate CoA-transferase, whereas propionate CoA-transferases have a motif of ENG and glutaconate CoA-transferases have a motif of E-G in the active centre. To ascertain the presence of the catalytic glutamate residue in the active site, it was characterized as described in the following chapter.

#### 4.2.2 Identification of the catalytic glutamate residue in the active site

From the amino acid sequences alignment and the two known structures of family I CoA-transferase, it was suggested that E238 was the most likely candidate for the formation of the enzyme-CoA thioester. To confirm it, E238 was mutated to glutamine, alanine, serine and aspartate. After successful expression in *E. coli* host cells and purification by a StrepTactin column, the yields of the mutant proteins were comparable to that of the wild type AbfT (41 – 67%), except that E238D which has a very low protein yield (2%). However, only this aspartate mutant retained 20% of the wild type specific activity, and all of others exhibited almost no CoA-transferase activity. As described in a previous publication about glutaconate-CoA transferase from *A. fermentas*, E54 of the  $\beta$ -subunit was also studied by mutagenesis [39]. The  $\beta$ E54D showed a low growth rate and a reduced protein yield similarly to E238D of AbfT. The specific activity of  $\beta$ E54D and two other mutants  $\beta$ E54A and  $\beta$ E54Q were negligible. However, the  $\beta$ E54D mutant exhibited a high hydrolase activity. Apparently, a water molecule can fit between the shorter aspartate residue and the thioester. Furthermore, upon incubation of the  $\beta$ E54Q mutant with a thioester, the transferase activity slowly recovered, probably due to transfer of  $\text{NH}_2$  instead of oxygen as shown in Fig. 4-6 (a, b). In contrast to glutaconate CoA-transferase, all AbfT mutants including E238D exhibited no acyl-CoA hydrolase activity, nor could the E238Q mutant be recovered. Moreover, the substrate specificity of the E238D mutant was identical to that of the wild type. Hence these results demonstrate that E238 plays a most important role for formation of the thioester intermediate, and AbfT appears to be much more flexible than glutaconate CoA-transferase, because the aspartate residue is able to take over the function of the glutamate residue.



### 4.2.3 Crystal structure and mutation studies

The successful purification and determination of the recombinant AbfT from *C. aminobutyricum* offered the possibility of uncovering its crystal structure, which was solved by the group of A. Messerschmidt (MPI of Biochemistry, Martinsried). The overall structure revealed a homodimeric protein with an elongated pocket between the C- and N-terminal domains or between the  $\alpha$ ,  $\beta$  subunits, which extends to the active site glutamate residue. It confirmed the determination of E238 as a key residue by site-directed mutagenesis in this work.

The three known 4-hydroxybutyrate CoA-transferase structures respective from *Shewanella oneidensis*, *Porphyromonas gingivalis* and *C. aminobutyricum* have been compared, which revealed a much related overall structure. The fold of the active site residues is identical in all three enzymes, as can be deduced by the amino acid sequence alignment. All of them contain a glutamate residue in the active centre bound to the CoA-thioester.

Moreover, it remained a question of the separate co-substrate binding site in AbfD hinted from glutaconate CoA-transferase. On the other hand, this enzyme is specific for C-5 and C-6 dicarboxylic acids like *trans*-glutaconate, *trans*-muconate as well as 2-hydroxyglutarate and glutarate. On the other hand, acetate, propionate, and to a lesser extent (*R*)-lactate, butyrate and *cis*-crotonate become esterified, which can be explained by the existence of two binding pockets. From the crystal structure of AbfT, two pockets have been seen. The left refers to the binding site for acetyl groups of CoA and the right could be the co-substrate binding site. Among the co-substrate binding pocket from the right side, Q213 could be the only residue for forming a hydrophilic contact to the 4-hydroxy group of 4-hydroxybutyrate, which is highly conserved in all 4-hydroxybutyrate CoA-transferases. However, 4-hydroxybutyrate could also be modeled into the left pocket with its C-1 carboxyl group in position of the acetyl carboxyl group and with the 4-hydroxy group in such a location that it can form hydrogen bonds to atom NE2 of H31. It is also conserved in the CoA-transferase from *P. gingivalis*, but in the enzyme from *S. oneidensis* H31 is replaced by a serine. To ascertain this hypothesis, the residues deduced from the 3D structure to be relevant for the substrate binding were mutated. The specific activities of the resulting proteins were measured and compared. H31G was expected to be inactive, because it does not provide a hydrophilic side chain. The reduced activity of H31S (2%) can be explained



by the shorter side chain of serine forcing the hydrophilic group deeper in the substrate pocket. In contrast to this, the H31N mutant has a longer side chain, and is able to make stronger hydrophilic contacts to the respective substrate, which can result in the enhancement of the activity (183%). Moreover, the relatively high activity of the H31A mutant cannot be explained easily. Surprisingly, it was observed in the crystal structure that S137 and D139 are located below the side chain of H31. Therefore, we considered it is also possible, when the side chain of H31 is removed by mutation to alanine, the substrate could have access to these hydrophilic groups. The mutants H31A/S137A and H31A/D139A exhibited CoA-transferase activities of 6 % and 60 %, which explained that S137 has ability to compensate the action of H31A mutant. It has to be considered, however, that all the activities were measured with butyryl-CoA as substrate. Therefore H31, which is thought to interact with the hydroxyl group of 4-hydroxybutyryl-CoA, is not necessary any more. This could explain the considerably higher activity of the H31N mutant as compared to that of the wild type.

Unexpectedly, all of H31 mutants are unstable upon storage at – 80 °C, especially in the case of H31N and H31A. Their activities were reduced from 320 and 125 U/mg to 137 and 8 U/mg, probably because the H31 residue is involved in the stability of the 3D structure.

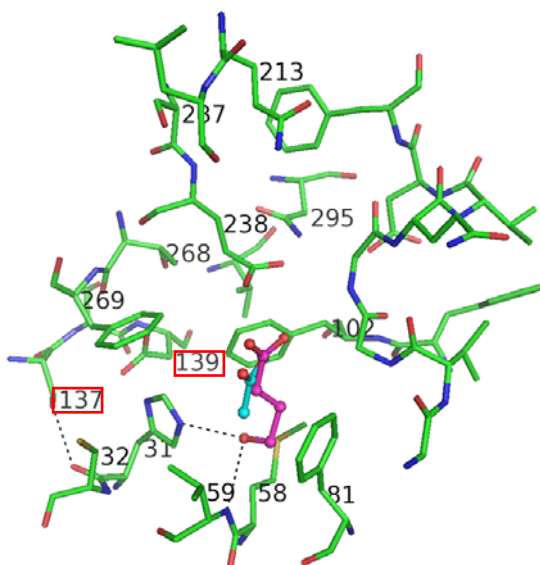


Figure 4-7. The position of S137 and D139 in the active centre. 4-hydroxybutyrate was manually docked into the substrate-binding pocket, which is colored in purple.

The mutants of M58S and M58T were made to examine the influence of a further hydrophilic group close to the imidazole ring of His31. Both mutants showed decreased activity (15% and 40%, respectively). The same value is valid for the double mutant H31A/M58S. The above evidence indicates that the hydrophilic group in place of M58 is not able to compensate for the action of His31.

#### 4.2.4 The crystal structure of enzyme & butyryl-CoA complex

The crystal structure of the complex between AbfT and butyryl-CoA has been determined at a resolution of 2.6 Å. The binding of butyryl-CoA in the active centre causes a conformational change of the active site loop from an open conformation in the apo-form to a closed conformation in the complex. The conformation change of this loop seems to be characteristic for all family I CoA-transferases. The butyryl-group is situated in an approximate *syn*-conformation in a substrate binding pocket, which has been identified in the mutation studies (4.2.3). This phenomenon could be the explanation, why AbfT cannot accept (*E*)-crotonyl-CoA as substrate. Similarly, glutaconate CoA-transferase, as a well studied family I CoA-transferase, accepts acetate, propionate, butyrate, (*Z*)-crotonate, glutarate and (*E*)-glutaconate, but not (*E*)-crotonate and (*Z*)-glutaconate [38]. Unexpectedly, the good substrate butyryl-CoA did not react with the active site glutamate of AbfT. A possibility for this result could be that no such thioester intermediate is formed at all, as observed in family II of CoA-transferases. To ascertain the existence of this thioester intermediate between E238 and CoASH, three methods have been used: inactivation of CoA-transferase by sodium borohydride, mechanism based fragmentation of the enzyme at the thioester by heating at 70 °C and kinetic measurements. All of results proved the formation of this enzyme-CoA thioester intermediate. The reason for no reaction between butyryl-CoA and E238 in the crystal structure could be the five-fold reduced enzymatic activity of butyryl-CoA compared to 4-hydroxybutyryl-CoA and/or by formation of enzyme-butyryl-CoA complex on ice, i.e. soaking of the crystals with butyryl-CoA. Furthermore, the kinetic data clearly favor a ping-pong mechanism typically for family I CoA-transferases.

### **4.3 4-Hydroxybutyryl-CoA dehydratase in new CO<sub>2</sub>-fixation pathway in *M. sedula***

*Metallosphaera sedula*, an extremely thermoacidophilic archaea, plays important roles during the metal mobilization in the natural environment. It grows optimally at pH 2.0 and 75 °C. A new CO<sub>2</sub>-fixation cycle via 3-hydroxypropionate and 4-hydroxybutyrate in *M. sedula* has been published [73,74]. Surprisingly, in this organism exist two different copies of 4-hydroxybutyryl-CoA dehydratase (MS\_1 and MS\_2). To uncover their functions and differences, their genes were expressed in *E. coli*, a widely used expression system to produce recombinant proteins. Unfortunately, MS\_1 was produced in an inactive form, although on SDS-PAGE it exhibited a high-level gene expression and protein purity, and MS\_2 in the pACYCDuet vector was not expressed successfully in the *E. coli* system. Up to now, *E. coli* has been used to produce thermostable proteins for biochemical characterization and crystallographic studies, but a large amount of thermophilic and hyperthermophilic proteins folded into their native state only under natural conditions of high temperature or in the presence of their native cofactors. Therefore, in future the native thermophilic hosts will be applied to produce the active MS\_1 and MS\_2 proteins [107].

## References

1. Wächtershäuser, G. (1990) Evolution of the first metabolic cycles, *Proc Natl Acad Sci U S A.* 87, 200-204.
2. Wächtershäuser, G. (1992) Groundworks for an evolutionary biochemistry: the iron-sulphur world, *Prog Biophys Mol Biol.* 58, 85-201.
3. Decker, K., Jungermann, K. & Thauer, R. K. (1970) Energy production in anaerobic organisms, *Angew Chem Int Ed Engl.* 9, 138-158.
4. Thauer, R. K., Kaster, A. K., Seedorf, H., Buckel, W. & Hedderich, R. (2008) Methanogenic archaea: ecologically relevant differences in energy conservation, *Nat Rev Microbiol.* 6, 579-591.
5. Stickland, L. H. (1935) Studies in the metabolism of the strict anaerobes (genus *Clostridium*): The oxidation of alanine by *C. sporogenes*. IV. The reduction of glycine by *C. sporogenes*, *Biochem J.* 29, 889-898.
6. Buckel, W. & Barker, H. A. (1974) Two pathways of glutamate fermentation by anaerobic bacteria, *J Bacteriol.* 117, 1248-1260.
7. Buckel, W., Golding, B.T. (1999) Radical species in the catalytic pathways of enzymes from anaerobes, *FEMS Microbiol. Reviews.* 22, 523-541.
8. Buckel, W. (1996) Unusual dehydrations in anaerobic bacteria: considering ketyls (radical anions) as reactive intermediates in enzymatic reactions, *FEBS Lett.* 389, 20-24.
9. Buckel, W. (2001) Unusual enzymes involved in five pathways of glutamate fermentation, *Appl Microbiol Biotechnol.* 57, 263-273.
10. Barker, H. A. (1937) On the fermentation of glutamic acid, *Enzymologia.* 2, 175 - 182.
11. Chen, H. P., Hsu, H. J., Hsu, F. C., Lai, C. C. & Hsu, C. H. (2008) Interactions between coenzyme B<sub>12</sub> analogs and adenosylcobalamin-dependent glutamate mutase from *Clostridium tetanomorphum*, *FEBS J.* 275, 5960-5968.
12. Brüggemann, H., Baumer, S., Fricke, W. F., Wiezer, A., Liesegang, H., Decker, I., Herzberg, C., Martinez-Arias, R., Merkl, R., Henne, A. & Gottschalk, G. (2003) The genome sequence of *Clostridium tetani*, the causative agent of tetanus disease, *Proc Natl Acad Sci U S A.* 100, 1316-1321.

13. Bothe, H., Darley, D. J., Albracht, S. P., Gerfen, G. J., Golding, B. T. & Buckel, W. (1998) Identification of the 4-glutamyl radical as an intermediate in the carbon skeleton rearrangement catalyzed by coenzyme B<sub>12</sub>-dependent glutamate mutase from *Clostridium cochlearium*, *Biochemistry*. 37, 4105-4113.
14. Gruber, K. & Kratky, C. (2002) Coenzyme B<sub>12</sub> dependent glutamate mutase, *Curr Opin Chem Biol*. 6, 598-603.
15. Buckel, W., Hetzel, M. & Kim, J. (2004) ATP-driven electron transfer in enzymatic radical reactions, *Curr Opin Chem Biol*. 8, 462-467.
16. Hans, M., Sievers, J., Müller, U., Bill, E., Vorholt, J. A., Linder, D. & Buckel, W. (1999) 2-hydroxyglutaryl-CoA dehydratase from *Clostridium symbiosum*, *Eur J Biochem*. 265, 404-414.
17. Kim, J., Hetzel, M., Boiangiu, C. D. & Buckel, W. (2004) Dehydration of (R)-2-hydroxyacyl-CoA to enoyl-CoA in the fermentation of alpha-amino acids by anaerobic bacteria, *FEMS Microbiol Rev*. 28, 455-468.
18. Müller, U. & Buckel, W. (1995) Activation of (R)-2-hydroxyglutaryl-CoA dehydratase from *Acidaminococcus fermentans*, *Eur J Biochem*. 230, 698-704.
19. Hans, M., Buckel, W. & Bill, E. (2008) Spectroscopic evidence for an all-ferrous [4Fe-4S]<sup>0</sup> cluster in the superreduced activator of 2-hydroxyglutaryl-CoA dehydratase from *Acidaminococcus fermentans*, *J Biol Inorg Chem*. 13, 563-574.
20. Hans, M., Bill, E., Cirpus, I., Pierik, A. J., Hetzel, M., Alber, D. & Buckel, W. (2002) Adenosine triphosphate-induced electron transfer in 2-hydroxyglutaryl-CoA dehydratase from *Acidaminococcus fermentans*, *Biochemistry*. 41, 5873-5882.
21. Hans, M., Buckel, W. & Bill, E. (2000) The iron-sulfur clusters in 2-hydroxyglutaryl-CoA dehydratase from *Acidaminococcus fermentans*. Biochemical and spectroscopic investigations, *Eur J Biochem*. 267, 7082-7093.
22. Gerhardt, A., Çinkaya, I., Linder, D., Huisman, G. & Buckel, W. (2000) Fermentation of 4-aminobutyrate by *Clostridium aminobutyricum*: cloning of two genes involved in the formation and dehydration of 4-hydroxybutyryl-CoA, *Arch Microbiol*. 174, 189-199.
23. Barker, H. A., D'Ari, L. & Kahn, J. (1987) Enzymatic reactions in the degradation of 5-aminovalerate by *Clostridium aminovalericum*, *J Biol Chem*. 262, 8994-9003.

24. Collins, M. D., Lawson, P. A., Willems, A., Cordoba, J. J., Fernandez-Garayzabal, J., Garcia, P., Cai, J., Hippe, H. & Farrow, J. A. (1994) The phylogeny of the genus *Clostridium*: proposal of five new genera and eleven new species combinations, *Int J Syst Bacteriol.* 44, 812-826.
25. Johnson, J. L. & Francis, B. S. (1975) Taxonomy of the Clostridia: ribosomal ribonucleic acid homologies among the species, *J Gen Microbiol.* 88, 229-244.
26. Hardman, J. K. & Stadtman, T. C. (1960) Metabolism of omega-amino acids. I. Fermentation of gamma-aminobutyric acid by *Clostridium aminobutyricum* n. sp, *J Bacteriol.* 79, 544-548.
27. Hardman, J. K. & Stadtman, T. C. (1960) Metabolism of omega-acids. II. Fermentation of delta-aminovaleric acid by *Clostridium aminovalericum* n. sp, *J Bacteriol.* 79, 549-552.
28. Hardman, J. K. & Stadtman, T. C. (1963) Metabolism of omega-amino acids. IV. gamma Aminobutyrate fermentation by cell-free extracts of *Clostridium aminobutyricum*, *J Biol Chem.* 238, 2088-2093.
29. Hardman, J. K. & Stadtman, T. C. (1963) Metabolism of omega-amino acids. III. Mechanism of conversion of gamma-aminobutyrate to gamma-hydroxybutyrate by *Clostridium aminobutyricum*, *J Biol Chem.* 238, 2081-2087.
30. Kwon, O. S., Park, J. & Churchich, J. E. (1992) Brain 4-aminobutyrate aminotransferase. Isolation and sequence of a cDNA encoding the enzyme, *J Biol Chem.* 267, 7215-7216.
31. Gerhardt, A. (1999) Molekulare Charakterisierung der Schlüsselenzyme des 4-Hydroxybutyrat-Stoffwechsels in *Clostridium aminobutyricum*: Dehydrogenase, CoA-Transferase und Dehydratase, *Doktorarbeit, Philipps Universität Marburg*.
32. Scherf, U., Söhling, B., Gottschalk, G., Linder, D. & Buckel, W. (1994) Succinate-ethanol fermentation in *Clostridium kluyveri*: purification and characterisation of 4-hydroxybutyryl-CoA dehydratase/vinylacetyl-CoA delta 3-delta 2-isomerase, *Arch Microbiol.* 161, 239-245.
33. Bartsch, R. G. & Barker, H. A. (1961) A vinylacetyl isomerase from *Clostridium kluyveri*, *Arch Biochem Biophys.* 92, 122-132.
34. Söhling, B. & Gottschalk, G. (1996) Molecular analysis of the anaerobic succinate degradation pathway in *Clostridium kluyveri*, *J Bacteriol.* 178, 871-880.
35. Kenealy, W. R. W., D.M. (1985) Studies on the substrate range of *Clostridium kluyveri*; the use of propanol and succinate, *Arch Microbiol.* 141, 187-194.
36. Bornstein, B. T. & Barker, H. A. (1948) The energy metabolism of *Clostridium kluyveri* and the synthesis of fatty acids, *J Biol Chem.* 172, 659-669.

37. Heider, J. (2001) A new family of CoA-transferases, *FEBS Lett.* 509, 345-349.
38. Buckel, W., Dorn, U. & Semmler, R. (1981) Glutaconate CoA-transferase from *Acidaminococcus fermentans*, *Eur J Biochem.* 118, 315-321.
39. Mack, M. & Buckel, W. (1995) Identification of glutamate  $\beta$ 54 as the covalent-catalytic residue in the active site of glutaconate CoA-transferase from *Acidaminococcus fermentans*, *FEBS Lett.* 357, 145-148.
40. Eikmanns, U. & Buckel, W. (1990) Properties of 5-hydroxyvalerate CoA-transferase from *Clostridium aminovalericum*, *Biol Chem Hoppe Seyler.* 371, 1077-1082.
41. Dimroth P, M. K., Eggerer H. (1975) On the mechanism of action of isocitrate lyase., *Eur J Biochem. Feb 3*, 267-273.
42. Scherf, U. & Buckel, W. (1991) Purification and properties of 4-hydroxybutyrate coenzyme A transferase from *Clostridium aminobutyricum*, *Appl Environ Microbiol.* 57, 2699-2702.
43. Jacob, U., Mack, M., Clausen, T., Huber, R., Buckel, W. & Messerschmidt, A. (1997) Glutaconate CoA-transferase from *Acidaminococcus fermentans*: the crystal structure reveals homology with other CoA-transferases, *Structure.* 5, 415-426.
44. Müh, U., Çinkaya, I., Albracht, S. P. & Buckel, W. (1996) 4-Hydroxybutyryl-CoA dehydratase from *Clostridium aminobutyricum*: characterization of FAD and iron-sulfur clusters involved in an overall non-redox reaction, *Biochemistry.* 35, 11710-11718.
45. Scherf, U. & Buckel, W. (1993) Purification and properties of an iron-sulfur and FAD-containing 4-hydroxybutyryl-CoA dehydratase/vinylacetyl-CoA delta 3-delta 2-isomerase from *Clostridium aminobutyricum*, *Eur J Biochem.* 215, 421-429.
46. Martins, B. M., Dobbek, H., Çinkaya, I., Buckel, W. & Messerschmidt, A. (2004) Crystal structure of 4-hydroxybutyryl-CoA dehydratase: radical catalysis involving a [4Fe-4S] cluster and flavin, *Proc Natl Acad Sci U S A.* 101, 15645-15649.
47. Kim, J. J., Wang, M. & Paschke, R. (1993) Crystal structures of medium-chain acyl-CoA dehydrogenase from pig liver mitochondria with and without substrate, *Proc Natl Acad Sci U S A.* 90, 7523-7527.
48. Kim, J. J. & Wu, J. (1990) Structural studies of medium-chain acyl-CoA dehydrogenase from pig liver mitochondria, *Prog Clin Biol Res.* 321, 569-576.



49. Kiema, T. R., Engel, C. K., Schmitz, W., Filppula, S. A., Wierenga, R. K. & Hiltunen, J. K. (1999) Mutagenic and enzymological studies of the hydratase and isomerase activities of 2-enoyl-CoA hydratase-1, *Biochemistry*. 38, 2991-2999.
50. Buckel, W. & Golding, B. T. (2006) Radical enzymes in anaerobes, *Annu Rev Microbiol*. 60, 27-49.
51. Buckel, W. (1980) The reversible dehydration of (*R*)-2-hydroxyglutarate to (*E*)-glutaconate, *Eur. J. Biochem*. 106, 439-447.
52. Çinkaya, I. (1996) 4-Hydroxybutyryl-CoA Dehydratase aus *C. aminobutyricum*. Untersuchung zum Reaktionsmechanismus mit regiospezifisch deuterierten Substraten, *Diplomarbeit, Philipps Universität Marburg*.
53. Çinkaya, I. (2002) Substrat-induzierte Radikalbildung in dem Eisen-Schwefel-Flavoenzym 4-Hydroxybutyryl-CoA Dehydratase aus *Clostridium aminobutyricum*, Ph. D. thesis, *Philipps Universität Marburg*.
54. Friedrich, P. (2003) Untersuchungen zur Substrat-Stereochemie der 4-Hydroxybutyryl-CoA Dehydratase und zum Mechanismus der 4-Hydroxybutyrat-CoA-Transferase aus *Clostridium aminobutyricum*, *Diplomarbeit, Philipps Universität Marburg*.
55. Fridrich, P. (2008) Substrats stereochemie and Untersuchungen zum Mechanismus der 4-Hydroxybutyryl-CoA Dehydratase aus *Clostridium aminobutyricum*, *Doktorarbeit, Philipps Universität Marburg*.
56. Scott, R., Näser, U., Friedrich, P., Selmer, T., Buckel, W. & Golding, B. T. (2004) Stereochemistry of hydrogen removal from the 'unactivated' C-3 position of 4-hydroxybutyryl-CoA catalysed by 4-hydroxybutyryl-CoA dehydratase, *Chem Commun (Camb)*, 1210-1.
57. Friedrich, P., Darley, D. J., Golding, B. T. & Buckel, W. (2008) The complete stereochemistry of the enzymatic dehydration of 4-hydroxybutyryl coenzyme A to crotonyl coenzyme A, *Angew Chem Int Ed Engl*. 47, 3254-3257.
58. Friedrich, P., Darley, D. J., Golding, B. T. & Buckel, W. (2008) Der stereochemische Verlauf der enzymatischen Wassereliminierung von 4-Hydroxybutyryl-Coenzym A zu Crotonyl-Coenzym A., *Angew. Chem*. 120, 3298-3301.
59. Kimura, M. & Yamaguchi, S. (1998) Medium-chain acyl-CoA dehydrogenase deficiency, *Ryoikibetsu Shokogun Shirizu*, 414-416.



60. Engst, S., Vock, P., Wang, M., Kim, J. J. & Ghisla, S. (1999) Mechanism of activation of acyl-CoA substrates by medium chain acyl-CoA dehydrogenase: interaction of the thioester carbonyl with the flavin adenine dinucleotide ribityl side chain, *Biochemistry*. 38, 257-267.
61. Beinert, H., Emptage, M. H., Dreyer, J. L., Scott, R. A., Hahn, J. E., Hodgson, K. O. & Thomson, A. J. (1983) Iron-sulfur stoichiometry and structure of iron-sulfur clusters in three-iron proteins: evidence for [3Fe-4S] clusters, *Proc Natl Acad Sci U S A*. 80, 393-396.
62. Beinert, H., Holm, R. H. & Munck, E. (1997) Iron-sulfur clusters: nature's modular, multipurpose structures, *Science*. 277, 653-659.
63. Beinert, H. (2000) Iron-sulfur proteins: ancient structures, still full of surprises, *J Biol Inorg Chem*. 5, 2-15.
64. Dunham, W. R., Palmer, G., Sands, R. H., Bearden, A. J., Beinert, H. & Orme-Johnson, W. H. (1971) Comments on "the interpretation of the EPR and Mössbauer spectra of two-iron, one-electron iron-sulfur proteins", *Biochem Biophys Res Commun*. 45, 1119-26.
65. Werst, M. M., Kennedy, M. C., Houseman, A. L., Beinert, H. & Hoffman, B. M. (1990) Characterization of the [4Fe-4S]<sup>+</sup> cluster at the active site of aconitase by <sup>57</sup>Fe, <sup>33</sup>S, and <sup>14</sup>N electron nuclear double resonance spectroscopy, *Biochemistry*. 29, 10533-10540.
66. Kent, T. A., Emptage, M. H., Merkle, H., Kennedy, M. C., Beinert, H. & Münck, E. (1985) Mössbauer studies of aconitase. Substrate and inhibitor binding, reaction intermediates, and hyperfine interactions of reduced 3Fe and 4Fe clusters, *J Biol Chem*. 260, 6871-6881.
67. Robbins, A. H. & Stout, C. D. (1989) Structure of activated aconitase: formation of the [4Fe-4S] cluster in the crystal, *Proc Natl Acad Sci U S A*. 86, 3639-3643.
68. Edmondson, D. & Ghisla, S. (1999) Flavoenzyme structure and function. Approaches using flavin analogues, *Methods Mol Biol*. 131, 157-179.
69. Edmondson, D. E. & Tollin, G. (1983) Semiquinone formation in flavo- and metalloflavoproteins, *Top Curr Chem*. 108, 109-138.
70. Manstein, D. J., Pai, E. F., Schopfer, L. M. & Massey, V. (1986) Absolute stereochemistry of flavins in enzyme-catalyzed reactions, *Biochemistry*. 25, 6807-6816.
71. Manstein, D. J., Massey, V., Ghisla, S. & Pai, E. F. (1988) Stereochemistry and accessibility of prosthetic groups in flavoproteins, *Biochemistry*. 27, 2300-2305.

72. Näser, U., Pierik, A. J., Scott, R., Çinkaya, I. & Buckel, W. (2005) Synthesis of  $^{13}\text{C}$ -labeled gamma-hydroxybutyrates for EPR studies with 4-hydroxybutyryl-CoA dehydratase., *Bioorg. Chem.* 33(1), 53-66.
73. Berg, I. A., Kockelkorn, D., Buckel, W. & Fuchs, G. (2007) A 3-hydroxypropionate/4-hydroxybutyrate autotrophic carbon dioxide assimilation pathway in Archaea, *Science*. 318, 1782-1786.
74. Ettema, T. J. & Andersson, S. G. (2008) Comment on "A 3-hydroxypropionate/4-hydroxybutyrate autotrophic carbon dioxide assimilation pathway in Archaea", *Science*. 321, 342; author reply 342.
75. Willadsen, P. & Buckel, W. (1990) Assay of 4-hydroxybutyryl-CoA dehydratase from *Clostridium aminobutyricum*, *FEMS Microbiol Lett.* 58, 187-191.
76. Diamant, S., Azem, A., Weiss, C. & Goloubinoff, P. (1995) Increased efficiency of GroE-assisted protein folding by manganese ions, *J Biol Chem.* 270, 28387-28391.
77. Southern, E. M. (1992) Detection of specific sequences among DNA fragments separated by gel electrophoresis., *Biotechnology*. 24, 122-139.
78. Hanahan, D. (1983) Studies on transformation of *Escherichia coli* with plasmids, *J Mol Biol.* 166, 557-580.
79. Saiki, R. K., Gelfand, D. H., Stoffel, S., Scharf, S. J., Higuchi, R., Horn, G. T., Mullis, K. B. & Erlich, H. A. (1988) Primer-directed enzymatic amplification of DNA with a thermostable DNA polymerase, *Science*. 239, 487-491.
80. Fisher, C. L. & Pei, G. K. (1997) Modification of a PCR-based site-directed mutagenesis method, *Biotechniques*. 23, 570-1, 574.
81. Kusukawa, N. & Yura, T. (1988) Heat shock protein GroE of *Escherichia coli*: key protective roles against thermal stress, *Genes Dev.* 2, 874-882.
82. Kusukawa, N., Yura, T., Ueguchi, C., Akiyama, Y. & Ito, K. (1989) Effects of mutations in heat-shock genes *groES* and *groEL* on protein export in *Escherichia coli*, *Embo J.* 8, 3517-3521.
83. Schmidt, T. G. & Skerra, A. (1994) One-step affinity purification of bacterially produced proteins by means of the "Strep tag" and immobilized recombinant core streptavidin, *J Chromatogr A.* 676, 337-345.

84. Bungert, S., Krafft, B., Schlesinger, R. & Friedrich, T. (1999) One-step purification of the NADH dehydrogenase fragment of the *Escherichia coli* complex I by means of Strep-tag affinity chromatography, *FEBS Lett.* 460, 207-211.
85. Lichty, J. J., Malecki, J. L., Agnew, H. D., Michelson-Horowitz, D. J. & Tan, S. (2005) Comparison of affinity tags for protein purification, *Protein Expr Purif.* 41, 98-105.
86. Erb, T. J., Berg, I. A., Brecht, V., Müller, M., Fuchs, G. & Alber, B. E. (2007) Synthesis of C<sub>5</sub>-dicarboxylic acids from C<sub>2</sub>-units involving crotonyl-CoA carboxylase/reductase: the ethylmalonyl-CoA pathway, *Proc Natl Acad Sci U S A.* 104, 10631-10636.
87. Erb, T. J., Brecht, V., Fuchs, G., Müller, M. & Alber, B. E. (2009) Carboxylation mechanism and stereochemistry of crotonyl-CoA carboxylase/reductase, a carboxylating enoyl-thioester reductase, *Proc Natl Acad Sci U S A.* 106, 8871-8876.
88. Bradford, M. M. (1976) A rapid and sensitive method for the quantitation of microgram quantities of protein utilizing the principle of protein-dye binding, *Anal Biochem.* 72, 248-254.
89. Laemmli, U. K. (1970) Cleavage of structural proteins during the assembly of the head of bacteriophage T4, *Nature.* 227, 680-685.
90. He, W.-Z. & Malkin, R. (1994) Reconstitution of iron-sulfur center B of photosystem I damaged by mercuric chloride, *Photosynth Res.* 41, 381-388.
91. Fish, W. W. (1988) Rapid colorimetric micromethod for the quantitation of complexed iron in biological samples, *Methods Enzymol.* 158, 357-364.
92. Smith, F. E., Herbert, J., Gaudin, J., Hennessy, D. J. & Reid, G. R. (1984) Serum iron determination using ferene triazine, *Clin Biochem.* 17, 306-310.
93. Wang, B. H. & Biemann, K. (1994) Matrix-assisted laser desorption/ionization time-of-flight mass spectrometry of chemically modified oligonucleotides, *Anal Chem.* 66, 1918-1924.
94. Crooks, G. E., Hon, G., Chandonia, J. M. & Brenner, S. E. (2004) WebLogo: a sequence logo generator, *Genome Res.* 14, 1188-1190.
95. Goloubinoff, P., Diamant, S., Weiss, C. & Azem, A. (1997) GroES binding regulates GroEL chaperonin activity under heat shock, *FEBS Lett.* 407, 215-219.
96. Hashimoto, H., Günther, H. & Simon, H. (1973) The stereochemistry of vinylacetyl-CoA-isomerase of *Clostridium kluyveri*, *FEBS Lett.* 33, 81-83.
97. Schulman, M. & Wood, H. G. (1975) Succinyl-CoA: propionate CoA-transferase from *Propionibacterium shermanii*, *Methods Enzymol.* 35, 235-242.

98. Selmer, T., Willanzheimer, A. & Hetzel, M. (2002) Propionate CoA-transferase from *Clostridium propionicum*. Cloning of gene and identification of glutamate 324 at the active site, *Eur J Biochem.* 269, 372-380.
99. Berthold, C. L., Toyota, C. G., Richards, N. G. & Lindqvist, Y. (2008) Reinvestigation of the catalytic mechanism of formyl-CoA transferase, a class III CoA-transferase, *J Biol Chem.* 283, 6519-6529.
100. Selmer, T. & Buckel, W. (1999) Oxygen exchange between acetate and the catalytic glutamate residue in glutamate CoA-transferase from *Acidaminococcus fermentans*. Implications for the mechanism of CoA-ester hydrolysis, *J Biol Chem.* 274, 20772-20778.
101. Kim, J., Darley, D., Selmer, T. & Buckel, W. (2006) Characterization of (R)-2-hydroxyisocaproate dehydrogenase and a family III coenzyme A transferase involved in reduction of L-leucine to isocaproate by *Clostridium difficile*, *Appl Environ Microbiol.* 72, 6062-6069.
102. Howard, J. B., Zieske, L., Clarkson, J. & Rathe, L. (1986) Mechanism-based fragmentation of coenzyme A transferase. Comparison of alpha 2-macroglobulin and coenzyme A transferase thiol ester reactions, *J Biol Chem.* 261, 60-65.
103. Ben-Zvi, A., De Los Rios, P., Dietler, G. & Goloubinoff, P. (2004) Active solubilization and refolding of stable protein aggregates by cooperative unfolding action of individual hsp70 chaperones, *J Biol Chem.* 279, 37298-37303.
104. Ben-Zvi, A. P., Chatellier, J., Fersht, A. R. & Goloubinoff, P. (1998) Minimal and optimal mechanisms for GroE-mediated protein folding, *Proc Natl Acad Sci U S A.* 95, 15275-15280.
105. Castanie, M. (1997) A set of pBR322-compatible plasmids allowing the testing of chaperone-assisted folding of proteins overexpressed in *Escherichia coli.*, *Anal Biochem.* 254, 150-152.
106. Kim, J. J. & Wu, J. (1988) Structure of the medium-chain acyl-CoA dehydrogenase from pig liver mitochondria at 3-A resolution, *Proc Natl Acad Sci U S A.* 85, 6677-6681.
107. Albers, S. V., Jonuscheit, M., Dinkelaker, S., Urich, T., Kletzin, A., Tampé, R., Driessen, A. J. & Schleper, C. (2006) Production of recombinant and tagged proteins in the hyperthermophilic archaeon *Sulfolobus solfataricus*, *Appl Environ Microbiol.* 72, 102-111.
108. Buckel W (1986) Biotin-dependent decarboxylases as bacterial sodium pumps: Purification

and reconstitution of glutaconyl-CoA decarboxylase from *Acidaminococcus fermentans*. *Methods Enzymol.* 125:547-558

## **Danksagung**

Mein besonderer Dank gilt Herrn Prof. Dr. W. Buckel für die interessante Themenstellung, die gute Betreuung, ständige Diskussionsbereitschaft und Förderung jeder Art.

Herrn Prof. Dr. L-O. Essen danke ich für die Bereitschaft, diese Arbeit als Zweitgutachter zu betreuen.

Herrn Prof. A. Messerschmidt, ihren Arbeitsgruppen und Dr. Berta Martins danke ich für die gute Zusammenarbeit im Rahmen der Kristallisation und insbesondere für das schnelle Lösen der dreidimensionalen Strukturen.

Dr. Peter Friedrich und Dr. Jihoe Kim danke ich für die zahlreichen Hilfestellung, die ständige Diskussionsbereitschaft und ihr großes Interesse an dieser Arbeit.

Ich danke Frau Iris Schall und Herrn Marco Hornung für die technische Unterstützung. Mein besonderer Dank gilt Frau Elke Eckel für die nette Zusammenarbeit und ihre Hilfe bei der experimentellen Arbeit.

Bei Frau Patricia Wagner und Frau Jutta Seip möchte ich für die freundliche Unterstützung während dieser Arbeit und beim Aufenthalt in Deutschland.

Mein ganz besonderer Dank gilt natürlich allen Mitarbeitern unsere Arbeitsgruppen. Zum einen für die Hilfe bei kleinen und großen Problemen, zum anderen für das angenehme Klima und die gute Zusammenarbeit.

Ein großes Dankeschön an meine Eltern, meinen Mann und meine Tochter für Liebe, Verständnis und die Unterstützung während meines Studiums.

## **Lebenslauf**

### **Persönliche Daten**

Name, Vorname: Zhang, Jin  
Geburtsdatum: 01.11.1976  
Geburtsort: Xi'an, V. R. China  
Familienstand: verheiratet, mit einer Tochter  
Nationalität: V. R. China

### **Schulbildung und Studium**

09.1988 – 07.1994 Gymnasium der Normal Universität Shannxi (V. R.China)  
09.1994 – 08.1999 Studium der klinischen Medizin (Bachelor) an der Medizinischen Universität Xi'an (V. R. China)  
08.1999 – 08.2000 Praktikum in dem provinziellen Volksklinikum Shaanxi  
08.2000 – 07.2001 Deutsch Intensivkurs an der Philipps-Universität Marburg  
10.2001 – 02.2006 Studium der Biologie (Diplom) an der Philipps-Universität Marburg  
Spezialisierung: Mikrobiologie, Virologie, Biochemie  
05.2005 – 02.2006 Diplomarbeit im Laboratorium für Mikrobiologie zur Thema:  
'Zum Mechanismus der 4-Hydroxybutyryl-CoA-Dehydratase' unter der Leitung von Prof. Dr. Wolfgang Buckel, Note 1.7  
03.2006 – 03.2010 Wissenschaftliche Mitarbeiterin im Laboratorium für Mikrobiologie bei Prof. Dr. Buckel

## Erklärung

Ich versichere, dass ich meine Dissertation

On the enzymatic mechanism of  
4-hydroxybutyryl-CoA dehydratase and 4-hydroxybutyrate CoA-transferase  
from *Clostridium aminobutyricum*

selbständig, ohne unerlaubte Hilfe angefertigt und mich dabei keiner anderen also der von mir ausdrücklich bezeichneten Quellen und Hilfen bedient habe. Die Dissertation wurde in der jetzigen oder einer ähnlichen Form noch bei keiner anderen Hochschule eingereicht und hat noch zu keinen sonstigen Prüfungszwecken gedient.

Marburg, 01.04.2010

Jin Zhang